

Materials Advances



Accepted Manuscript

This article can be cited before page numbers have been issued, to do this please use: S. K. Panja, A. R. Patel, A. D. Fazal, T. D. Solanky, S. Dhibar and S. Kumar, *Mater. Adv.*, 2025, DOI: 10.1039/D5MA00750J.



This is an Accepted Manuscript, which has been through the Royal Society of Chemistry peer review process and has been accepted for publication.

Accepted Manuscripts are published online shortly after acceptance, before technical editing, formatting and proof reading. Using this free service, authors can make their results available to the community, in citable form, before we publish the edited article. We will replace this Accepted Manuscript with the edited and formatted Advance Article as soon as it is available.

You can find more information about Accepted Manuscripts in the <u>Information for Authors</u>.

Please note that technical editing may introduce minor changes to the text and/or graphics, which may alter content. The journal's standard <u>Terms & Conditions</u> and the <u>Ethical guidelines</u> still apply. In no event shall the Royal Society of Chemistry be held responsible for any errors or omissions in this Accepted Manuscript or any consequences arising from the use of any information it contains.



11

12

13

14

15

16

17

18

19

20

21

22

23

24

25

26

27

28

29

30

1 Recent Advances and Challenges in Graphene-Based Advances

2 Nanomaterials for Photocatalytic CO₂ Reduction

- 3 Abhishek R. Patel, Anas D. Fazal, Trupti D. Solanky, Subhendu Dhibar, Sumit
- 4 Kumar,^{3*} Sumit Kumar Panja,^{1*}
- ¹Material Chemistry Laboratory, Tarsadia Institute of Chemical Science, Uka Tarsadia
- 6 University, Maliba Campus, Gopal Vidyanagar, Bardoli-Mahuva Road, Surat-394350,
- 7 Gujarat, India.
- ²Department of Physics, Indian Institute of Technology, Patna-801106, Bihar, India
- ³Department of Chemistry, Magadh University, Bodh Gaya-824234, Bihar, India

Abstract

Photocatalytic CO₂ reduction is a viable solar-driven approach to sustainably synthesize fuels and chemicals which provides great potential in response to the urgent threat of increasing atmospheric CO₂. Recently, graphene-based nanomaterials have arisen as extremely compelling platforms due to their large surface area, superior electrical conductivity and tunable electrical properties. This highlighted how new developments in graphene-based photocatalysts as CO2 reduction including fundamental reaction mechanisms, thermodynamics, kinetics as well as light-induced charge separation. The presentation assessed different forms of grapheme (Graphene Oxide (GO), Reduced Graphene Oxide(rGO), doped graphene and 3D graphene) both with respect to their synthesis, functionality and the role of functionalization including for co-catalysts. Certain aspects of improved charge transport and catalytic activity are presented in the coupling of graphene with metal oxides, semiconductors, metals, carbon nitrides and Z-scheme systems. The review critically evaluates previous findings on the influence of differing synthesis methods on morphology, performance and included mechanistic information from spectroscopic and density functional theory (DFT) based studies. In addition to advances like single-atom catalysis, hybrid systems and machine learning based design, the review also discusses issues of catalyst stability, scalability and environmental issues. In the conclusion, future directions for developing graphene-based systems towards

- effective, scalable and sustainable CO₂ photoreduction are also provided in Spatial Adolorsou 31
- review. 32

36

37

38

39

40

41

42

43

44

45

46

47

48

49

50

51

52

53

54

55

56

60

- Keywords: Photocatalysis, Graphene Oxide (GO), Reduced Graphene Oxide (rGO), 33
- CO₂ reduction; Charge transfer dynamics. 34

1. Introduction

Increasing levels of CO₂ in the atmosphere is an important factor associated with global climate change and presents a massive challenge to human and environmental systems [1]. CO₂ emissions have dramatically increased in the past century due to fossil fuel combustion, industrial processes and changes in land-use that have resulted in significant increases to global temperatures, extreme weather events as well as ocean acidification[2]. It is critical to reduce CO₂ levels in order to create better climate stability and ultimately sustainability [3]. Photocatalysis employs semiconductors to absorb light resulting in the formation of electron-hole pairs that drive cellular redox processes to convert CO2 into hydrocarbons species such as methane, methanol and formic acids [4, 5]. Despite the interest surrounding this research, it is often obstructed by challenges surrounding conversion efficiency, poor selectivity and rapid recombination of photo-generated charge carriers.

Recently, graphene-based nanomaterials have attracted great attention as new components for photocatalytic systems [6]. Graphene-based materials in particular graphene and its derivatives, e.g., GO, rGO and functionalized hybrids have shown great potential to enhance photocatalytic performance based on a multitude of properties when compared to more traditional photocatalysts including the large surface area to mass ratio, high electron mobility, chemical stability/tolerance towards oxidation and ease of modification of surface chemistry [7, 8]. Graphenebased materials may enhance photogenerated charge separation, enhance light absorption spectra and improve CO₂ adsorption to overcome limitations in more

traditional photocatalyst systems [9-11]. 57

There is now considerable interest in investigating graphene-based nanomaterials for 58

photocatalytic CO₂ reduction from the scientific community and we have already seen 59

significant increases in publications and research activities in the past ten years.

Interest in the area was less significant after 2015, though prior to that research control graphene-based photocatalysts were also pretty limited, more so in and around 2010[12, 13]. This largely came down to the outcome that the coupling of photocatalytic systems with graphene was a relatively new process and mechanism. As the researchers recognized the potential of the electrical properties, functionalities, large surface area and unique role as an electron mediator, the pressure to research increased. After the cumulative number of research papers on graphene in photocatalytic systems peaked around 2015, pressure again began to build due to global climate crisis challenges, with an especially high need for improvements in sustainable energy technology (to at least align in the same direction as work carried out in fulfilling the promise of advancements in hydrocarbon energy technologies). Newer syntheses, improved quality of graphene and hybrid photocatalysts between semiconductor materials (i.e., TiO₂, g-C₃N₄) and MOFs, created new constructive waves in the research environment [14-16].

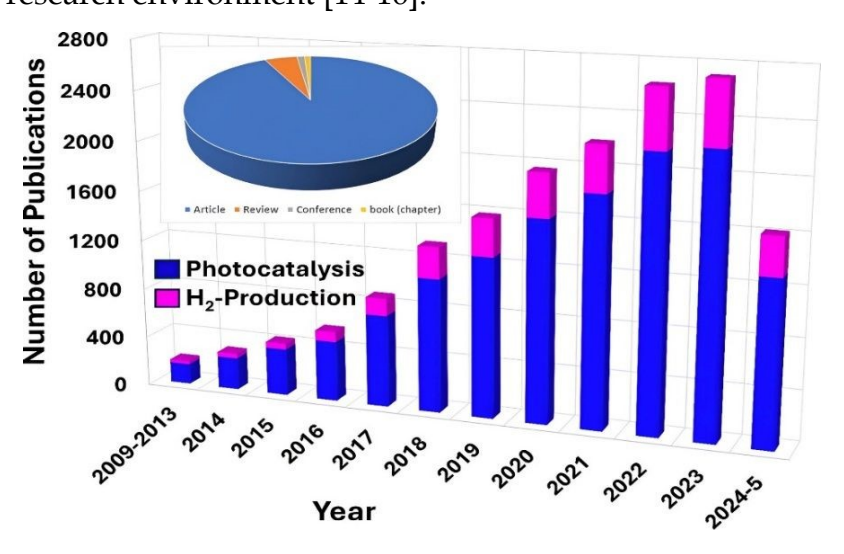


Fig. 1 Publications per year about graphene-based nanomaterials for photocatalytic reduction of CO₂ ,Reprinted with the Ref. ^[17], copyright@**2024**, RSC.

In the past few years, the overall number of publications has generally gone up with a high frequency in high-quality journals in supplements with physics, chemistry and environmental engineering being the most prolific disciplines are due to the multidisciplinary nature (**Fig.1**). Overall, converging assumptions point towards a maturing technological state and teaching a collaborative approach to research devoted to using graphene and graphene nanostructures in purposeful experiences

93

94

95

96

97

98

99

100

101

102

103

104

105

109

110

111

- containing photocatalytic reactions aimed at reduction for possible commercialization Adoption Adoption at the last transfer of the las
- 85 toward carbon neutral and carbon negative technologies.
- 86 This study reviews recent developments in graphene-based nanomaterials use in CO₂
- 87 reduction by photocatalytic processes. It reviews the different types of graphene
- 88 composites and how they can enhance photocatalytic activity (and the scientific
- 89 principles), addresses current challenges, compares performance between systems
- 90 and discusses subsequent research avenues to advance this exciting subject into real-
- 91 life and industrial applications.

2. Fundamentals of Photocatalytic CO₂ Reduction

2.1 Basic Principles and Reaction Mechanisms

To initiate redox reactions in the surface-driven, light-induced process of photocatalytic CO₂ reduction, semiconductors are used as photocatalysts that absorb photons.[18, 19] The photons excite electrons (e⁻) in the valence band (VB) to the conduction band (CB) as long as they have an energy equal to or greater than the bandgap energy (Eg) of the photocatalyst. When an electron is promoted to the CB, a hole (h⁺) is created in the VB and the VB is now positively charged.

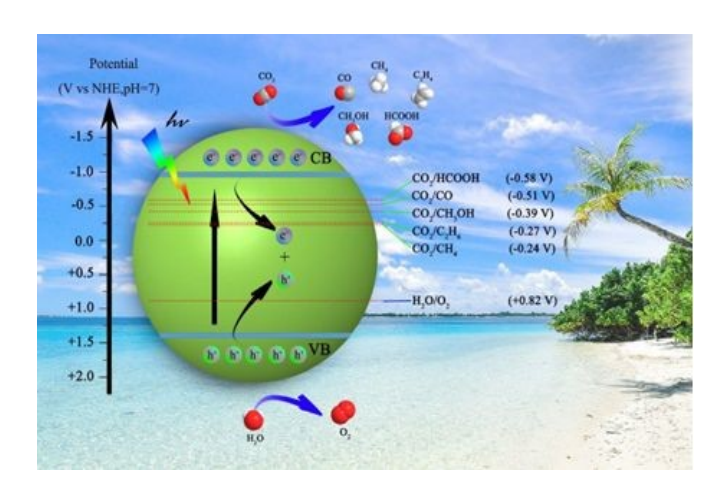
Semiconductor + hv
$$\rightarrow e^{-}(CB) + h^{+}(VB)$$

The holes tend to participate in water oxidation to provide protons and maintain charge neutrality, while the photogenerated electrons can thermally decompose the significantly adsorbed CO₂ molecules [20, 21]. Depending upon the particular nature of the catalyst and reaction conditions, the reduction of CO₂ may follow a number of paths with potentially complex multi-electron transfer steps.

106
$$CO_2 + 2H^+ + 2e^- \rightarrow CO + H_2O (E^0 = -0.53V \text{ vs. NHE})$$

107 $CO_2 + 2H^+ + 2e^- \rightarrow HCOOH (E^0 = -0.61V)$
108 $CO_2 + 8H^+ + 8e^- \rightarrow CH_4 + 2H_2O (E^0 = -0.24V)$

These reactions are thermodynamically uphill and require catalysts that can facilitate multi-electron processes with minimal energy input and shown in (Fig. 2) [20].



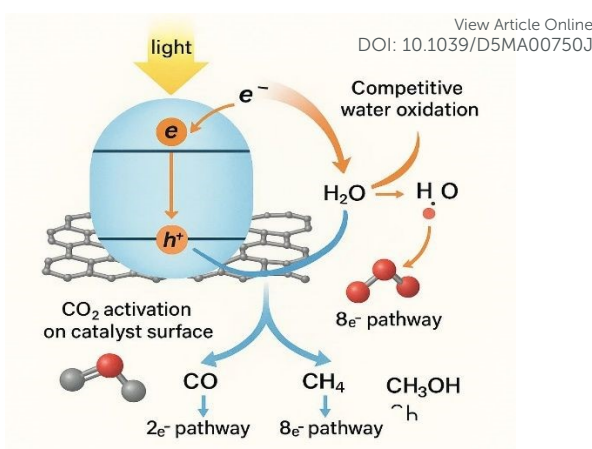


Fig. 2 (A) Band edge alignment and redox potentials for photocatalytic CO₂ reduction with H₂O, (B) General mechanism of graphene-based photocatalytic CO₂ reduction pathways, Reprinted with the Ref. [22],Copyright@**2020**, RSC.

2.2 Thermodynamics and Kinetics of CO₂ Photoreduction

CO₂ is a linear and stable compound with a strong C=O bond (bond energy of 750kJ/mol) it is difficult to activate [23, 24]. Thermodynamic reductions of CO₂ to products such as CO, CH₄ or CH₃OH must overcome significant energy barriers and be utilized in conjunction with the redox potentials of the photocatalyst (**Fig. 3**). In terms of kinetic functionality, the pathway to CO₂ reductions competes with hydrogen evolution reaction (HER) which is often thermodynamically favourable [25].

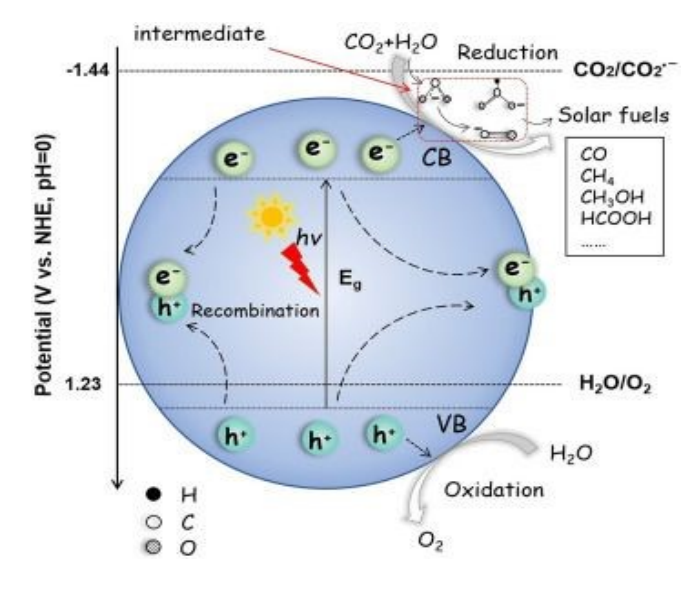


Fig. 3 Schematic Representation of Thermodynamics and Kinetics of CO₂ Photoreduction Reprinted with the Ref. [26], copyright@**2020**, Elsevier.

So, kinetic control through catalyst surface modification, active site engineering 955 MA007503

selective adsorption of CO₂ vs H⁺ is important to increase selectivity [27].

Additionally, product formation is also very sensitive to the number of electrons

transferred: CO and HCOOH are 2e⁻ products while CH₄ and CH₃OH are 8e⁻ and 6e⁻

products, respectively, making this kinetically more complicated.

2.3 Desired Products and Selectivity Control Reactions

Selectivity remains a central challenge in photocatalytic CO₂ reduction due to the coexistence of multiple reaction intermediates (COOH, CHO, CH₂OH) and competing reduction pathways that lead to diverse products [28,29]. Depending on the stabilization and transformation of these intermediates, the system can yield CO, HCOOH, CH₄, or CH₃OH, which serve as valuable chemical feedstocks, hydrogen carriers or high energy density fuels. However, the intrinsic competition with the hydrogen evolution reaction (HER) and the difficulty in controlling electron-proton transfer steps often result in poor product distribution and low carbon efficiency. Consequently, improving product selectivity is not merely a matter of enhancing catalytic activity but also of directing the reaction mechanism toward well-defined and desirable pathways which is essential for practical applications in solar-to-fuel conversion.

A variety of strategies have been developed to enhance selectivity in CO₂ photoreduction. Catalyst composition and morphology play a pivotal role, where controlled doping with transition metals or nonmetals modulates electronic structures and adsorption energies, thereby stabilizing key intermediates and suppressing side reactions [30]. Similarly, rational engineering of the electronic band structure governs the separation and distribution of photogenerated charge carriers, influencing surface coverage and the reduction potential available for CO₂ activation [31]. Beyond intrinsic material properties, the introduction of surface functional groups provides specific anchoring sites that stabilize critical intermediates, improving the probability of their conversion into targeted products. In addition, external factors such as electrolyte pH, CO₂ partial pressure and the incorporation of co-catalysts can further tune reaction kinetics, facilitating selective product formation under optimized operating conditions [32].

Graphene-based materials have emerged as highly effective platforms for improving coloring selectivity in CO₂ reduction owing to their unique physicochemical features. The conjugated π-network and superior electron mobility of graphene enable rapid charge transfer and efficient stabilization of electron-rich intermediates, thereby minimizing unwanted back-reactions. Furthermore, the tunability of graphene through heteroatom doping, covalent functionalization, and formation of heterostructures provides versatile pathways to modulate CO₂ adsorption strength and intermediate stabilization. These attributes, combined with graphene's ability to integrate synergistically with semiconductors and metal nanoparticles, make graphene-based photocatalysts promising candidates for achieving high selectivity toward desired products, thus offering a rational route toward efficient and sustainable CO₂-to-fuels conversion.

2.4 Role of Light Harvesting and Charge Separation

To use the photocatalytic process effectively, good light harvesting is important. Ideally, photocatalysts should absorb a wide spectral extent, especially in the visible region (~400–700 nm) where most solar energy is located [28, 29]. Many traditional photocatalysts (such as TiO₂) has large bandgaps (>3.0 eV) that prevents further efficient use of the sunlight [30].

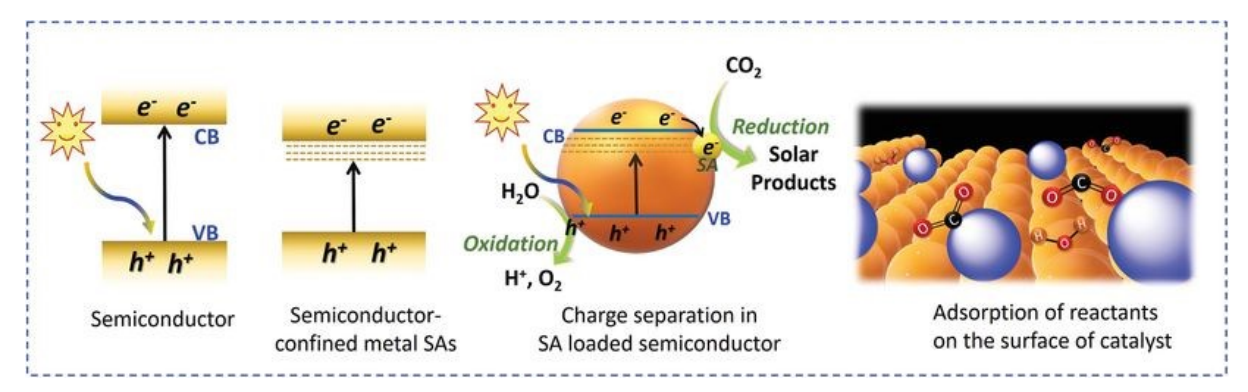


Fig. 4 Schematic Representation of light Harvesting and charge separation, Reprinted with the Ref [31], copyright@**2020**, Wiley Online Library.

Since photogenerated electron-hole pairs rapidly recombine and this can drastically reduce quantum efficiency, charge separation efficiency is thus also very important and shown in (**Fig.4**)[32]. The following are some strategies for increasing light absorption and reducing recombination. The overall performance of photocatalytic

systems is characterized by the synergy that can be established through increased light A007503

absorption, rapid charge carrier mobility and CO₂ adsorption on catalyst surfaces [33,

187 34].

2.4.1 Factors and areas of consideration

Bandgap engineering has been widely recognized as a fundamental strategy for improving photocatalytic CO₂ reduction efficiency. By tailoring the band structure, photocatalysts can extend their light absorption into the visible range while maintaining the redox potentials required for CO₂ activation and subsequent multi-electron transfer processes. Techniques such as heteroatom doping introduce impurity energy levels that narrow the bandgap and tune the electronic structure, while the construction of heterojunctions between semiconductors creates internal electric fields that facilitate charge separation. These modifications not only improve solar spectrum utilization but also influence the adsorption and stabilization of key intermediates, thereby enhancing both activity and selectivity. In particular, graphene-based heterojunctions with semiconductors provide unique advantages by integrating extended light absorption with efficient charge transport pathways.

Z-scheme photocatalytic systems represent another promising approach, drawing inspiration from the architecture of natural photosynthesis. In these systems, two semiconductors are coupled in a manner that preserves the strong reduction potential of one and the strong oxidation potential of the other, while photogenerated electrons and holes in the less energetic bands recombine internally. This spatial and energetic separation allows for simultaneous CO₂ reduction and water oxidation with high efficiency. Incorporating graphene into Z-scheme systems further enhances their performance, as graphene can act as a solid-state conductive bridge, promoting ultrafast charge transfer while suppressing recombination. Recent studies have demonstrated that such graphene-based Z-scheme systems exhibit superior stability and selectivity compared to conventional type-II heterojunctions, making them highly attractive for solar fuel production.

Surface plasmon resonance (SPR) effects associated with noble-metal decoration provide an additional avenue for enhancing photocatalytic CO₂ reduction. Metals such as Au, Ag, and Cu can generate localized electromagnetic fields under light

Open Access Article. Published on 13 November 2025. Downloaded on 18/11/2025 9:21:00 PM.

BY-NG

This article is licensed under a Creative Commons Attribution-NonCommercial 3.0 Unported Licence.

irradiation, leading to strong absorption in the visible region and the excitation of place of high-energy "hot" electrons. These hot carriers can be injected into adjacent semiconductors or graphene-based supports, where they participate directly in CO₂ reduction reactions. Moreover, the synergistic combination of plasmonic metals with graphene facilitates rapid hot-electron transfer due to the high conductivity and extended π-conjugation of graphene, thus suppressing charge recombination and improving reaction selectivity. Graphene itself also contributes by serving as an electron sink and conductive channel, enabling spatial charge separation across hybrid interfaces. Together, bandgap engineering, Z-scheme architectures, plasmonic enhancement, and graphene-mediated charge transport constitute complementary and mutually reinforcing strategies that can be rationally combined to overcome the efficiency and selectivity bottlenecks in photocatalytic CO₂ conversion.

Although notable progress has been made with traditional photocatalysts for CO₂

reduction, their overall efficiency is still restricted by inherent challenges such as fast charge carrier recombination, narrow light absorption, and a limited number of surface-active sites for CO_2 activation. To overcome these drawbacks, researchers have increasingly focused on graphene and graphene-based nanomaterials, which offer outstanding electrical conductivity, large specific surface area, and chemically tunable interfaces. These features facilitate efficient charge separation and transfer, enhanced light harvesting when coupled with semiconductors, and improved catalytic reactivity. The subsequent section provides an in-depth discussion of the structure, properties, and photocatalytic roles of graphene and its derivatives in advancing CO_2 conversion technologies.

3. Graphene and Graphene-Based Nanomaterials

3.1 Structure and Properties of Graphene

Graphene is a 2D carbon allotrope made up of a single atomic layer of sp²-hybridized carbon atoms arranged in a honeycomb lattice and shown in (**Fig. 5**) [35]. This unique atomic arrangement gives graphene many exceptional physicochemical properties that make it a much-studied material with significant potential for a wide range of applications, including photocatalysis[36]. Logically, every carbon atom is connected

to three neighbours in graphene, forming a stable and delocalized π -electron system across the entire sheet [37]. The delocalization of electrons leads to the desired properties of graphene electroconductivity, thermal stability, and typical mechanical stability. For example, the intrinsic carrier mobility of graphene at room temperature is above 200,000 cm² V⁻¹ s⁻¹, with thermal conductivity beyond 5000 W m⁻¹ K⁻¹. Graphene also has excellent flexibility and only absorbs ~2.3 % of visible light, giving it apparent transparency, such as for optical electronic applications. It has the theoretical highest surface area: 2630 m² g⁻¹ (simply meaning a large surface area for chemical reactions or adsorption).[38]

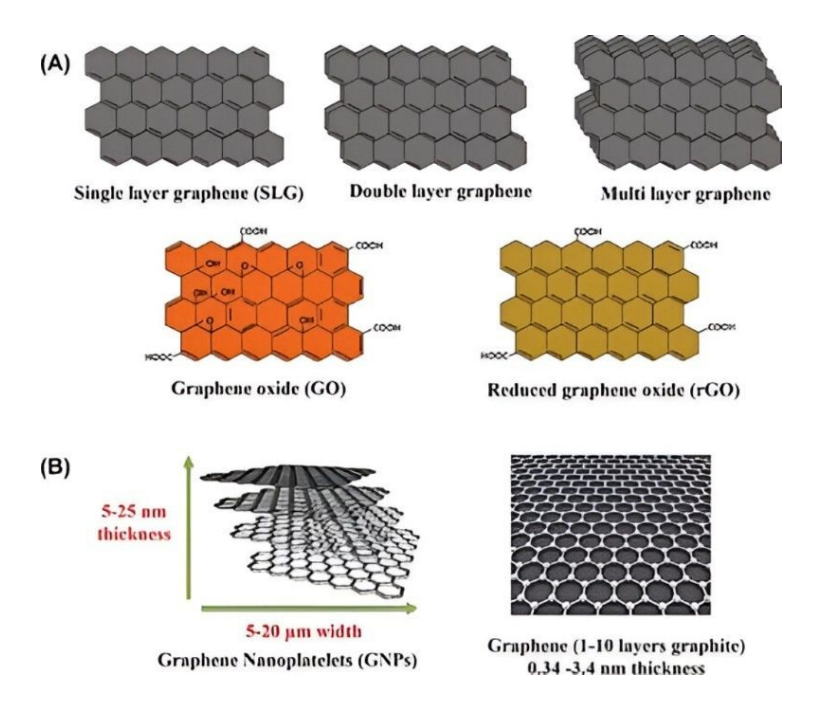


Fig. 5 A) Different structural forms of graphene and its derivatives: Single-layer graphene (SLG), Double-layer graphene, Multi-layer graphene, GO with oxygen-containing functional groups, RGO with partially restored graphitic structure (B) Morphological representations of graphene-based materials: Graphene nanoplatelets (GNPs) with 5–25 nm thickness and 5–20 µm lateral size ,Few-layer graphene (1–10 layers) with thickness of 0.34–3.4 nm. Reprinted with the Ref. [39]copyright@2019, Dove Medical Press.

The unique characteristics make graphene a perfect medium for electron transport and interfacial charge transfer processes specifically, which is vital for photocatalytic processes [40]. However, pristine graphene is chemically inert, therefore lacks a bandgap which prevents it from being useful by itself in this area of electronics [41]. Therefore, researchers have looked into graphene-based derivatives and composites to both overcome the limitations of pristine graphene and take advantage of its conductive and mechanical properties.

View Article Online

DOI: 10.1039/D5MA00750J

3.2 Derivatives of GO, rGO, Doped Graphene, 3D Graphene

To prepare graphene for real photocatalytic and catalytic applications, numerous derivatives have been created [42]. The goals of the derivatives generally relate to introducing chemical functionalities, creating a bandgap, increasing dispersibility in solvents, and establishing synergistic effects with other catalytic materials[43].

Figure: 6 Structural model of GO showing oxygen-containing functional groups such as hydroxyl (–OH), epoxy (–O–), carbonyl (C=O), and carboxyl (–COOH) groups distributed on the basal plane and edges of the graphene sheet. Reprinted with the Ref. [39]copyright@2019, Dove Medical Press.

GO is a heavily oxidized version of graphene, with many oxygen-containing functional groups (e.g., hydroxyl, epoxy, and carboxyl) attached to its sheet structure (**Fig. 6**). These oxygen-containing groups disrupt the conjugated π-electron system (cause pi conjugation to cease), thereby diminishing the electrical conductivity of GO, but markedly increasing its hydrophilicity and chemical reactivity [44]. GO is easily dispersible in water, and other polar protic solvents, thereby permitting its use as an important scaffolding material to support subsequent growth and immobilization of photocatalysts [45]. Importantly GO when incorporated to make a composite material with photocatalysts, shows improved interfacial interactions, charge transfer and increased photocatalytic activity due to its higher density of functional groups and defect sites[46].

Fig. 7 Structural model of rGO, showing a partially restored sp² carbon network with residual oxygenticle Online containing functional groups such as hydroxyl (-OH), epoxy (-O-), and carboxyl (-COOH) groups remaining on the basal plane and edges. Reprinted with the Ref. [39]copyright@**2019**, Dove Medical Press.

RGO can be chemically, thermally or electrochemically reduced GO leaving behind a partially restored π-conjugated network, some reduction in the oxygen content and the possibility of partially restoring GO electrical conductivity, making rGO a better candidate for electron mediator than GO itself [47]. The reduction also creates defects and residual functional groups that can impact interfacial properties and device performance. However, rGO provides a balance between good conductivity and sufficient surface functional groups, when surface functionality is important in encapsulating many photocatalytic systems (**Fig.7**)[48].

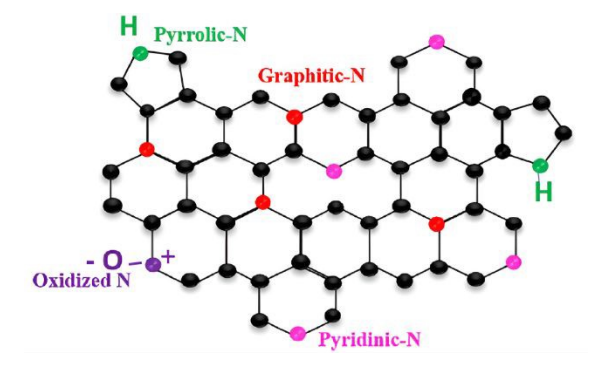


Fig. 8 Schematic representation of nitrogen-doped graphene showing different nitrogen configurations, including pyridinic-N, pyrrolic-N, graphitic-N, and oxidized-N within the graphene lattice. These doped sites significantly influence the electronic structure, surface reactivity, and catalytic activity of graphene-based materials, Reprinted with the Ref [49],copyright@2021,Springer.

Doped graphene is graphene with heteroatoms (like nitrogen (N), boron (B), sulphur (S) or phosphorus (P)) incorporated into the lattice as a substitution for carbon atoms or attached to the surface (**Fig. 8**). Doping creates changes in the electronic structure of graphene, creating localized states within the bandgap and changing work function of the graphene [50, 51]. For example, N-doped graphene has been shown to have better electron donor ability, so some of doped graphene's interactions increase catalytic reaction activity and lead to an increased interaction with nanoparticles of metals or semiconductors[52]. Each of these changes improve photocatalytic ability, through better charge separation and transfer.

View Article Online

319

320

321

322

323

324

325

326

327

328

329

330

331

332

333

334

335

336

337

338

339

340

341

342

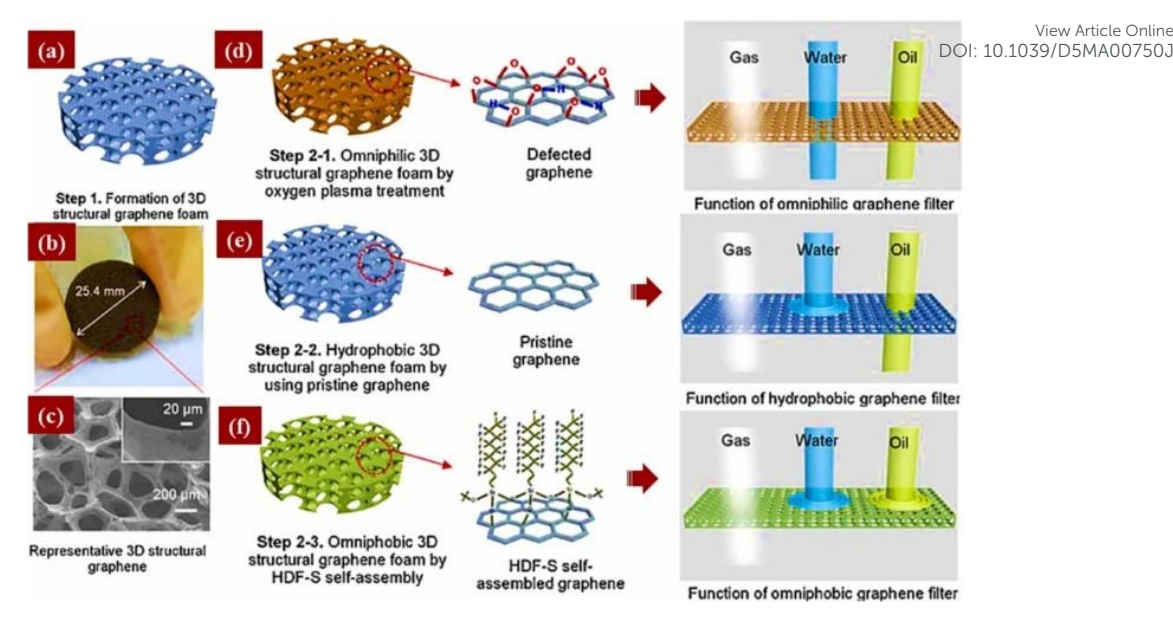


Fig. 9 Graphene foam contains a variety of various functional groups for use in the selective separation of gas, water, and oil. (a) Structure of graphene-foam. (b) 3D-graphene foam picture. (c) SEMmicrograph porous structures. (d) Gas, water, and oil travel through deformed graphene. (e) Pure graphene foam accepts gas and oil yet blocks water. (f) HDF-S-covalently bonded graphene can filter gases, Reprinted with the Ref [53], copyright@2018, Wiley Online Library.

Three-dimensional (3D) graphene architectures[54] (e.g., graphene aerogels, foams, and hydrogels) provide a macroporous and mesoporous scaffold, high surface area, significantly enhanced mechanical stability and favourable mass transport properties (Fig.9) [55-57]. These traits can be leveraged to support photocatalytic nanoparticles and encourage light absorption and reactant diffusion [46]. Furthermore, these 3D graphene support materials can provide continuous conductive pathways for charge migration, which will help reduce electron-holes recombination process.[56] In general, these graphene-based nanomaterials can be intelligently chosen or designed based on the requirements of the photocatalytic system, for example, light absorption capabilities, charge transportation features, reactant adsorption and/or interfacial interactions.

3.3 Methods of Synthesis and Functionalization of Graphene and its derivatives

Graphene and its derivatives have unique physicochemical properties that can be synthesized and functionalized to enhance those properties and tailor them for specific applications[57]. This is particularly appropriate for photocatalysis for CO₂ reduction. Graphene synthesis is separated into two major categories - top down and bottom up (**Fig.10**) [58].

View Article Online DOI: 10.1039/D5MA00750J



Fig. 10 Methods of Synthesis and Functionalization of Graphene and its derivatives, Reprinted with the Ref [59], copyright@2022, Springer.

The **top-down** method involves the exfoliation of bulk graphite into single individual graphene sheets [60]. Mechanical exfoliation can produce high quality graphene, but is not scalable. Chemical exfoliation methods, like the Hummers method and its variations, are often employed for GO synthesis. Chemical exfoliation uses powerful oxidizing agents (e.g. KMnO₄, H₂SO₄) in the oxidation of graphite adding oxygenated groups which separate the interlayers and promote exfoliation. The GO produced can then be reduced to rGO via chemical (e.g. hydrazine, ascorbic acid), thermal, or electrochemical routes[61].

Bottom-up methods use graphene from molecular precursors, generally through chemical vapor deposition. Chemical vapor deposition puts graphene films into high purity, large-area films on metal substrates (Cu or Ni) [62]. CVD has great potential in different electronic and optoelectronic applications, but it is not considered practical for the production of graphene based photocatalytic composites due to cost and scalability [59].

The functionalization of graphene is needed to bring usable chemical groups, improve compatibility with other materials, and ultimately improve electronic properties[63]. Covalent functionalization takes place when chemical groups bond to the carbon lattice (often through reactions with the oxygenated groups in GO, for example), provides stable bonds and improved dispersibility for composites; however, this process may limit the use of the conjugated structure of graphene and limit conductivity. Non-covalent functionalization generally introduces molecules or nanoparticles from the enveloping compound to the sp2 framework of graphene through π–π interactions, hydrogen bonding and/or electrostatic interactions[64, 65].

In photocatalytic applications, functionalization strategies usually consisting problem of perfect online decorating graphene with metal or metal oxide nanoparticles (TiO₂, ZnO or CdS); anchoring co-catalysts; or doping with heteroatoms to improve the potential of light absorption, reactive sites and to improve charge separation [66]. Generally, methods of synthesis/functionalization are the major factors in impacting the overall performance of the graphene-based composites synthesized.

3.3.1 Chemical synthesis methods for graphite oxide

Extensive research has focused on understanding the structure of GO, the primary precursor for graphene materials. GO is typically synthesized by intercalating and oxidizing graphite powder using strong acids (e.g., HCl, H₂SO₄, HNO₃) and oxidizing agents (e.g., NaNO₃, KMnO₄, KClO₃). Several chemical synthesis methods (also see Table 1) discussed below. Each method differs in its oxidants, advantages, disadvantages, and resulting carbon-to-oxygen (C/O) ratios.

Brodie's oxidation method was the first to synthesize GO by reacting graphite with KClO₃ along with HNO₃ at around 60 °C for three to four days.[67, 68] The process involved repeated oxidation steps and drying at 100 °C. Although effective, it has major drawbacks, including long reaction times and the emission of toxic gases.

Staudenmaier method improved Brodie's process by using a mixture of concentrated HNO₃, H₂SO₄, and gradually added KClO₃ to achieve higher oxidation in a single vessel.[69] The reaction involved controlled heating, stirring, and subsequent cooling with water, which is followed by filtration and washing. It produces highly oxidized GO but major disadvantages are long reaction times, explosion risks, and toxic chlorine gas release.

Original Hummer's method introduced a faster and safer alternative for synthesizing GO using KMnO₄ and NaNO₃ as oxidants in conc. H_2SO_4 with graphite.[70] The reaction proceeds through controlled temperature stages (0–4 °C, 35 °C, and 98 °C). It takes about two hours. After oxidation, H_2O_2 is added to reduce residual manganese compounds, followed by washing and drying to obtain GO. The mechanism involves four stages, which are Intercalation, Convection-diffusion, Oxidation and Purification. During Intercalation, H_2SO_4 and $NaNO_3$ generate HNO_3 and reactive oxygen species that open graphite layers. $KMnO_4$ reacts with H_2SO_4 to form Mn_2O_7 , which

intercalates between layers in the step of Convection-diffusion. Further 10 Metalogo Continuous intercalates between layers in the step of Convection-diffusion.

decomposes into O_2 and O_3 , oxidizing graphite into graphite oxide. The purification

403 is performed using H_2O_2 and HCl, it removes residual manganese compounds.

Improved Hummers methods aim to enhance the efficiency, yield, and environmental

safety while reducing toxic emissions. These modifications fall into several main

406 categories.

405

409

411

412

413

417

418

422

424

430

 $H_2SO_4/KMnO_4$ -based methods eliminates $NaNO_3$, preventing toxic NO_2/N_2O_4

release without reducing yield.[71] It enables large-scale, eco-friendly GO synthesis,

with oxidation levels adjustable by KMnO₄ concentration and drying temperature.

 H_2O_2 acts as a terminating agent, and its quantity influences the C/O ratio. The

reaction involves three stages: acid intercalation, oxidation to pristine graphite oxide,

and hydration to form GO. A "mild oxidation" variant (lower KMnO4 ratio) yields

more crystalline, water-dispersible GO suitable for high-conductivity graphene.

Introduced by Marcano et al., H₂SO₄-H₃PO₄/KMnO₄-based methods replace NaNO₃

with a 9:1 H₂SO₄:H₃PO₄ mixture, increasing oxidation efficiency and yield while

eliminating toxic gas formation.[72] It allows better temperature control (35–50 °C)

and produces three times more GO than the original method. Further optimization

studies refined intercalators and drying steps for faster, cost-effective, and scalable

419 production.

In case of Ferrate-assisted oxidation, KMnO₄ is partially replaced with K₂FeO₄, which

has higher oxidizing power and operates under milder conditions (<5 °C, 35–95 °C),

improving efficiency while reducing acid use and environmental impact. During

423 KMnO₄-free methods, Eco-friendly alternatives, such as K₂FeO₄, ozone, peracetic

acid, and electrochemical oxidation, avoid toxic manganese by-products. Though

oxidation levels may be lower, these methods offer safer, scalable production routes.

426 Microwave-assisted oxidation approach rapidly heats reactants via dielectric heating,

reducing synthesis time from several days to about 20 minutes at 100 °C. It yields GO

428 with higher C/O ratios (less oxygenated) but is significantly faster and energy-

429 efficient.[73, 74]

3.4 Graphene as an Electron Mediator and Co-Catalyst

Graphene-based nanomaterials are essential electron mediators and co-catalysts in ΔΕ (CO₂ reduction and photocatalysis processes (**Fig. 11**). Both roles are important for charge separation, interfacial charge transfer, and the recombination suppression of photogenerated electron-hole pairs[75]. As an electron mediator, graphene illustrated an effective electron transport pathway between the photocatalyst and the reaction interface[76]. The high electrical conductivity of graphene and its massive π-conjugated system allows excited electrons to readily transfer from a semiconductor photocatalyst to graphene, a charge sink or electron reservoir, to prevent hols recombination and remain energized carriers[77]. In TiO₂/graphene composites, for example, photogenerated electrons can migrate away from TiO₂ to graphene and, subsequently, to CO₂ molecules disposed on the surface, providing for multi-electron reductions. The unique capacity of graphene produced directional charge flow allowing for the increase in the overall quantum efficiencies the system[78, 79].

Graphene serves as a support co-catalyst that supplies active sites for adsorption and activation of CO₂ and other materials (**Table 1**). Functional groups, defects, or impurities (dopants) in the graphene surface can serve as anchoring sites or functional catalytic sites [76]. For example, in nitrogen-doped graphene, the lone pair electrons of nitrogen can react with CO₂ and catalytically activate and reduce it[78]. Metal nanoparticles deposited onto graphene, and the support themselves, can work together to enhance catalytic activity. The electron rich graphene substrate can stabilize metal active sites, facilitate charge transfer, and modulate the electronic environment of the catalytic centres.

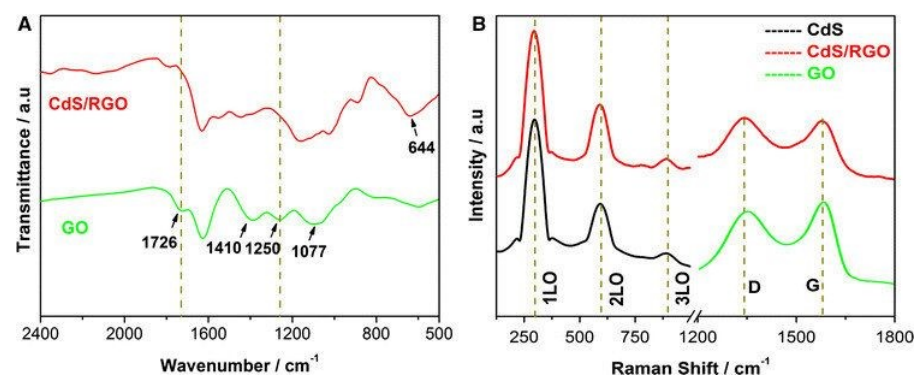


Fig. 11 (A) FT-IR-profiles of GO and CdS-RGO (B) Raman-spectra of GO-CdS-nanoparticles-and-CdS-RGO, Reprinted with the Ref [80], copyright@2020, Springer.

458

459

460

461

462

463

464

465

466

View Article Online DOI: 10.1039/D5MA00750J

Graphene composites with semiconductors can form a Schottky junction or heterojunction, which facilitates charge separation and selective pathway for reaction. CdS/rGO systems provide an example, where rGO facilitates the charge process by improving mobility of the electrons and also minimizing the photo corrosive degradation of CdS material. Similarly, graphene composites with perovskites improves electron transport enhancing rapid electron transport potential, stability, and superior photocatalytic performance[75, 81].

Table 1: Summary of synthesis methods and their impact on catalytic performance

SN.	Synthesis Method	Typical Procedure	Surface Area	Defect Density	Impact on Catalytic Activity	Remarks	Ref.
1	Hummers' Method (Chemical Oxidation/ Reduction)	Oxidation of graphite→ Graphene oxide → Reduction to rGO	Moderate- High (depends on reduction)	High (due to oxygen functional groups, vacancies)	Enhances active sites and electron transfer but may introduce recombinati on centers	Common, scalable; quality depends on reduction degree	[82]
2	Hydrother mal/Solvot hermal	Graphene oxide mixed with precursors , treated at high T & P	High (porous, few-layer structures)	Moderate (controlle d defect formation)	Good dispersion of co- catalysts, strong interfacial contact improves activity	Suitable for hybrids (e.g., graphene-metal oxides)	[83]
3	Chemical Vapor Deposition (CVD)	Hydrocar bon gases decompos ed on metal substrate	Very High (high crystallinit y, large domain size)	Low (near defect- free)	Excellent charge transport; but fewer catalytic sites unless doped/func tionalized	Expensive, limited scalability	[84]

						View A DOI: 10.1039/D5/	rticle Online MA00750J
4	Exfoliation (Liquid phase or Electroche mical)	Sonication , shear, or electroche mical delaminati on of graphite	Moderate- High (depends on exfoliation efficiency)	Variable (controlle d via process)	Balances conductivity and defect density, useful for heterojuncti ons	Green methods possible; lower yield than chemical oxidation	[85]
5	Doping- assisted synthesis (N, S, B, P doping)	Graphene prepared with heteroato ms introduce d during synthesis or post-treatment	Moderate	Controlled defect sites (heteroato m- induced)	Creates active sites, improves CO ₂ adsorption and electron transfer	Strongly enhances selectivity for CO/CH ₄	[86]

4. Recent Progress in Graphene-Based Photocatalytic Systems

Graphene-based materials can benefit photocatalytic systems and help reduce CO₂ levels. When combined with different functional materials, such as metal oxides, semiconductors, metals and carbon-based materials, they can result in advanced nanocomposites with better charge separation, light absorption capacity, and surface reaction sites [87, 88]. This section will talk about the recent developments in these five fields: graphene/metal oxide nanocomposites, graphene/semiconductor heterojunctions, graphene/metal-based nanohybrids, graphene/carbon nitride and their 2D/2D heterostructures, and graphene-based Z-scheme photocatalytic systems[89, 90].

4.1 Graphene/Metal Oxide Nanocomposites

Metal oxides are some of the most studied photocatalytic materials due to their advantageous band structures, photostability, and availability, including tungsten trioxide (WO₃), zinc oxide (ZnO), and titanium dioxide (TiO₂) (Fig. 12) [91]. Unfortunately, the fast recombination of photogenerated charge carriers and the limited visible light absorption often decreases the actual photocatalytic performance of metal oxides. One successful strategy to overcome these limitations has been to

Open Access Article. Published on 13 November 2025. Downloaded on 18/11/2025 9:21:00 PM.

This article is licensed under a Creative Commons Attribution-NonCommercial 3.0 Unported Licence.

combine these systems with graphene[92].Graphene/metal oxide nanocomposites acide online have emerged as highly effective photocatalytic systems owing to the synergistic effects facilitating charge separation, light absorption, and surface reaction kinetics[93].In these nanocomposites, graphene behaves as a conductive support and electron mediator, and metal oxides are the primary photocatalysts. Graphene in combination with TiO₂, ZnO, Fe₂O₃, and CuO not only improves photocatalytic performance in CO₂ reduction under UV light, but also performs well in visible light[94, 95].

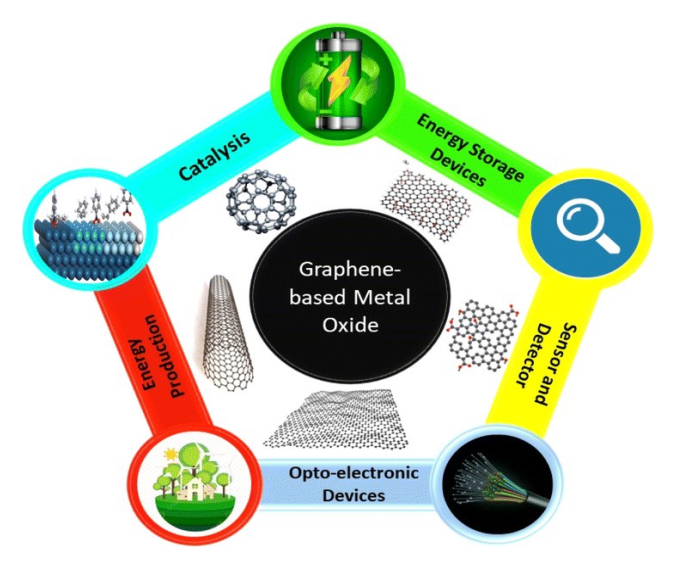


Fig. 12 Nanocomposites of Graphene/Metal Oxide, Reprinted with the Ref [96], copyright@**2024**, RSC.

Graphene/ TiO_2 has been studied more than most other systems. Graphene is critical to improving the photocatalytic efficiency of TiO_2 , as it increases light absorption in the visible area and reduces electron-hole recombination[97, 98]. However, due to the high electron mobility and high surface area of graphene, electrons can be transferred quickly from the TiO_2 conduction band to a graphene sheet to lengthen the life of photogenerated charge carriers. In addition, graphene has multiple active sites for CO_2 adsorption, which is important for increasing photocatalytic conversion efficiency[99, 100].

Graphene enhances the CO_2 photoreduction activity of many ZnO-based nanocomposites. It is said that the graphene sheets intercalate and transport electrons from the heated ZnO which reduces charge-recombination and improves the production of the key intermediates CO_2^- and $HCOO^-[101-104]$. Because of its Π -

510

511

512

513

514

515

516

517

518

519

520

521

522

523

524

525

526

527

528

529

530

531

532

533

534

535

536

537

538

conjugated electronic framework, graphene can produce enhanced interactions with A00750J CO_2 through π - π stacking allowing for improved gas collection and activation on its surface[105]. Graphene also enhances the photocatalytic activity of other visible-light responsive metal oxides such as Fe₂O₃ and CuO. Overall, the charge transport, and increased absorption of light energy that is seen in graphene/Fe₂O₃ composites comparatively to Fe₂O₃ was likely due to the small bandgap of Fe₂O₃[106]. Graphene performs similarly in the case of CuO as well since the heterojunction also has a considerable charge transport factor while stabilizing reactive species for the CO₂ reduction pathways[107]. The synthetic methods including hydrothermal synthesis, sol-gel procedures and in situ growth are important factors that affect interfacial contact, particle size distribution and electron coupling between graphene and metal oxides. Efficient charge transport through the nanocomposite is dependent on creating strong interfacial contacts that optimize electron transport pathways and facilitate lower barriers for charge migration[108, 109]. Graphene/metal energy nanocomposites are versatile photocatalysts that may be engineered for higher CO₂ conversion performance, by tailoring materials design i.e., composition, shape, and interfacial properties in unprecedented detail. Some recent studies have further highlighted the importance of rational design

strategies in advancing photocatalytic systems for energy and environmental applications (**Table 2**). ZnO-based heterostructures continue to attract attention due to their cost-effectiveness and stability, though their intrinsic drawbacks necessitate heterojunction engineering [110]. Both S-scheme and Z-scheme heterostructures have demonstrated exceptional improvements in charge separation and redox capability, with Nb₂O₅/La₂O₃ and ZnO-g-C₃N₄-CuO systems showing outstanding hydrogen evolution rates and strong stability.[111-113] Similarly, the integration of CNTs with Sr-doped ZnO and the ternary ZnO-Cu-CdS composite reveal that synergistic effects between dopants, carbon supports, and mediators such as Cu can significantly enhance light absorption, interfacial charge transfer, and pollutant degradation.[112, 114] These advances not only improve photocatalytic efficiency but also broaden

Open Access Article. Published on 13 November 2025. Downloaded on 18/11/2025 9:21:00 PM.

application versatility, spanning H_2 production, dye degradation and $\Omega_{A00750J}$ reduction.[115]

541

Table: 2 Comparative performance of graphene-based photocatalysts for CO₂ reduction

SN	Catalyst System	Synthesis Method	CO ₂ Conversion Rate	Product Selectivity	Quantum Efficiency (QE)	Stabilit y (h)	Ref.
1	rGO-TiO ₂ nanocomposite	Hydrothermal assembly (GO + Ti precursor)	~45-80 µmol g ⁻¹ h ⁻¹	CO (70%), CH ₄ (20%), H ₂ (10%)	0.5–1.2%	15-20 h	[116]
2	Graphene-ZnO heterojunction	Solvothermal growth of ZnO on GO	~30-60 µmol g ⁻¹ h ⁻¹	CO (65%), CH ₄ (25%)	0.3-0.8%	10-15 h	[117]
3	N-doped Graphene- Cu₂O	In-situ reduction with nitrogen precursor	~120 µmol g ⁻¹ h ⁻¹	CH ₄ (55%), CO (40%)	~2.1%	30 h	[118]
4	Graphene-g- C ₃ N ₄ 2D/2D heterostructure	Thermal polymerization of urea + GO	~150 µmol g ⁻¹ h ⁻¹	CO (80%), CH ₄ (15%)	~2.5%	40 h	[119]
5	rGO-Ag-TiO ₂ plasmonic system	Photo deposition of Ag NPs on rGO-TiO ₂	~200 µmol g ⁻¹ h ⁻¹	CO (90%), trace CH ₄	~3.0%	50 h	[120]
6	Graphene- MoS ₂ hybrid	Hydrothermal co-assembly	~100 µmol g ⁻¹ h ⁻¹	CO (75%), CH ₄ (20%)	1.8%	25 h	[121]
7	B-doped Graphene-TiO ₂	Sol-gel with boron precursor	~85 µmol g ⁻¹ h ⁻¹	CH ₄ (60%), CO (30%)	1.0-1.5%	20 h	[122]

543

544

545

546

547

548

549

550

551

552

4.2 Graphene/Semiconductor Heterojunctions

Besides the classic metal oxides, graphene has been paired with a number of semiconductors with lower band gaps and tunable properties to generate competitive photocatalytic heterojunctions[123, 124]. There have been a large number reporting the hybridization of graphene with the semiconductor's bismuth vanadate (BiVO₄), molybdenum disulphide (MoS₂), cadmium sulphide (CdS), and graphitic carbon nitride (g-C₃N₄) along with hybrid hierarchically porous catalytic metal oxides where the changing properties to metal oxides were complimentary as shown in (**Fig.13**) [125].

View Article Online DOI: 10.1039/D5MA00750J

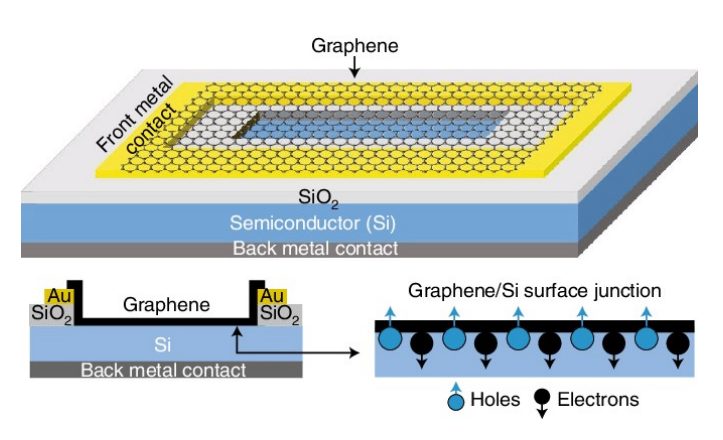


Fig:13 Schematic of a graphene on-semiconductor Si heterojunction photovoltaic cell Top, Reprinted with the Ref [126], copyright@**2019**, Nature.

Kim et al. successfully synthesized ZnO nanostructures with nanoneedle and nanowall morphologies directly on few-layer graphene sheets.[127] In their approach, mechanically exfoliated graphene was transferred onto SiO₂/Si substrates, followed by the growth of ZnO using a metal-organic vapor phase epitaxy (MOVPE) process carried out without any catalyst assistance. The study revealed that both the aspect ratio and spatial arrangement of the ZnO nanostructures—whether aligned vertically or organized in rows—were strongly influenced by the growth temperature, which affected nucleation behavior at the step edges of the graphene surface. Furthermore, the optical characteristics of the ZnO/graphene hybrids were examined through photoluminescence (PL) spectroscopy conducted in the 17–200 K temperature range, providing insights into their structural and electronic quality.

Zinc sulfide (ZnS), one of the earliest studied semiconductors, shares structural and electronic similarities with ZnO but offers distinct advantages such as wider band gaps (3.72 eV for cubic and 3.77 eV for hexagonal forms), making it ideal for UV-selective optoelectronic applications like photodetectors and sensors.[128, 129] Although various low-dimensional ZnS nanostructures have been synthesized, systematic studies on ZnS nanostructure arrays have only recently advanced, unveiling new opportunities to exploit their unique properties.[130] Furthermore, growing research on ZnS-graphene nanocomposites highlights the synergistic interaction between the two materials, leading to improved photocatalytic and electronic performance.

4.3 Graphene/Metal-based Nanohybrids

581 This article is licensed under a Creative Commons Attribution-NonCommercial 3.0 Unported Licence. 582 583 584 Open Access Article. Published on 13 November 2025. Downloaded on 18/11/2025 9:21:00 PM. 585 586 587 588 589

590

578

579

580

Photo-corrosion represents a significant limitation to direct bandgap semiconduction as significant limitation as significa like CdS (~2.4 eV) which have relatively good properties for visible spectrum light harvesting. Beyond stabilizing the photocatalyst, encapsulating CdS with graphene would help with charge separation[131]. Acting as an electron sink, graphene minimizes recombination losses and improves durability, by lowering operating rates while light is present. The CdS/graphene systems have experienced promising CO₂ reduction rates and high quantum yields[132].

Another layered semiconductor with better catalytic properties and hydrogen evolution properties is MoS₂[133]. When combined with graphene, MoS₂ can reduce CO₂ by facilitating charge transfer and providing extra edge sites[134]. MoS₂/graphene composites demonstrate high rates of conversion of CO₂ to CH₄ when exposed to visible light and the fact that they are hybrids ensures good interfacial contact and effective separation of photogenerated carriers[135].



591 592

593

594

595

596

597

598

599

Fig. 14 Graphene/Metal-based Nanohybrids, Reprinted with the Ref [96], copyright@2024, RSC.

In order to solve cost issues, the incorporation of accessible non-noble metals (Ni, Co, Cu) has emerged [136]. These metals are catalytic, and have adequate proximity to graphene, and increased efficiencies of electron transport pathways. Ni/graphene composites provide enhanced CO₂ adsorption and activation abilities, making them appealing candidates for photoreduction applications[137]. Co and Cu NP's help support the dynamics of charge carriers while also participating in multi-electron

transfer processes[138].In metal type nanohybrids shown in (**Fig.14**) or graph in dicicle Online functions as a conductive support medium and as a functional medium to stabilize metal particles, limit aggregation, and manipulate electrical properties at the interface, thus improving photocatalytic performance[139].

4.4 Graphene/Carbon Nitride and 2D/2D Heterostructures

2D/2D heterostructures of graphene and other two-dimensional materials provide a new architecture to help in photocatalysis as shown in (**Fig.15**). In a layered composite format, conducive photocatalytic CO_2 conversion occurs because composites allow improved proximity, faster charge transport, and light absorption [140].

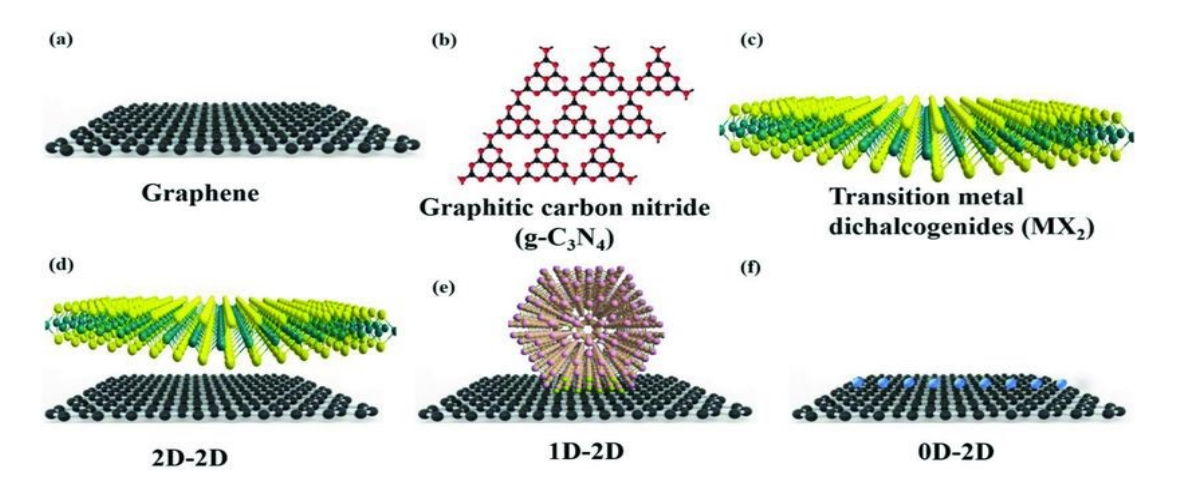


Fig. 15 Frontiers of 2D-materials used in catalysis and their heterostructures, Reprinted with the Ref [141], copyright@**2019**, Wiley Online Library.

Graphene/g-C₃N₄ 2D/2D heterostructures represent a new area of interest due to their synergistic properties. g-C₃N₄ absorbs visible light and has photocatalytic activity, while graphene has solid-state conductivity and promotes charge transport[142]. Thus, a combination of these material properties provides substantial improvements to the standard photocatalytic performance observed in methane and methanol yields under simulated solar light exposure. Other two-dimensional materials, such as MoS₂, WS₂, and layered double hydroxides (LDHs), have been used as van der Waals heterojunctions with graphene[143]. These heterojunctions improve charge separation with electric fields formed in-plane and overlapping conduction and/or valence bands[144]. A heterojunction of MoS₂/graphene hybrid

Open Access Article. Published on 13 November 2025. Downloaded on 18/11/2025 9:21:00 PM.

BY-NC

This article is licensed under a Creative Commons Attribution-NonCommercial 3.0 Unported Licence.

superstructures improves CO₂ reduction reaction activity and stability because the dicte online edges of MoS₂ form catalytic sites and graphene is a very effective conductor [145]. The very thin dimension of 2D materials generates a high surface-to-volume ratio, resulting in a greater density of exposed active sites, drastically reduces the charge diffusion distances, and has the potential to improve CO₂ and photoreduction kinetics, but facilitates coupling to light-harvesting systems like sensitizers and dyes [146, 147].

4.5 Graphene based Z-scheme Photocatalytic Systems

Z-scheme systems incorporate two semiconductors to accomplish efficient charge separation while utilizing both reduction and oxidation potentials, simulating natural photosynthesis as shown in (**Fig.16**) [148]. In Z-scheme transistor topologies, graphene has been and is used as an electron mediator, allowing for fast electron transport and therefore improved charge carrier dynamics[149]. In traditional Z-scheme processes with two semiconductors, a redox mediator physically connects two semiconductors with semi-ideal band alignment and free charge movements and generates problems of low efficiencies and back reflexes[150]. For example, graphene facilitates electron transfer from g-C₃N₄ to TiO₂ pigment so that the redox potentials stay high and the photocatalytic efficiency of the CO₂ photoreduction products improves[151, 152].

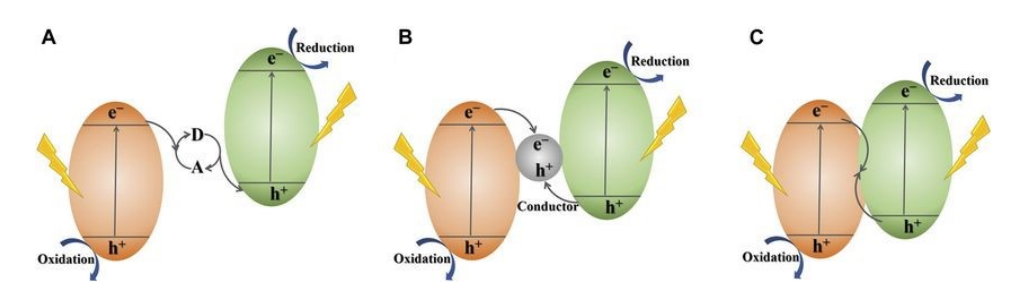


Fig. 16 Schematic illustration of different types of Z-scheme photocatalytic systems: (A) traditional Z-scheme photocatalytic system, (B) all-solid-state Z-scheme photocatalytic system, (C) direct Z-scheme photocatalytic system, Reprinted with the Ref [153], copyright@2024, Frontiersin.

There have also been dual-component systems that involve graphene improving the interfacial contact, as well as reducing direct charge recombination, such as BiVO₄/Graphene/g-C₃N₄ and CdS/Graphene/ZnIn₂S₄. These arrangements utilize

the conductive pathway of graphene in order to create directed charge flow which hadorson enhances quantum efficiencies and product yield[154].

In addition, heterojunctions are more structurally robust when supported with graphene allowing for greater resistance to changing environmental situations[155]. High rates of CO2 reduction have become achievable due to the wide variety of applications humans have created for such designs, particularly under visible to solar light[156]. All and all, Z-scheme graphene-based systems are a complex photocatalytic architecture which should promote reduction and charge recombination losses while maximizing light harvesting and redox potential. The potential for these to scale up solar to fuel technology is exciting[157-161].

In recent years, various other graphene-based composites have emerged as highly efficient photocatalysts for CO₂ reduction owing to their superior conductivity, large surface area, and ability to promote charge separation. A concise summary of representative systems, their photocatalytic performance, and the resulting products is presented in **Table 3**.

Table: 3 Overview of CO₂ photocatalytic conversion into solar fuels and value-added chemicals using graphene-based composite photocatalysts

Composite photocatalyst	Light source	Reaction medium	Main products	Photocatalytic performance	[Ref.]
Graphene- WO ₃ nanobelt	Xenon lamp, 300	CO ₂ and gaseous	CH ₄	Conversion rate: $0.89 \mu mol h^{-1}$ (after 8 h of irradiation)	[162]
composite	W	H ₂ O			
ZnIn2S4/N-	Xenon	84 mg	CO,	CH ₄ : 1.01 μmol ·h ⁻¹ ·g ⁻¹	[163]
graphene	lamp (300	NaHCO ₃ ,	CH₃OH,	CO: 2.45 µmol ·h ⁻¹ ·g ⁻¹	
	W)	2M H ₂ SO ₄	CH ₄	CH ₃ OH: 1.37 μmol ·h ⁻¹ ·g ⁻¹	
Graphene-g-	Daylight	CH ₄	CH ₄	5.87 µmol g ⁻¹ (after 9 hour)	[164]
C_3N_4	bulb, 15 W			2.3-fold than that for g-C ₃ N ₄	
(15 wt%)					
Modified	300-Watt	CH₃OH	CH ₃ OH	Conversion rate: 0.172 µmol	[165]
graphene oxide	halogen			$g^{-1} h^{-1}$	
(GO)	lamp			(Six-fold higher than the	
	irradiation			pure TiO2)	
Cu-Nanoparticle	one-pot	Cu(NO ₃) ₂ ·3		Conversion rate: 6.84 µmol	[166]
Decorated	microwave	H ₂ O in		g-cat-1h-1	
Graphene Oxide	process (2	ethylene		(60 times higher than that for	
	h of visible	glycol		pristine GO)	
	irradiation)			,	
Platinum	Xenon		C ₂ H ₅ OH	Conversion rate: 1,130	[167]
modified rGO	lamp, 300		and	nmol/(h cm²)	
with	W		CH₃COOH		
TiO ₂ nanotubes					

Graphene derivative TiO2	Mercury vapour lamp		Methanol, Ethanol	Ethanol production Rate: 144.7 µmol g ⁻¹ h ⁻¹ at pH 11.0. Methanol production Rate: 47.0 µmol g ⁻¹ h ⁻¹ at pH 4.0.	11,697 Article Online 0.1039705MA00750J
Noble metal nanoparticles (Pt, Pd, Ag, Au) immobilized on rGO-TiO ₂	Xenon arc lamp, 500 W (6 h of light irradiation)	CO ₂ and H ₂ O vapor	CH ₄	Conversion rate: 1.70 µmol g_{cat}^{-1}	[169]
Graphene- supported TiO ₂ nanocrystals with coexposed [110] and [115] facets (G/TiO ₂ - 001/101)	300 W Xe arc lamp	CO ₂ + H ₂ O	СО	70.8 mmol g ⁻¹ h ⁻¹ CO yield	[170]
Reduced graphene oxide (rGO)-copper oxide nanocomposites	visible light irradiation	CO ₂	Methanol	Pristine CuO nanorods showed low photocatalytic activity due to fast charge-carrier recombination, producing only 175 µmol g ⁻¹ methanol. rGO-Cu ₂ O nanocomposites exhibited a fivefold improvement, yielding 862 µmol g ⁻¹ methanol. rGO-CuO nanocomposites achieved a sevenfold improvement, yielding 1228 µmol g ⁻¹ methanol.	[171]
GO-supported oxygen-TiO ₂	xenon arc lamp (400 nm)	CO ₂ and H ₂ O vapor	Methane	Methane (CH ₄) yield: 3.450 µmol gcat ⁻¹	[172] 2017
CuO/Cu ₂ O nanowire (NW) arrays grafted with reduced graphene oxide (CuO/Cu ₂ O NWAs@rGO)	Xenon arc lamp, 500 W	CO ₂ + H ₂ O	СО	Enhanced CO production compared to bare CuO/Cu ₂ O NWAs due to slower charge recombination and efficient electron transfer through rGO nanosheets Carbon monoxide (0.31 and 0.20 mmol cm-2)	[173]
Pt-sensitized graphene- wrapped defect- induced blue- colored TiO ₂	300 W Xenon lamp	Continuous flow- through CO ₂ + H ₂ O	CH ₄ , C ₂ H ₆	259 µmol g ⁻¹ CH ₄ , 77 µmol g ⁻¹ C ₂ H ₆ (7.9% AQY; 5.2% CH ₄ , 2.7% C ₂ H ₆), stable for 42 h	[174]
graphene oxide modified with cobalt metallated aminoporphyrin	450 W Xenon lamp	CO ₂	Formic acid	Formic acid yield: 96.49 µmol in 2 h.	[175]

In ₂ O ₃ -rGO nanocomposites	Visible light	$CO_2 + H_2O$	CH ₄	953.72 μmol g ⁻¹	176 7 Article 0.1039/B5MA0
α-Fe ₂ O ₃ –ZnO rod/reduced graphene oxide (rGO) heterostructure	Visible light & UV- Vis light Xenon Lamp	CO ₂ + H ₂ O	CH₃OH	Under visible light: $1.8 \mu mol$ $g^{-1} h^{-1}$, total $5.3 \mu mol$ g^{-1} in $3 h$; Under UV-Vis: $3.2 \mu mol$ $g^{-1} h^{-1}$, total $9.7 \mu mol$ g^{-1} in $3 h$; $\sim 10 \times higher than ZnO$; stable (90% activity retained after 3 cycles)	[177]
Poly(3- hexylthiophene) nanoparticles/g raphene oxide (P3HT NPs/GO)	Visible light (sunlight)	Gas-phase CO ₂	CH₃OH (methanol), CH₃CHO (acetaldehy de)	CO ₂ -to-CH ₃ OH production: 3.4× higher than pristine GO; total solar fuel yield: 5.7× higher than GO; improved dispersion with SDS nearly 2× higher yield than without SDS; overall solar-to-fuel conversion efficiency 13.5× higher than GO	[178]
Chlorophyll- Cu/graphene (Chl- Cu/graphene)	Visible light (420 nm)	$CO_2 + H_2O$	C ₂ H ₆ (only product)	68.23 μmol m ⁻² h ⁻¹ C ₂ H ₆ yield; 1.26% AQE; high selectivity and stability over 18 h	[179]
Au-TiO ₂ decorated N- doped graphene (ANGT-x, optimized ANGT2)	Xenon lamp, 300 W (1 > 420 nm)	CO ₂ + H ₂ O vapor	Methane (CH ₄ , highly selective)	Electron consumption rate: 742.39 μmol g⁻¹ h⁻¹ (for ANGT2); catalytic activity ~4× higher than ANGT0 and ~60× higher than binary Au-TiO ₂ ; best reported PCO ₂ R rate under comparable conditions	[180]
rGO-grafted NiO-CeO ₂ nanocomposite	Xenon lamp, 300 W	$CO_2 + H_2O$	Formaldeh yde (HCHO)	421.09 μmol g ⁻¹ h ⁻¹ (≈4× higher than pristine CeO ₂)	[181]
G-Ti _{0.91} O ₂ hollow spheres	300 W xenon lamp	CO ₂ and H ₂ O vapor	CO, CH ₄	CO: 8.91 µmol ·g ⁻¹ ·h ⁻¹ CH ₄ : 1.14 µmol ·g ⁻¹ ·h ⁻¹ ~5× higher total CO ₂ conversion than Ti _{0.91} O ₂ spheres; CO dominant; enhanced charge separation, electron transfer to graphene, and photon- trapping from hollow structure	[182]
CuxO/graphene oxide (GO)/Cu- MOF (Cu-BTC) ternary composite photocathode	Xenon lamp150 W, AM 1.5 flter (100 mW cm-2)	Aq. electrolyte + CO ₂	Ethanol, Methanol and Propanol	Ethanol yield: 162 μM cm⁻² after 4 h; improved charge separation and CO ₂ binding confirmed by DFT; Cu-BTC composites reported alcohol yields up to 2217 nmol h⁻¹ cm⁻² (MeOH, EtOH, PrOH)	[183]
RGO-CdS nanorods (0.5 wt% RGO)	Visible light, 300 W xenon lamp	CO ₂ and H ₂ O vapor	CH ₄	2.51 mmol 'h ⁻¹ 'g ⁻¹ ; >10× higher than pure CdS; outperforms Pt–CdS under same conditions; RGO acts	[184]

1				as electron	View Article Online
				acceptor/transporter,	0.1039/D5MA00750J
				enhancing charge separation	
				and CO ₂ adsorption	
SWCNT-TiNS	UV (365	CO ₂	CH ₄	Under UV: SEG-TiNS	[185]
(1D-2D) and	nm) and	(water-	1	showed up to 3.5× higher	
SEG-TiNS (2D-	visible	saturated		CH ₄ production vs TiNS,	
2D)	(>380 nm)	atmosphere		while SWCNT-TiNS	
nanocomposites	light)		showed 2× improvement.	
1		,		Under visible: SWCNT-	
				TiNS showed up to 5.1 ×	
				improvement, SEG-TiNS	
				3.7×, compared to TiNS.	
				SEG-TiNS superior under	
				UV (73.5% more CH ₄ than	
				SWCNT-TiNS), while	
				SWCNT-TiNS superior	
				under visible due to	
				photosensitization.	
Graphene-TiO ₂	300 W	$CO_2 + H_2O$	CH ₄ , C ₂ H ₆	C ₂ H ₆ , 16.8 μmol h ⁻¹ g ⁻¹ ;	[186]
(G-TiO ₂ , 2 wt%	xenon	vapor	C114/ C2116	CH ₄ , 8 μmol h ⁻¹ g ⁻¹ ;	
graphene)	lamp	system		Solar fuel production rate is	
graphene	lamp	System		1.7-fold of TiO ₂	
Ag NW-	Visible	H ₂ O (for	H ₂ , CO,	H ₂ : 70.6 µmol (7× higher	[187]
RGO/CdS NW	light, 300	water-	CH ₄ ,	than CG-2 wt%); CO: 3.648	
(ACG-2 wt%)	W xenon	splitting),	reduced	μmol g ⁻¹ ; CH ₄ : 1.153 μmol	
(11CG-2 W 170)	lamp	H ₂ O/CO ₂	nitro-	g^{-1} ; nitro-aromatic reduction	
	lamp	(for CO_2)	aromatic	enhanced compared to CG-2	
		reduction)	compound	wt%	
		reduction	compound	W (70	
Au-	Visible	CO ₂ saturat	CH ₃ OH	18.80 ppm cm ⁻² h ⁻¹ methanol	[188]
Cu/graphene/C	light, 300	ed H ₂ O		production rate	
u2O (3D coaxial	W xenon				
NW array)	lamp				
Cu ₂ O/RGO	Simulated	$CO_2 + H_2O$	CO, CH ₄	Nearly 6× higher activity	[189]
	solar light,			than optimized Cu ₂ O and	
	500 W			50× higher than	
	xenon			Cu ₂ O/RuOx after 20 h;	
	lamp			apparent quantum yield	
	(400 nm)			~0.34% at 400 nm; enhanced	
				photocurrent and stability	
				due to efficient charge	
				separation and RGO	
				protection	
ZnO-RGO	Simulated	CO ₂ saturat	CH₃OH	4.6 μmol h ⁻¹ g ⁻¹ ; 1.7 times	[190]
	solar light,	ed		higher than pure ZnO	
	500 W	NaHCO ₃ so			
	xenon	lution			
	lamp				
Fe2V4O13/RGO	Visible	CO ₂ and	CH ₄	2.3 µmol h ⁻¹ g ⁻¹ ; 1.5-fold	[191]
/CdS	light, 300	H ₂ O vapor		higher than Fe ₂ V ₄ O ₁₃ -CdS	
	W xenon				
	lamp				
	· •	1	1	1	

666

667

668

669

670

671

672

673

674

675

676

677

678

679

680

681

682

683

Graphene-TiO ₂	Mercury lamp (200 W)	CO ₂ , triethylami ne vapor	СО	CO conversion rate: 1.26 µmol mg ⁻¹	11097 Article O 0.10397195MA007
MOF-808/ reduced graphene oxide	Xenon lamp	CO ₂ , H ₂ O	СО	CO conversion rate: 14.35 µmol ·g-1	[193]
ZnO/N-doped reduced graphene oxide	Xenon lamp (300 W)	84 mg NaHCO ₃ , 2M H ₂ SO ₄	СН₃ОН	CH ₃ OH conversion rate: 1.51µmol ·h ⁻¹ ·g ⁻¹ (2.3 and 4.7 times higher than that of the pristine ZnO and commercial ZnO)	[194] 2021
RGO-P25; SEG-P25	UV light: 100 W mercury vapor lamp Visible light: 60 W daylight bulb	CO ₂ and H ₂ O vapor	CH ₄	Under UV light: $-1.9 \ \mu mol \ m^{-2} \ h^{-1},$ comparable to TiO_2 $-8.5 \ \mu mol \ m^{-2} \ h^{-1}, 4.5 \ times$ higher than TiO_2 Under visible light: $-1.3 \ \mu mol \ m^{-2} \ h^{-1}, 2.3 \ times$ higher than TiO_2 $-4.0 \ \mu mol \ m^{-2} \ h^{-1}, 7.2 \ times$ higher than TiO_2	[195]

5. Mechanistic insight and charge dynamics in graphene based photocatalytic CO₂ Reduction

Rational design of graphene-based materials with enhanced photocatalytic properties necessitates some understanding of the mechanisms governing photocatalytic CO₂ reduction. The addition of graphene and its derivatives can significantly alter band structures, light harvesting efficiencies, and charge carrier dynamic behaviours[196]. In this section, we will also discuss the nature of interfaces that separate and transport charge in conjunction with graphene's contributions to improve the performance of photocatalysts, as well as the theoretical and experimental frameworks that support these operational mechanisms[197].

5.1 Charge separation and migration at graphene interfaces

The effective production, separation, and transportation of photo-induced electronhole pairs are key to photocatalytic efficiency. Rapid recombination of these carriers due to charge carrier motion limits the number of electrons available for reducing CO₂ on typical semiconductor photocatalysts[198]. The unique structure of graphene acts as both a mediator and an electron acceptor at the interface to eliminate this challenge[199]. Photogenerated electrons from the CB are transferred to the graphene

sheet because of the energy level alignment and difference in the two Fermi levels icle Online when semiconductors like TiO₂, ZnO, or g-C₃N₄ are combined with graphene, or rGO[200]. Transfer of these electrons decreased their chance to recombine and increases their time to interact with the adsorbed CO₂ on the surface as shown in (Fig.17) [201, 202].

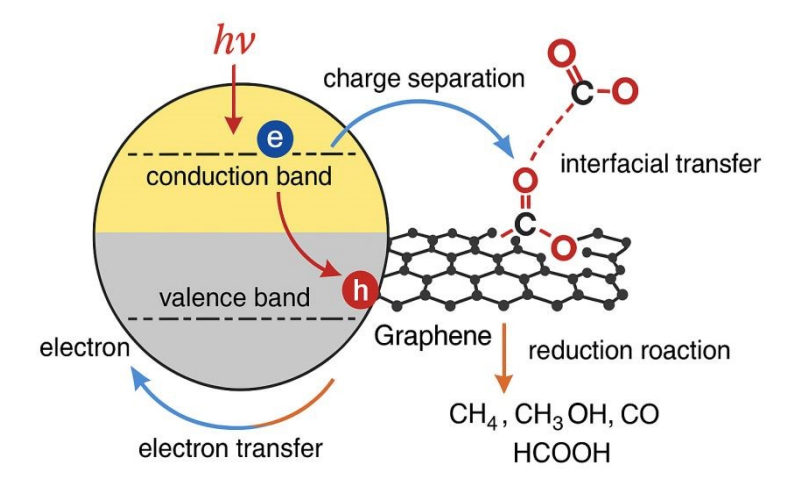


Fig.17 Mechanistic insights in charge transfer dynamics. Reprinted with the [203], copyright@2025, RSC.

Moreover, the two-dimensional structure and high conductivity (~10⁴ S/cm) of graphene provide a rapid and directional pathway for charge migration[204]. This network of conductive sheets reduces the distance between separate photocatalytic nanoparticles and therefore facilitates a more uniform distribution of charge carriers across the surface of the catalyst, and greater electron migration between adjacent particles[205].

5.2 Synergistic roles of graphene in light absorption and carrier mobility

Even without a bandgap, pristine graphene lacks the characteristics of an intrinsic photoactive substance; nonetheless, when combined with other materials it can improve light harvesting and charge transportation capabilities in photocatalysts[206]. By limiting nanoparticle agglomeration in the composite and ultimately increasing light scattering centers throughout the composite material, graphene enhances the light absorption via improved light harvesting[207]

View Article Online DOI: 10.1039/D5MA00750J

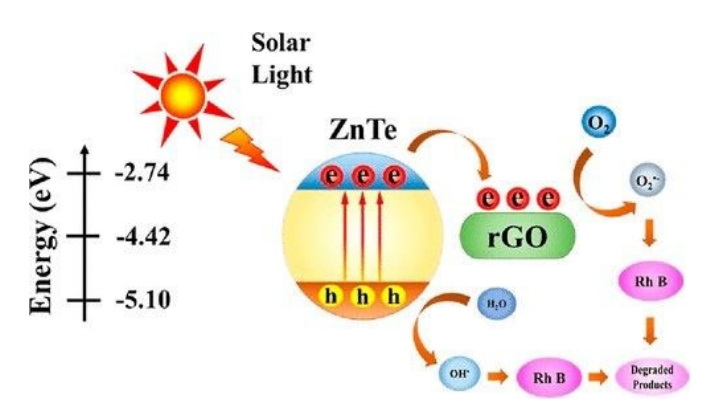


Fig.18 Plausible Mechanism of the Photocatalytic Degradation Process of RhB Containing the R–ZT Catalyst under Solar Light Irradiation, Reprinted with the Ref [208], copyright@2022, ACS.

In addition, when graphene is mixed with plasmonic metals like Au or Ag, it will modify the optical response of the composite system[209]. The localized surface plasmon resonance (LSPR) of noble metal-graphene hybrids will lead to an enhancement in visible light absorption and induce hot electrons that may be transported to graphene and used in CO₂ reduction as shown in (Fig.18) [210].Graphene also significantly enhances the mobility of charge carriers. Due in large part to the delocalized π-electron system, the energy wasted when carriers migrate is minimized since it offers a fast transport path. Graphene can act as reasonably inert, solid-state electron mediators in Z-scheme photocatalytic setups, recombining less energetic electrons and holes from the two different semiconductors in a selective manner, while still retaining the high redox potential of the remaining charge carriers[13, 211, 212]

5.3 Experimental and theoretical investigation

A large body experimental and theoretical evidence supports the application of graphene modifications to photocatalytic reactions [213]. Charge dynamics in graphene-based photocatalysts have been assessed by the use of methods such as surface photovoltaic (SPV) measurements, electrochemistry and impedance spectroscopy (EIS) measurements, photoluminescence (PL) spectroscopy, and time-resolved fluorescence [214-216].

View Article Online

727

728

729

730

731

732

733

734

735

736

737

738

739

740

741

742

743

744

745

746

747

748

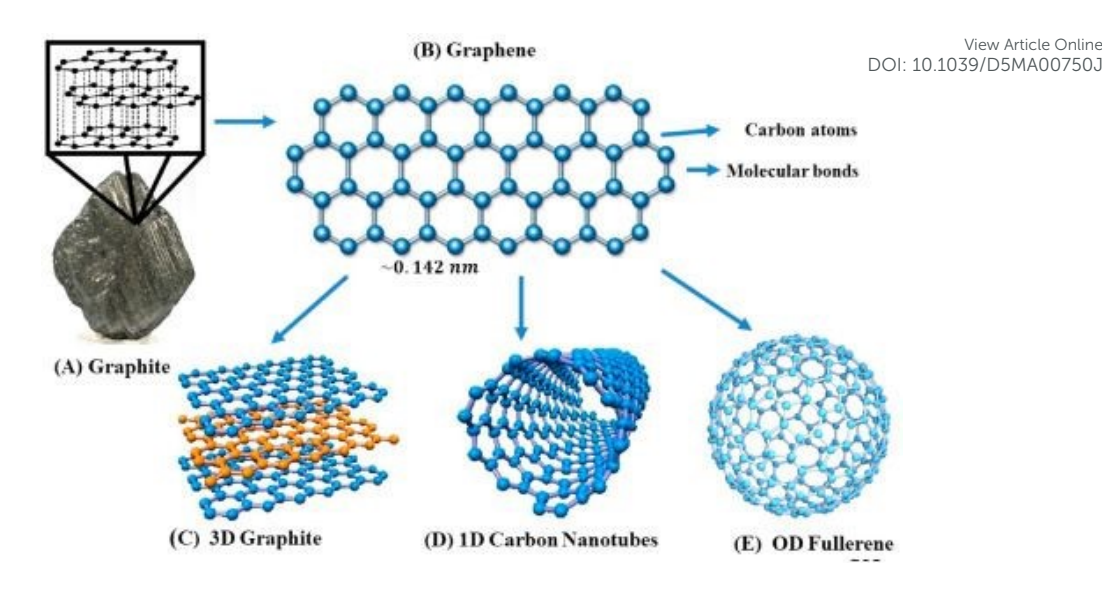


Fig.19 The Schematic illustration of the Origin and the transformation of graphite to graphene's atomic structure. The transformation process shows that graphene, a 2D basic unit of carbon can be folded into (C) 3-D Graphite (D) rolled into 1-D Nanotubes (E) and folded into 0-D Fullerene, Reprinted with the Ref [217], copyright@2023, ACS.

For examples shown in (Fig.19), hybrids containing graphene often showed reduced emission intensity in PL spectra, which indicates reduced electron-hole recombination[218]. The increased interfacial conductivity was demonstrated by EIS measurements, which generally show reduced charge-transfer resistance for graphene-based composites as compared to clean semiconductors[219, 220]. Transient absorption spectroscopy (TAS) and time-correlated single photon counting (TCSPC) offer direct insight of charge carrier lifetimes, with graphene-based materials with much increased lifetimes - often by orders of magnitude[221, 222]. Surface photovoltage imaging experiments showcase better charge separation and charge carrier dispersion on graphene-modified surfaces[223].

Modelling approaches utilizing DFT have assisted in elucidating interfacial charge transfer, modification of the band structure, and CO₂ adsorption energies[224]. DFT simulations suggest charge transfer to heteroatom-doped graphene (for example N-doped, B-doped) exhibits higher CO₂ binding energy and far lower energy barriers for multi-electron transfer processes[225]. Coupling with graphene may better align semiconductor conduction or valence band edge with CO₂ reduction redox potentials, as simulations have indicated [226, 227].

View Article Online

DOI: 10.1039/D5MA00750J

Open Access Article. Published on 13 November 2025. Downloaded on 18/11/2025 9:21:00 PM.

5.4 Graphene induced defect engineering and bandgap modulation

Defects can markedly alter the electrical properties and reactivity of graphene for both intrinsic defects and defects created during synthesis[228]. Specifically, functional groups, vacancies, Stone-Wales defects and dopants allow for effective sites for CO₂ adsorption and activation, due to their capacity to modify the band structure and introduce localized electronic states[229, 230]. Defect engineering in GO or rGO opens up possibilities for bandgap tuning and reactive oxygen-bearing functionalities (such as -OH, -COOH, -C=O) that not only act as anchoring sites for the nanoparticles, also allows for dipole and hydrogen bonding with CO₂ molecules to enhance contact of CO₂ with the reaction sites[231, 232]. These defects can also be potential charge trapping sites to stabilize catalytic intermediates and extend charge separation steps[233].

Heteroatom doping with N, S, B, or P can change the electronic density and bandgap of graphene to improve photocatalytic activity further. For example, N-doped graphene establishes electron-rich regions which can facilitate proton-coupled electron transfer and activation of CO₂ because of the lone pairs which donate electrons to nearby carbon atom(s)[195, 234]. Engineering the band structure of graphene in a heterojunction is also possible with 2D/2D heterojunctions. Heterojunctions with layered materials such as MoS₂ or g-C₃N₄ provide strong interfacial interaction with few 2D materials while spatially separating electrons and holes through the band alignments result in staggered band alignments (type-II or Z-scheme)[235, 236].

Oxygen-doped graphene (GO and rGO) plays a particularly important role due to the abundance of oxygen-containing functional groups, which not only improve the dispersibility of graphene but also provide abundant active sites for anchoring semiconductor species[237]. Residual oxygen groups in rGO are reported to enhance electron transfer by serving as electron-accepting and shuttling sites, while also inducing bandgap narrowing in semiconductor composites through chemical bonding (e.g., Ti–O–C linkages) as shown in (Fig.20) [238]. This leads to red-shifts in light absorption and enhanced photocatalytic performance. However, oxygen

functionalities also introduce a trade-off: while they increase absorptivity variable online porosity, they may reduce carrier mobility by disrupting the π-network. Interestingly, graphene oxide can also act as a standalone semiconductor with a tunable bandgap, although its photoactivity is limited by instability under prolonged irradiation.

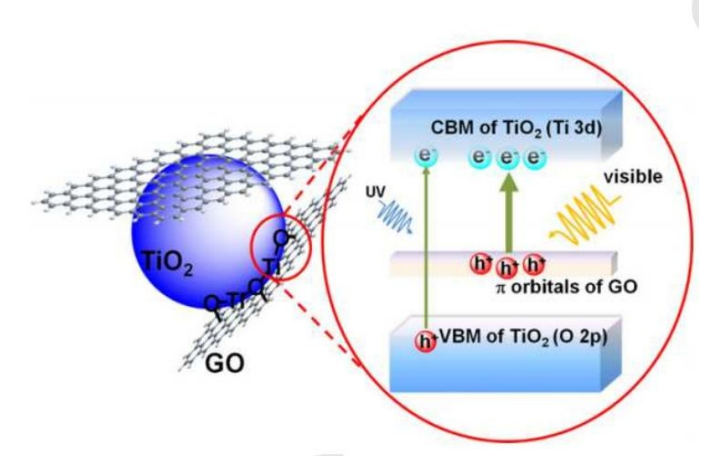
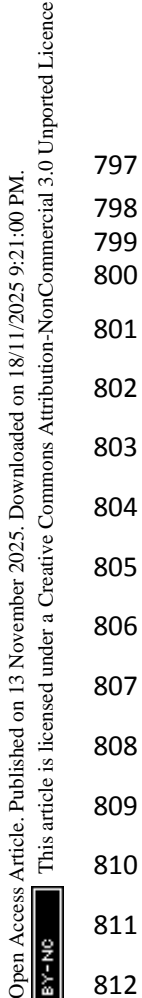


Fig. 20 Schematic representation of Ti-o-c chemical bonding which introduce a localized state and render band gap narrowing, Reprinted with the Ref[239] copyright@**2019**, Springer.

Nitrogen-doped graphene (NGR) has attracted significant attention as a superior alternative to rGO due to its ability to preserve more of the sp² carbon network while introducing active nitrogen sites[240]. Nitrogen atoms contribute additional relectrons, thereby improving the electronic density of states near the Fermi level and markedly enhancing conductivity compared to rGO as shown in (Fig.21) [241]. This increased conductivity promotes efficient electron-hole separation, delays recombination, and boosts photocatalytic durability. Furthermore, different nitrogen configurations—graphitic, pyridinic, and pyrrolic—introduce distinct surface states that act as catalytic centres and improve interfacial contact with semiconductor nanoparticles, thereby strengthening photocatalyst–support interactions.



813

814

815

816

817

818

819

820

821

822

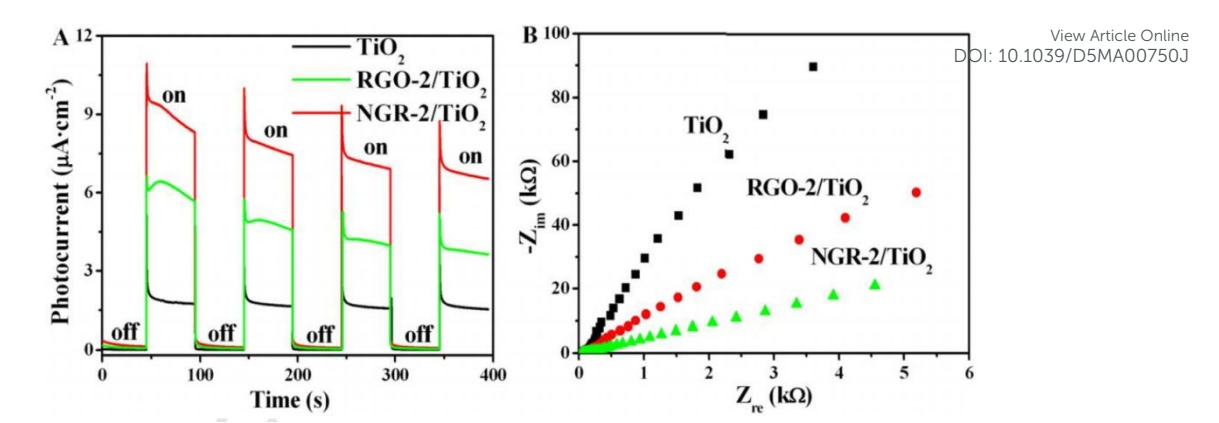


Fig 21. Left: the transient photocurrent of Tio₂, RGO/ Tio₂ and NGR/ Tio₂ to a chopped light irradiation. Right: Nyquist plot of electrochemical impedance spectra for Tio₂, RGO/ TiO₂ and NGR/ TiO₂, Reprinted with the Ref[242], copyright@2025, Elsevier.

Phosphorus-doped graphene (P-G) has also shown promise, as P atoms induce semiconducting behaviour in graphene and open a tunable bandgap (up to ~2.85 eV), enabling visible-light-driven photocatalysis[243]. The incorporation of P atoms reduces defect density while simultaneously enhancing the material's electronic properties. In particular, P-doping Favors hydrogen evolution reactions under visible light, outperforming GO and rGO analogues in photocatalytic hydrogen generation[244].

Sulfur doping, particularly in nitrogen-sulfur co-doped graphene quantum dots (N, S-GQDs), further extends visible-light absorption due to new surface states introduced by sulfur functionalities (C=S, S=O)[245]. These dopants enable broad absorption bands in the visible region and confer sensitizing properties, allowing GQDs to act as efficient electron donors when coupled with semiconductor photocatalysts like TiO₂[246]. The enhanced photoluminescence and surface charge properties imparted by sulfur doping strengthen the structure-activity relationship in such composites.

these heteroatom modifications significantly broaden the Taken together, photocatalytic capabilities of graphene-based materials. Oxygen doping primarily facilitates surface reactivity and bandgap modulation, nitrogen doping enhances conductivity and electron mobility, phosphorus doping introduces stable bandgap engineering with reduced defect states, and sulfur doping expands visible-light utilization. The synergy of these dopants not only improves charge separation and

826

827

828

829

830

831

832

833

834

835

836

837

838

839

840

841

842

843

844

845

846

847

848

849

850

851

852

transport but also enables selective production of solar fuels and chemicals wild MA00750J tailored reaction conditions.

6. Influence of synthesis strategies on photocatalytic efficiency

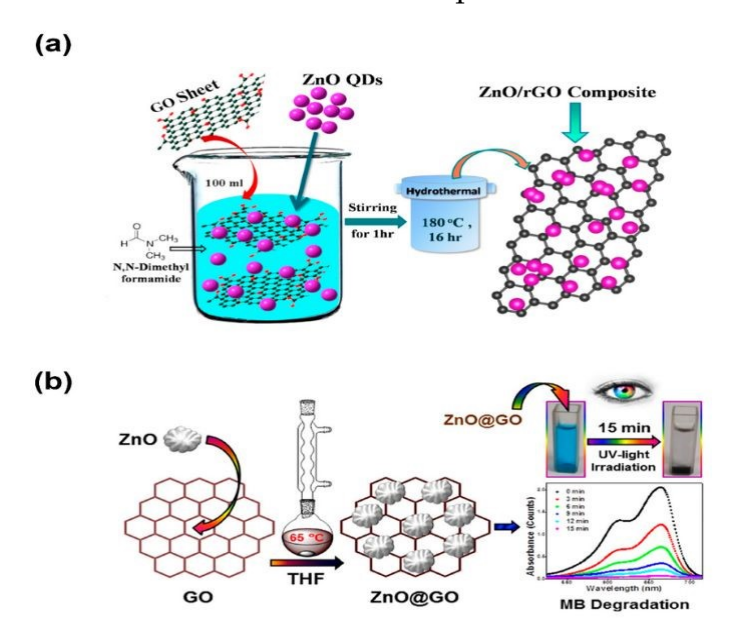
The structural attributes of graphene-based photocatalysts chiefly determined through the synthesis approaches of the working moieties - are directly related to their performance in CO₂ reduction[247]. The various approaches will affect the shape, defect density of the material, crystallinity, surface chemical properties and interfacial contact between the graphene component and the active components of the composite all impact the catalytic efficiency, charge separation and light absorption[248]. This section will raise discussion about the impact that various synthesis approaches have on the photocatalytic activity and sustainability of graphene-based materials, focusing on hydrothermal, electrochemical, photoreduction and green synthesis processes.

6.1 Hydrothermal / Solvothermal approach

Graphene-based nanocomposites are frequently developed by hydrothermal and solvothermal methods, which are also economic and scalable methods with the possibility of producing well-crystallized forms that may have good interfacial contact between graphene and active components[249]. During the hydrothermal/solvothermal method shown in (Fig.22), GO or rGO is readily dispersed with metal precursors in aqueous or organic solutions before heating and pressurizing a sealed autoclave [250]. Over these heating and pressurizing conditions, nucleation and growth of semiconductor or metal oxide nanoparticles (e.g., TiO₂, ZnO, BiVO₄) can occur directly on the peeled-off GO or rGO sheets. Greater interfacial coupling is also known to improve photocatalytic CO₂ reduction via better electron transfer and suppressing electron-hole recombination. Fine tunings of synthesis conditions have the potential to induce vast differences in the catalytic activity of hydrothermally synthesized materials. A good example is how different reaction temperatures alter the crystallinity of the precipitated nanoparticles. Elevated temperatures often help promote the crystallinity or order of solid, thus minimizing structural defects that act as recombination sites for charge carriers, whilst

also increasing the lifetime of charge carriers. This outcome was associated with ZnO-

graphene hybrids, where increased CO₂ to CO conversion efficiencies of crystallinity resulted from elevating the hydrothermal temperature from 120 °C to 180 °C, and several crystallinity defects resulting in reduced conversion efficiencies. Conversely, if the temperature is too high charge carriers can act as glues between nanoparticles resulting in agglomeration which reduces both the surface area and number of active sites in a sample which can subsequently decrease CO₂ adsorption ability. Time is also critical; longer hydrothermal times frequently enhance stability and increase the relative size and homogeneity of nanoparticles, whilst promoting better interactions in the hybrid structure of nanoparticles-graphene. However, prolonged growth also reduces defect density which may limit the availability of catalytically active sites. In contrast, shorter reaction times can generate smaller nanoparticles with higher defect density, potentially increasing catalytic activity by creating additional active centers, albeit at the expense of structural stability.



The pH of the precursor solution and the concentration of metal salts are just as important as temperature and time for nucleation and growth of the nanoparticles.

On graphene, we typically produced smaller, more evenly dispersed nanoparticles

from faster nucleation rates at higher pH. This is important for the effective electron

transport of the composite. The precursor concentration affects loading density of the A007503 nanoparticles: mid-range concentrations evenly distribute the loaded nanoparticles and help maintain graphene conductivity and improve electron-hole separation, while extreme concentrations can lead to nanoparticle collisions with one another, blocking graphene surfaces and limiting charge mobility. The ultimate impact on photocatalytic activity, photon absorption and CO₂ reduction rate is dependent on the balance of factors of crystallinity, defect density, surface chemistry and interfacial contact - all determined collectively from a balance of these interdependent factors[253].

6.2 Electrochemical and photoreduction method

For producing graphene-based photocatalysts both electrochemical and photoreduction technologies have become attractive alternatives to conventional chemical reduction. As they can be applied in relatively mild conditions, and because they offer precise control of both the level of reduction and nanoparticle deposition, both methods are considered to be "greener" since they do not use harsh reducing chemicals. For these reasons, they are suitable for making composites with electrical and structural properties which can be tuned to directly affect their efficiency for photocatalytic CO₂ reduction.

Electrochemical Reduction, involves the application of an electrical bias to GO films or dispersions in an electrolyte medium, removing oxygen functional groups while partially reforming sp²-hybridized carbon networks[254]. Extent of reduction is directly linked to applied potential, reduction time, and electrolyte composition[255]. GO deoxygenation accelerates with applied voltage; the higher the applied voltage, the greater the extent of deoxygenation, increasing electrical conductivity and enabling rapid electron transfer across rGO films. However, excessive reduction may strip too many oxygenated groups from the rGO, leading to a decrease in surface polarity and the number of CO₂ adsorption sites, marking a negative effect on catalytic selectivity. Reduction duration is equally important in rGO production: short reduction times yield partially rGOs with a predominance of oxygen functionalities that subsequently act as anchoring sites for metal nanoparticles, while long reduction times increase conductivity, but decrease oxidation and thus limit surface

907

908

909

910

911

912

913

914

915

916

917

918

919

920

921

922

923

924

925

926

927

928

929

930

931

932

933

934

935

936

reactivity.[256] As ionic strength and metal cation presence can regulate nanopartisticle online nucleation and dispersion, the electrolyte's composition can also influence this process. When noble metals (Ag, Au, and Pt) or TiO₂ are deposited on rGO substrates by electrochemical reduction, for example, there is a close interfacial contact, which aids in effective electron transmission and better charge separation at the graphenesemiconductor interface.

On the other hand, photoreduction is a process that makes use of light irradiation (typically UV or visible light) along with appropriate sacrificial agents (for example, ethanol, methanol, or other organic donors) to reduce GO, or reduce metal ions to graphene sheets in parallel to reducing GO. This is advantageous because it delivered a nanohybrid where there was a clean surface free from any (chemical) residual, unlike traditional chemical reduction routes. The parameters of photoreduction that influence it include: (1) the wavelength of light, and the intensity of light; (2) the time of illumination using the light; and (3) the concentration of sacrificial agent present. Short wavelength UV light, gives high energy photons that can drive highly efficacious GO reduction, and rapid nanoparticle nucleation; while visible-lightassisted photoreduction, is greener and more amenable to scale up. Long illumination times will likely enhance the level of reduction, and nanoparticle loading; however, excessive illumination can result in particle overgrowth or photothermal agglomeration. Additionally, sacrificial agent concentration also plays a role: moderate concentrations will facilitate the efficient transfer of photogenically generated electrons to GO or metal precursors, and high concentrations will result in either incomplete reductions or residual by-products that may passivate catalytic sites.

Electrochemical and photoreduction techniques are most effective when creating nanohybrids with uniformly dispersed nanoparticles good interfacial contact and tunable surface chemistry. These characteristics promote charge transfer efficiency, increase carrier lifetimes, and provide large active surface sites for the adsorption and activation of CO₂, all of which in turn have a direct influence on the catalytic efficiency. Additionally, these techniques produce low energy and less toxic byproducts while allowing for nominally room- to low-temperature reactions, benefiting

937 sustainability goals for the scalable production of graphene by MAOO750J 938 photocatalysts [257].

6.3 Green synthesis and sustainability concern

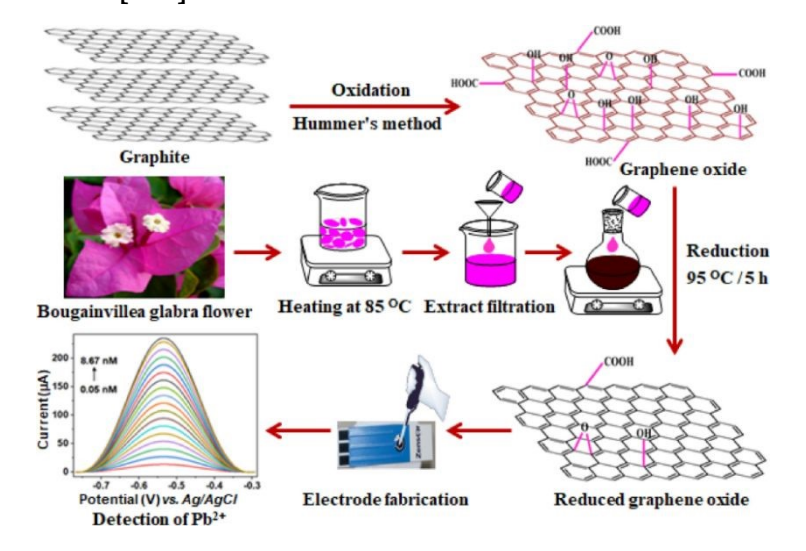
Due to growing emphasis on green chemistry, green synthesis protocols for graphene-based photocatalysts have gained significant attention[258]. With regard to conventional protocols that occasionally employ toxic solvents, high redox agents or high energy requirements, green protocols involve non-toxic solvents, biological redox agents or energy-saving protocols such as microwave-assisted or mechanochemical syntheses. The new technologies both minimize environmental effects and offer new surface functionalities that enhance photocatalytic CO₂ reduction[259].

One of the most frequently adopted green methods is biogenic and plant-extract-mediated reduction. Plant-derived, fungus-derived, or bacterial extracts comprise polyphenols, flavonoids, alkaloids and sugars that serve both as reducing and stabilizing agents while converting GO to rGO and depositing metal nanoparticles. The composition of the extracts directly affects catalytic properties. Polyphenol-laden extracts improve the incorporation of the surface graphene's oxygenated functional groups, increasing hydrophilicity and CO₂ adsorption ability. Flavonoids and proteins however, may act as a capping agent and decrease nanoparticle size and improve dispersion[260].

Microwave-assisted synthesis is another sustainable approach, where precursors are fairly uniformly heated quickly, and the time of reaction and energy consumption is reduced significantly versus traditional hydrothermal processing. The microwave power and exposure time will greatly determine the end material properties. In general, higher microwave power leads to better crystallinity and interfacial coupling, by promoting a faster reduction of GO and nucleation of metal/semiconductor nanoparticles. Extreme microwave power or excessive irradiation times can cause uncontrolled growth or agglomeration of nanoparticles, decrease the active surface area and affect mass transfer. With that stated, optimal microwave parameter manipulation allows the creation of highly porous nanocomposites with controlled shapes, large surface areas and enhanced light absorption efficiency.

Mechanochemical (solvent-free) synthesis is another environmentally-fried three continuous method that does not require an organic solvent. In the mechanochemical process, graphene sheets and catalyst precursors are closely combined by mechanical forces, including ball milling. The choices in milling speed, duration of milling, and ball-to-powder mixing ratio will directly affect the surface roughness, defects, and anchoring of nanoparticles on graphene. For example, in terms of CO₂ adsorption or electron-hole separation, short or low energy-modified milling may create mild defects, allowing for better homogenous dispersion of catalyst in the graphene encapsulated sample. In contrast, large defects created by long milling time (or high energy) can serve as charge recombination sites, reducing the overall catalytic activity of the catalyst. Therefore, optimization is required in order to properly assess the trade-off between the disadvantage of deterioration of structural integrity, and the opportunity to engineer better defects from persistent mill.

Taken collectively, green synthesis methods offer benefits that are considerable in terms of scalability and sustainability and options for tuning the electrical and structural properties of graphene-based photocatalysts as shown in (Fig.23). Often, they lead to composites with lower crystallinity and more heterogeneity compared to conventional hydrothermal or chemical methods, which can detract from long-term stability and reproducibility. Therefore, future studies should focus on optimizing these methods for green chemistry and catalysis, perhaps allowing controlled parameter tuning and hybridization, such as biogenic reduction followed by microwave irradiation[261].



6.4 Morphological tunning and surface area control

The catalytic efficiency of graphene-based photocatalysts is typically determined by controlling morphology and surface design rather than the selection of the synthesis method[263]. The morphological parameters of the composite material which contribute to photocatalytic efficiency through their influence on light absorption, charge separation, kinetics of surface reaction and CO₂ adsorption are equally as important as the innate electrical properties of the material[264]. Therefore, it is progressively more common to use rational modification of morphology when seeking to optimize catalytic efficiencies.

The finest strategy to produce a 3D graphene material is to produce it in the form of hydrogels, foams or aerogels. These are composite structures usually produced via hydrothermal self-assembly or freeze-drying, yielding connected porous networks comprising extremely high porosity and large surface areas[265]. Not only does increased porosity increase light exposure into the catalyst matrix and mass transfer of the CO₂ molecules to/from the active site, but increased porosity also increases active sites due to the increased surface area. For example, size distribution of pores will be affected by the rate at which it is frozen. Rapid freezing yields small closed holes with potential accessibility issues, while slow freeze-drying creates larger interconnecting pores, which can be beneficial for gas diffusion. Thus, this parameter can directly affect the kinetics of CO₂ adsorption and reduction.

The size and spatial distribution of nanoparticles on graphene supports are important factors. During synthesis, the kinetics of nucleation, the use of surfactants or templates, and the concentration of precursors can be varied and achieve morphological control. Smaller and more uniformly dispersed particles form more catalytically active sites and smaller distance of electron transport channel. However, overcrowding of particles from excessive nucleation can reduce graphene's conductivity and disrupt charge mobility. On the other hand, larger nanoparticles can decrease the density of surface-active sites while promoting crystallinity. Producing a suitable morphology will require controlling the syntheses conditions in such a way

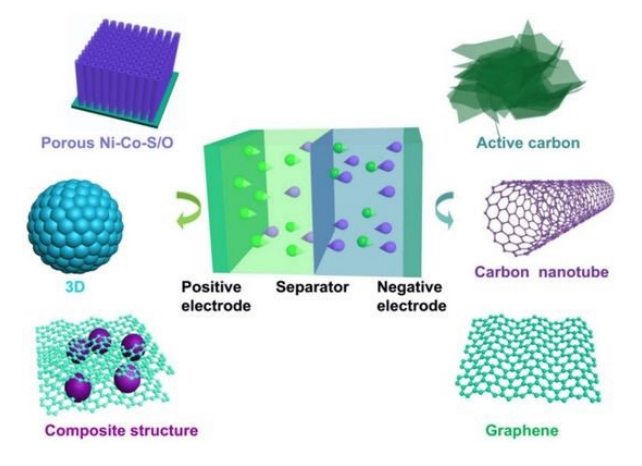
1023

1024

charge separation.

Morphological modification also depends upon defect engineering. Localized states that act as charge-trapping or catalytic sites are added to graphene's band structure when structural defects such as vacancies, edge sites and even heteroatom dopants (N, S, and B) are embedded (i.e., with an atomic localization)[266]. Because defects modified during the synthesis improve CO₂ adsorption via more significant binding interactions with intermediates such as CO₂ as formed and adsorbed at these sites, defects also help morphology-based modification. Defects must be controlled since stability might be compromised and non-radiative recombination could be enhanced if defect densities are too high. For example, nitrogen-doped graphene aerogels can exhibit increased selectivity to the production of CO by stabilizing COOH intermediates, but too much nitrogen-doping can lead to distortion of the carbon lattice structure which can reduce conductivity.

Finally, hierarchical and mesoporous structures enhance photocatalytic performance by combining mesopores (to provide a greater active surface area) and macropores (for mass transfer). Template-assisted synthesis allows precise control on pore size and connectivity. Surfactant/template to precursor ratio is important; if too little surfactant is used the porous structure may partially collapse, while more surfactant loading typically adds to the pore volume and surface area. The use of morphological control mechanisms provides the following synergistic balance of surface area, mass transport and charge transfer dynamics.



1044

1041

1042

1043

1048

1049

1050

1051

1052

1053

1054

Fig. 24 Taking Advantage of Graphene's Surface Area for Advanced Applications, Reprinted with Article Online
the Ref [267], copyright@2025, MDPI.

Surface engineering and morphological tuning are successful strategies for increasing photocatalytic CO₂ reduction capability in graphene-based composites as shown in (Fig.24)[268]. From careful manipulation of physical features (i.e., pore shape, nanoparticle size and dispersion, and defect density) it is possible to optimize light harvesting, facilitate charge separation, and uncover a large number of catalytic sites. The strategies we have proposed help bridge the gap between material development and functional performance.

Table 4: Summary of Synthesis Methods and Their Impact on Catalytic Properties

SN	Synthesis Method	Key Parameter	Effect on Material Properties	Impact on CO ₂ Photocatalysis	Ref.
1	Hydrothermal/ Solvothermal	Temperature	Higher crystallinity at elevated temperature; excessive heating causes nanoparticle aggregation and surface area loss	Improves charge carrier lifetime; excessive temperature reduces CO ₂ adsorption	[269]
2	Hydrothermal/ Solvothermal	Reaction Time	Longer times → larger particles, lower defect density; shorter times → smaller particles, higher defect density	Balances stability and catalytic site density	[270]
3	Hydrothermal/ Solvothermal	pH / Precursor Concentratior	Controls nucleation density and nanoparticle dispersion on graphene	Enhances interfacial contact and electron transfer	[271]
4	Electrochemical Reduction	Applied Potential	Higher voltage improves conductivity but may reduce surface oxygen groups	Improves electron mobility but may lower CO ₂ binding	[272]
5	Electrochemical Reduction	Electrolyte Composition	Ionic strength and cations influence nanoparticle deposition density and distribution	Better nanoparticle anchoring, enhanced interfacial charge separation	[273]
6	Photoreduction	Light Wavelength & Intensity	UV enables fast GO reduction; visible-light more sustainable but slower	Generates clean- surface composites with high electron transfer	[274]
7	Photoreduction	Sacrificial Agent Concentration	Moderate levels promote efficient reduction; excess may leave residues and passivate sites	Affects nanoparticle loading and catalytic efficiency	[275]

8	Green Synthesis (Biogenic)	Extract Composition	Polyphenols, flavonoids add functional groups enhancing CO ₂ adsorption and selectivity	Improves selectivity and CO ₂ affinity; variability limits reproducibility	MA00750J
9	Green Synthesis (Microwave- assisted)	Microwave Power & Duration	Rapid, uniform heating improves crystallinity; excessive power causes agglomeration	Reduces reaction time and energy input; optimized power enhances porosity and activity	[277]
10	Green Synthesis (Mechanochemi cal)	Milling Speed / Time	Creates defects and dispersion; excessive milling may cause too many recombination centres	Enhances CO ₂ adsorption via defects; excessive defects cause recombination losses	[278]
11	Morphological Tuning	Freeze-drying Rate	Slow rate → larger pores, better diffusion; fast rate → smaller, closed pores	Enhances mass transport and light penetration	[279]
12	Morphological Tuning	Surfactant / Template Ratio	Controls mesopore volume, active surface exposure	Increases active surface area and catalytic site exposure	[280]
13	Defect Engineering	Dopant Concentration	Introduces localized charge-trapping sites; excess doping distorts lattice, lowers conductivity	Stabilizes intermediates and boosts selectivity; excess defects hinder performance	[281]

7. Photocatalytic Performance Evaluation

7.1 Experimental Conditions and Reactor Configurations

The evaluation of photocatalytic performance requires standardized and reproducible experimental setups. The three main reactor configurations employed are slurry reactors, flat-panel reactors, and microreactors each providing distinct benefits for light distribution and reactant flow. To ensure comparability, parameters such as light intensity (W/m²), irradiation wavelength, CO₂ pressure and flow rate and reaction temperature must be carefully controlled.[282] For instance, slurry reactors with simulated solar light (AM 1.5G, 100 mW/cm²) have been widely used, while microreactors allow higher precision with CO₂ pressures up to 2 bar and light intensities ranging from 50–150 mW/cm². The use of monochromatic LEDs (420–650 nm) in some studies enables direct correlation between catalyst absorption

1072 This article is licensed under a Creative Commons Attribution-NonCommercial 3.0 Unported Licence 1073 1074 1075 Open Access Article. Published on 13 November 2025. Downloaded on 18/11/2025 9:21:00 PM. 1076 1077 1078 1079 1080 1081 1082 1083 1084

1085

1086

1087

1088

1089

1090

1091

1092

1093

1094

1095

1096

1097

1071

providing more detailed insights into charge transfer MAOO750J and activity, 1069 mechanisms. 1070

7.2 Effect of CO₂ Pressure, Light Source, and Co-Catalysts

Photocatalytic activity exhibits high sensitivity to external operating conditions. Increasing CO2 pressure enhances reactant solubility and adsorption, leading to higher yields[283]. For example, graphene-TiO₂ composites achieved a CO production rate of 120 µmol g⁻¹ h⁻¹ at 1 atm CO₂, which increased to 210 µmol g⁻¹ h⁻¹ when the pressure was raised to 3 atm. Similarly, the choice of light source strongly influences activity: visible light irradiation ($\lambda > 420$ nm, 300 mW/cm²) resulted in a 2.3-fold higher CH₄ yield for N-doped graphene/g-C₃N₄ compared to UV-only excitation. The addition of co-catalysts such as Pt, Cu, or Ni facilitates electron trapping and catalytic site formation. For instance, Pt-decorated graphene-ZnO composites exhibited an AQE of 6.2% under 365 nm irradiation, significantly higher than the bare composite (2.8%).

7.3 Performance Metrics its Yield, Selectivity and Quantum Efficiency

The primary performance indicators for CO₂ photoreduction include product yield (umol g⁻¹ h⁻¹), product selectivity (%), apparent quantum efficiency (AQE), and solar-to-fuel efficiency (STF)[284]. Recent reports demonstrate that significantly graphene-based hybrids outperform conventional photocatalysts[258]. For example, graphene-Cu₂O systems achieved a CO yield of 320 µmol g⁻¹ h⁻¹ with 82% selectivity under AM 1.5G illumination (100 mW/cm²), while TiO₂ under identical conditions produced only 75 µmol g⁻¹ h⁻¹ with 45% selectivity. Similarly, graphene/g-C₃N₄ composites delivered CH₄ yields of 210 μmol g⁻¹ h⁻¹ with AQE values of 5–8%, whereas pristine g-C₃N₄ typically showed <2% AQE. Reaction profiles are routinely characterized via gas chromatography (GC) for gaseous products and high-performance liquid chromatography (HPLC) for liquid intermediates.

7.4 Benchmarking with Conventional and Other Advanced Photocatalysts

Open Access Article. Published on 13 November 2025. Downloaded on 18/11/2025 9:21:00 PM.

Systematic benchmarking against conventional and advanced photocatally the control provides quantitative insight into the role of graphene[285]. For instance, under identical AM 1.5G conditions, graphene–perovskite composites achieved CO₂ conversion rates of 410 μmol g⁻¹ h⁻¹ with 85% CO selectivity and stability exceeding 120 h, compared to bare perovskites which exhibited only 160 μmol g⁻¹ h⁻¹ with 62% selectivity. Likewise, graphene-modified ZnO maintained stable activity over 100 h, while pure ZnO lost 40% of its activity within 30 h. Statistical analysis and recent studies reveals consistent trends: (i) graphene incorporation enhances quantum efficiencies from 1–3% to 5–12%; (ii) CO₂ conversion rates increase 2–5 fold relative to pristine semiconductors; and (iii) selectivity toward CO and CH₄ improves by 20–40%. These results underscore the importance of graphene as an electron mediator and structural stabilizer, establishing reliable structure–activity relationships for future catalyst design as shown in (Fig.25).

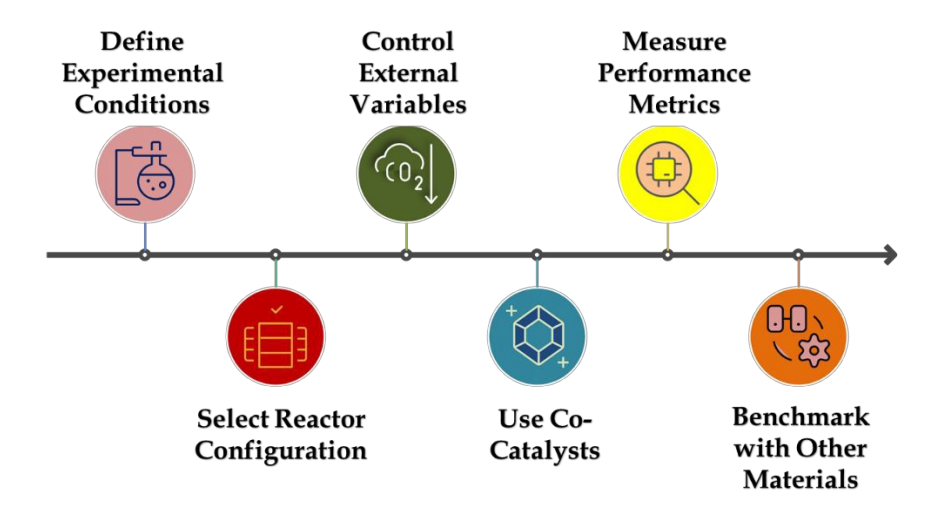


Figure: 25 Experimental setup and performance evaluation of graphene

8. Challenges and Limitations

8.1 Stability and Recyclability of Graphene-Based Catalysts

Extended use of graphene based photocatalysts often causes oxidation, mechanical delamination or photodegradation. Examination of recyclability calls for stability tests involving several photocatalytic cycles and extended illumination. Protective coverings or core-shell construction could help to reduce degradation issues.

8.2 Scale-Up and Cost-Effectiveness

1140

1141

1142

1143

1144

1145

1146

1147

1148

1149

1150

1151

1121

1122

1123

1124

1125

1126

The commercial deployment of these materials faces challenges because of large scale A00750.1 synthesis difficulties and uniformity problems and high production costs despite positive lab-scale results. The development of continuous hydrothermal synthesis and roll-to-roll graphene film production techniques represents current research directions for scalability [286]. The evaluation of economic viability requires a balance between material costs and energy consumption and catalyst durability.

8.3 Standardization of Testing Protocols

The current differences in testing methods produce results that are both inconsistent and non-comparable between different research groups. International consortia and standard-setting organizations are promoting uniform approaches which include catalyst pre-treatment and analytical instrument calibration and error reporting.

Graphene-based nanomaterials (GBN) have been developed with the purpose of

8.4 Toxicity and Environmental Impact of Nanomaterials

photo catalytically reducing CO₂ emissions, meaning GBNs could have a large positive impact on the environment, however, their potential health and environmental risks must be considered. Several studies have reported that GO and rGO cause mammalian cells oxidative stress, membrane damage and inflammation depending on their surface chemistry, size, and dose. In aquatic ecosystems, GBNs have been shown to interact with microorganisms, algae, and fish in ways that impact growth, reproduction, and metabolism, which raises ecotoxicological concern. Chronic exposure to GO has been linked to diminished algal primary productivity and with accumulated discharge of GO in higher trophic levels. And with GBN persistence in soil and water running the risk of unknown cumulative effects, pathways for degradation such as photodegradation, microbial breakdown, and oxidative transformation are only understood in part. [287]. In response to these concerns, regulatory groups have started to take action. The European Chemicals Agency (ECHA) and the U.S. Environmental Protection Agency (EPA) have stressed that nanomaterial safety evaluations and life-cycle assessments of graphene-based materials should be nano specific. However, the regulatory environment is still evolving, and very few regulations established have standardized protocols for toxicity testing, disposal, and risk assessment. Hence, when considering

1153

1154

1155

1156

1157

1158

1159

1160

1161

1162

1163

1164

1165

1166

1167

1168

1169

the safety of graphene nanomaterials in photocatalytic technologies, future studies Ado0750J must prioritize systematic research on environmental fate and bioaccumulation potential, as well as implementation of safe-by-design practices as shown in (**Fig.26**).

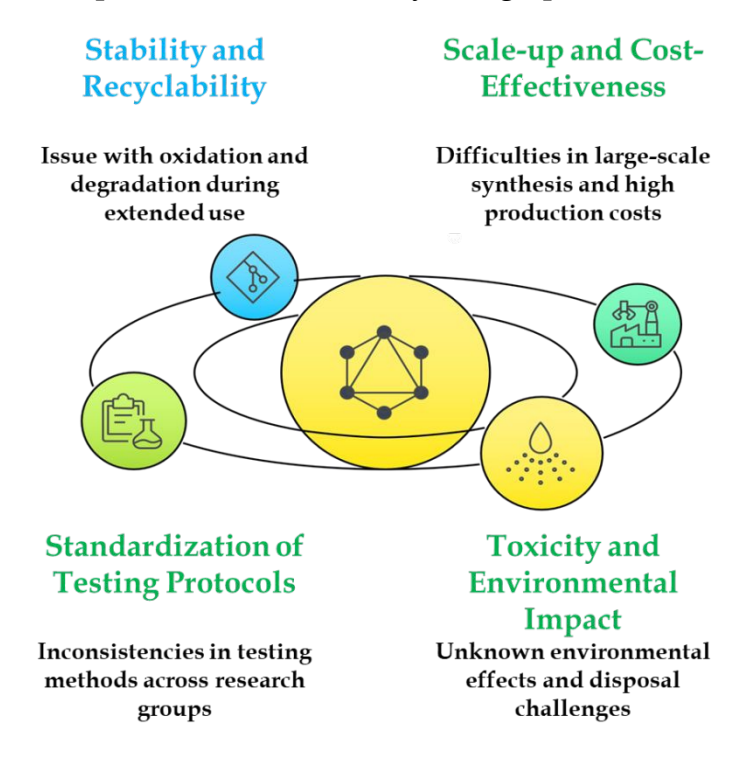


Fig. 26 Overcoming challenges in graphene-based catalysts for CO₂ reduction.

9. Recent Advances and Emerging Trends

9.1 Machine Learning and AI in Photocatalyst Design

Machine learning (ML) algorithms, such as random forests and neural networks, are being trained on databases of photocatalytic performance to predict new material combinations with high efficiency. These tools accelerate discovery cycles and reduce experimental workload by identifying key descriptors for performance.

9.2 Single-Atom Catalysts and Defect Engineering (SACs)

SACs doped into the lattice of graphene or anchored on it provide customized electronic environments and optimized atomic efficiency[288]. Especially for multi-electron reduction pathways, these active sites exhibit high turnover frequencies (TOFs) and selectivity. By improving reactivity and establishing anchoring sites, defect engineering enhances SACs.

9.3 Hybrid Systems: Graphene with MOFs, COFs, and Perovskites

Open Access Article. Published on 13 November 2025. Downloaded on 18/11/2025 9:21:00 PM.

The combination of graphene with MOFs, COFs and perovskites produces on the combination of graphene stability and conductivity with MOFs and COFs and their functionality and porosity and perovskites superior optoelectronic properties. The CO₂ photoreduction process benefits from these combinations because they create multiphase catalytic pathways and synergistic charge separation mechanisms.

9.4 Photocatalysis under Visible and Near-Infrared Light

The spectrum needs to be made more usable for solar applications. Graphene-based composites are being designed to absorb in the visible and near-infrared spectrums by using doping techniques, plasmonic coupling, or up conversion. This increases the solar-to-fuel conversion rates and enables the effective harvesting of low-energy photons.

9.5 Integration with Solar Fuels and Artificial Photosynthesis Systems

The development of artificial photosynthesis approaches nears completion through the integration of graphene-based photocatalysts into the complete system that include photoanodes, cathodes and membrane separators. The integrated platforms enable sustainable carbon-neutral energy cycles through direct fuel production of methane or methanol from CO₂ and water by using sunlight as shown in (**Fig.27**)[289].

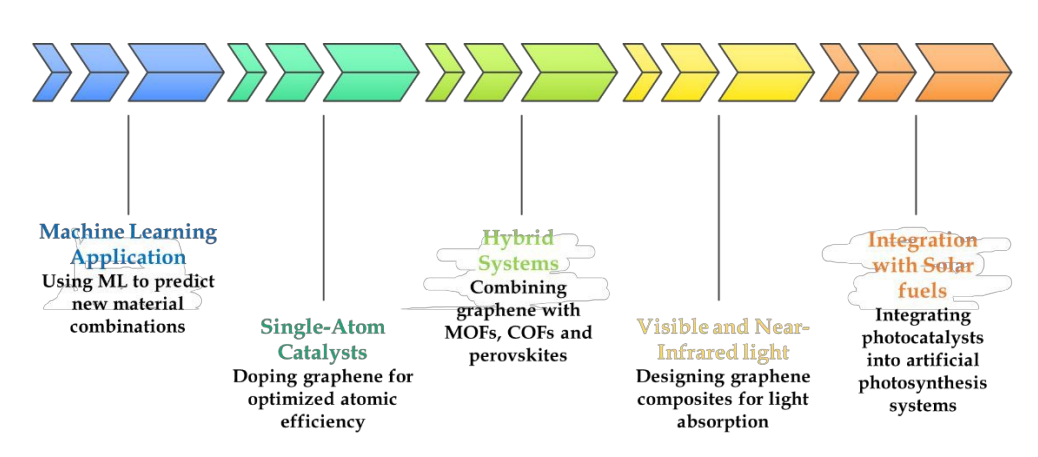


Fig. 27 Advances in photocatalysis in CO₂ reduction

10. Future Perspectives and Roadmap

10.1 Research Gaps and New Directions

The field of nanotechnology faces ongoing challenges regarding charge dynamics at the nanoscale and material stability and multifunctionality. The main research

directions for the future should focus on high-throughput screening and sophistics (Addicte Online in situ characterization tools and machine learning for guided material discovery.

10.2 Toward Commercial-Scale CO₂ Photoreduction

The advancement of technologies beyond the laboratory settings requires pilot-scale studies to demonstrate economic viability, dependability and integration with CO₂ capture units. The validation of real-world performance and technology scaling requires essential collaboration between academic institutions and industrial partners and government officials[290].

10.3 Policy, Funding, and Interdisciplinary Collaborations

The advancement of graphene research depends on the public and private funding initiatives which enable laboratory discoveries to become deployable technologies. Systemic innovation will emerge from interdisciplinary partnerships between materials science and chemical engineering and environmental policy and economics researchers.

10.4 Vision for Graphene-Based Nanomaterials in Climate Solutions

Graphene-based photocatalysts present a viable route for the sustainable use of CO₂. These materials can make a substantial contribution to climate mitigation by utilizing solar energy to transform greenhouse gases into useful fuels and chemicals. To achieve a carbon-neutral future, next-generation graphene hybrids and their integration into integrated energy systems will be essential as shown in (**Fig.28**)[291].

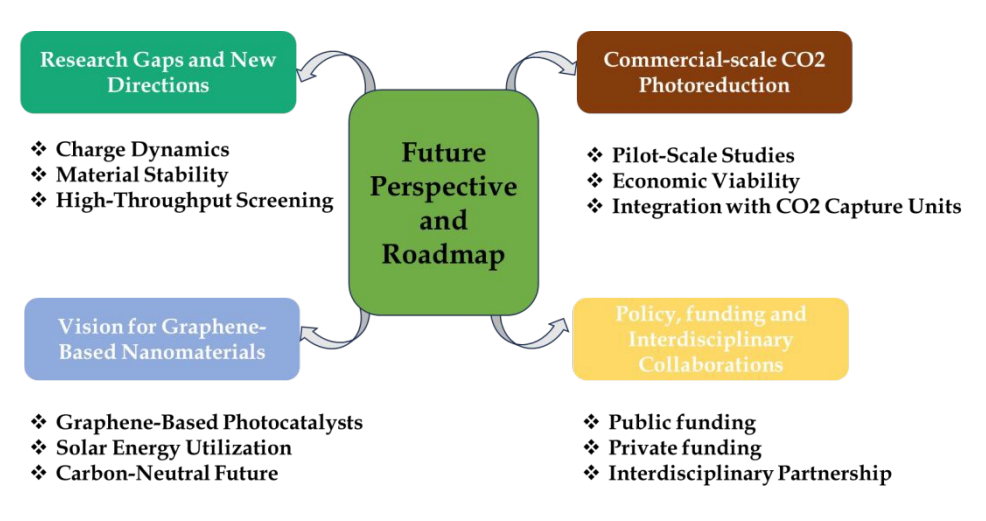


Fig. 28 Future perspective and roadmap of nanotechnology for CO2 reduction

1219

1220

1221

1222

1223

1224

1225

1226

1227

1228

1229

1230

1231

1232

1233

1234

1235

1236

1237

1238

1239

1240

1241

1242

1243

1244

1245

1246

Open Access Article. Published on 13 November 2025. Downloaded on 18/11/2025 9:21:00 PM.

PY-NC

This article is licensed under a Creative Commons Attribution-NonCommercial 3.0 Unported Licence.

View Article Online DOI: 10.1039/D5MA00750J

11. Conclusion

Photocatalytic carbon dioxide (CO₂) reduction provides a viable pathway toward sustainable energy conversion and carbon management; however, challenges with low efficiency, poor selectivity and limited stability will continue to hinder the commercialization of photocatalytic CO₂ systems. Recent advances in the field of graphene-based nanomaterials demonstrate that their remarkable capabilities (high surface area, increasing conductivity, tunable chemistry and electron mediators) can resolve many of these impediments. The incorporation of graphene into semiconductor, metal oxide, metal and carbon nitride systems has provided significant enhancements in light absorption, charge separation and inference stabilization of key intermediates during additional reactions and resultantly increased yields of CO₂ in the form of CO, CH₄, CH₃OH and HCOOH. Further advances including bandgap, Z-scheme, plasmonic enhancements and surface functionalization have illustrated the flexibility of graphene as a co-catalyst to tune the selectivity of CO₂ photoreduction, as well as to serve as a structural platform. However, there are still major challenges to overcome. Stability through long-term operation, scalability of synthesis pathways and the footprint of produced graphene at large scales are important factors that need to be addressed. Furthermore, although several reviews focus on model systems and laboratory conditions, our implementation of systems into commercial solar driven reactors remains limited. As such, the research needed to solve these technical issues will require the integration of several techniques, rational engineering of interfaces, precise control over heteroatom doping and the appropriate hybridization with metals and semiconductors, such that efficiency and selectivity can be achieved at scale. Looking forward, the combination of emerging technologies such as single-atom catalysis, machine learning-assisted catalyst design and green synthesis routes offers new opportunities for tailoring graphene-based systems toward high-performance CO₂ reduction. The synergistic integration of experimental and theoretical insights will be critical to unraveling complex reaction mechanisms and guiding the rational design of next-generation photocatalysts. With continued innovation, graphene-based

1247	nanomaterials hold immense potential to accelerate the realization of efficient atticle online and the contract of the realization of the contract of the realization of the contract of the contract of the realization of the contract of the contract of the realization of the contract of					
1248	scalable and sustainable CO ₂ -to-fuel conversion technologies, bridging the gap					
1249	between laboratory success and practical application.					
1250	Conflicts of interest					
1251	There are no conflicts to declare.					
1252	Notes					
1253	The authors declare no competing financial interests.					
1254	Acknowledgment					
1255	Abhishek, Anas and Trupti thank to Government of Gujarat for financial support					
1256	under SHODH fellowship; (File No. KCG/SHODH/2023-24/202301737,					
1257	KCG/SHODH/2023-24/2022011739 and KCG/SHODH/2023-24/202301735). SKP					
1258	acknowledges Tarsadia Institute of Chemical Science, Uka Tarsadia University, Surat-					
1259	394350, Gujarat, India for providing the infrastructure and instrument facilities.					
1260	Author Contributions					
1261	Abhishek R. Patel: Writing - Original Draft & editing; Anas D. Fazal: Writing -					
1262	Original Draft & editing; Trupti D. Solanky: Writing - Original Draft; Subhendu					
1263	Dhibar: Writing - Original Draft. Sumit Kumar: Writing - Original Draft, Funding					
1264	Acquisition, Resources, Supervision; Sumit Kumar Panja: Writing - Original Draft,					
1265	Funding Acquisition, Resources, Supervision.					
1266	Author ORCID					
1267	ARP : https://orcid.org/0009-0001-5443-6489					
1268	ADF: https://orcid.org/0009-0008-0112-9320					
1269	TDS : https://orcid.org/0009-0005-4965-0519					
1270	SD: https://orcid.org/0000-0002-9683-1540					
1271	SK : https://orcid.org/0000-0002-5695-5944					

1274 References:

1272

1273

1275

Uncategorized References

SKP: https://orcid.org/0000-0001-5658-0452

- 1276 [1] M. Kabir et al., Climate change due to increasing concentration of carbon dio Major Relicio Online
- and its impacts on environment in 21st century; a mini review, Journal of King Saud
- 1278 University-Science 35 (2023) 102693.
- 1279 [2] F.S. Islam, Clean coal technology: the solution to global warming by reducing the
- 1280 emission of carbon dioxide and methane, American Journal of Smart Technology and
- 1281 Solutions 4 (2025) 8.
- 1282 [3] S. Kharchuk, From Closed-Loop Cycles to a Clean Future: Reducing CO₂ Emissions
- by 60-90% through Enhanced Legacy Technologies-So We Do Not Become Petrified
- Relics of Our Own Misjudgments, Available at SSRN 5241304 (2024).
- 1285 [4] R. Naz, M. Tahir, Recent Developments in Metal-free Materials for Photocatalytic
- and Electrocatalytic Carbon Dioxide Conversion into Value Added Products, Energy
- 1287 & Fuels 39 (2025) 6127.
- 1288 [5] L.-L. Wu, L.-Q. Yang, W.-X. Liu, T.-Y. Hang, X.-F. Yang, Research progress on
- photocatalysts for CO2 conversion to liquid products, Rare Metals (2025) 1.
- 1290 [6] M. Gholami, R. Sedghi, Graphene-Based Photocatalysts for Hydrogen Production
- and Environmental Remediation, Springer, 2024, p. 535-562.
- 1292 [7] H. Liu, M. Yu, X. Tong, Q. Wang, M. Chen, High temperature solid oxide
- electrolysis for green hydrogen production, Chemical Reviews 124 (2024) 10509.
- 1294 [8] D.M.H. Pham, New and Traditional Density Functional Theory Methods for
- 1295 Unveiling Mechanisms of Green Chemistry Processes, (2025).
- 1296 [9] F. Zhang, J. Liu, L. Hu, C. Guo, Recent Progress of Three-Dimensional Graphene-
- Based Composites for Photocatalysis, Gels 10 (2024) 626.
- 1298 [10] H. Khan, Graphene based semiconductor oxide photocatalysts for photocatalytic
- 1299 hydrogen (H2) production, a review, International Journal of Hydrogen Energy 84
- 1300 (2024) 356.
- 1301 [11] M.R.A. Foisal, A.B. Imran, Graphene-Based Photocatalysts for Hydrogen
- 1302 Production and Environmental Remediation, Springer, 2024, p. 499-534.
- 1303 [12] J. Low, J. Yu, W. Ho, Graphene-based photocatalysts for CO2 reduction to solar
- fuel, The journal of physical chemistry letters 6 (2015) 4244.
- 1305 [13] Y.-H. Chen, J.-K. Ye, Y.-J. Chang, T.-W. Liu, Y.-H. Chuang, W.-R. Liu, S.-H. Liu,
- 1306 Y.-C. Pu, Mechanisms behind photocatalytic CO2 reduction by CsPbBr3 perovskite-

- graphene-based nanoheterostructures, Applied Catalysis B: Environmental 284 (2021) Allice Online
- 1308 119751.
- 1309 [14] A. Sewnet, M. Abebe, P. Asaithambi, E. Alemayehu, Visible-light-driven g-
- 1310 C3N4/TiO2 based heterojunction nanocomposites for photocatalytic degradation of
- 1311 organic dyes in wastewater: a review, Air, Soil and Water Research 15 (2022)
- 1312 11786221221117266.
- 1313 [15] S.B. Nehru, N. Perumal, Y.P. Subbarayalu, Sustainable water treatment: Synthesis
- and characterization of g-C3N5/NiCo2S4 heterojunction nanocomposite for efficient
- visible light-induced degradation of highly hazardous organic pollutants, Journal of
- 1316 Water Process Engineering 73 (2025) 107712.
- 1317 [16] P. Kyokunzire, G. Jeong, S.Y. Shin, H.J. Cheon, E. Wi, M. Woo, T.T. Vu, M. Chang,
- 1318 Enhanced nitric oxide sensing performance of conjugated polymer films through
- incorporation of graphitic carbon nitride, International Journal of Molecular Sciences
- 1320 24 (2023) 1158.
- 1321 [17] M.A. Ahmed, S.A. Mahmoud, A.A. Mohamed, Unveiling the photocatalytic
- potential of graphitic carbon nitride (gC 3 N 4): a state-of-the-art review, RSC advances
- 1323 14 (2024) 25629.
- 1324 [18] L. Wang, J. Yu, Interface science and technology, Elsevier, 2023, p. 1-52.
- 1325 [19] J. Kim, K. Lee, S. Choi, N. Jo, Y.S. Nam, Catechol Quinone as an Electron-Shuttling
- 1326 Spot Conjugated to Graphitic Carbon Nitride for Enhancing Photocatalytic Reduction,
- 1327 Chemistry of Materials 36 (2024) 5037.
- 1328 [20] M. Aresta, A. Dibenedetto, A. Angelini, Catalysis for the valorization of exhaust
- carbon: from CO2 to chemicals, materials, and fuels. Technological use of CO2,
- 1330 Chemical reviews 114 (2014) 1709.
- 1331 [21] M.Z. Rahman, C.B. Mullins, Understanding charge transport in carbon nitride for
- enhanced photocatalytic solar fuel production, Accounts of chemical research 52
- 1333 (2018) 248.
- 1334 [22] D. Qin et al., Recent advances in two-dimensional nanomaterials for
- photocatalytic reduction of CO 2: insights into performance, theories and perspective,
- 1336 Journal of materials chemistry A 8 (2020) 19156.

- 1337 [23] Y. Guo, S. Zhong, J. Huang, CO 2 Photo/Electro-Conversion Mechanism, Company of Manager 1337 [23] Y. Guo, S. Zhong, J. Huang, CO 2 Photo/Electro-Conversion Mechanism, Company of Manager 1337 [23] Y. Guo, S. Zhong, J. Huang, CO 2 Photo/Electro-Conversion Mechanism, Company of Manager 1337 [23] Y. Guo, S. Zhong, J. Huang, CO 2 Photo/Electro-Conversion Mechanism, Company of Manager 1337 [23] Y. Guo, S. Zhong, J. Huang, CO 2 Photo/Electro-Conversion Mechanism, Company of Manager 1337 [23] Y. Guo, S. Zhong, J. Huang, CO 2 Photo/Electro-Conversion Mechanism, Company of Manager 1337 [23] Y. Guo, S. Zhong, J. Huang, CO 2 Photo/Electro-Conversion Mechanism, Company of Manager 1337 [23] Y. Guo, S. Zhong, Company of Manag
- 1338 Conversion and Utilization: Photocatalytical and Electrochemical Methods and
- 1339 Applications (2023) 17.
- 1340 [24] P. Kalra, C.M. Suresh, N. Rashid, P.P. Ingole, 5
- 1341 PhotoelectrocatalyticCarbonDioxide, Photoelectrochemical Generation of Fuels (2022)
- 1342 149.
- 1343 [25] R. Gandhi, A. Moses, S.S. Baral, Fundamental study of the photocatalytic
- 1344 reduction of CO2: A short review of thermodynamics, kinetics and mechanisms,
- 1345 Chemical and Process Engineering 43 (2022) 223.
- 1346 [26] L. Liu, S. Wang, H. Huang, Y. Zhang, T. Ma, Surface sites engineering on
- semiconductors to boost photocatalytic CO2 reduction, Nano Energy 75 (2020) 104959.
- 1348 [27] B. Petrovic, M. Gorbounov, S.M. Soltani, Influence of surface modification on
- 1349 selective CO2 adsorption: A technical review on mechanisms and methods,
- 1350 Microporous and mesoporous materials 312 (2021) 110751.
- 1351 [28] X. Wang, F. Wang, Y. Sang, H. Liu, Full-spectrum solar-light-activated
- photocatalysts for light-chemical energy conversion, Advanced Energy Materials 7
- 1353 (2017) 1700473.
- 1354 [29] A. Nawaz, A. Kuila, N.S. Mishra, K.H. Leong, L.C. Sim, P. Saravanan, M. Jang,
- 1355 Challenges and implication of full solar spectrum-driven photocatalyst, Reviews in
- 1356 Chemical Engineering 37 (2021) 533.
- 1357 [30] S. Peiris, H.B. de Silva, K.N. Ranasinghe, S.V. Bandara, I.R. Perera, Recent
- development and future prospects of TiO2 photocatalysis, Journal of the Chinese
- 1359 Chemical Society 68 (2021) 738.
- 1360 [31] C. Hiragond, N. Powar, J. Lee, S.I. In, Single-Atom Catalysts (SACs) for
- 1361 Photocatalytic CO2 Reduction with H2O: Activity, Product Selectivity, Stability, and
- 1362 Surface Chemistry, Small 18 (2022). https://doi.org/10.1002/smll.202201428
- 1363 [32] G.Z.S. Ling, S.F. Ng, W.J. Ong, Tailor-engineered 2D cocatalysts: harnessing
- electron-hole redox center of 2D g-C3N4 photocatalysts toward solar-to-chemical
- conversion and environmental purification, Advanced Functional Materials 32 (2022)
- 1366 2111875.

- 1367 [33] K. Huang, C. Li, H. Li, G. Ren, L. Wang, W. Wang, X. Meng, Photocatal of Manager and Manager
- applications of two-dimensional Ti3C2 MXenes: a review, ACS Applied Nano
- 1369 Materials 3 (2020) 9581.
- 1370 [34] J. Ma, T.J. Miao, J. Tang, Charge carrier dynamics and reaction intermediates in
- 1371 heterogeneous photocatalysis by time-resolved spectroscopies, Chemical Society
- 1372 Reviews 51 (2022) 5777.
- 1373 [35] S. Bhattacharyya, Carbon Superstructures: From Quantum Transport to Quantum
- 1374 Computation. CRC Press, 2024.
- 1375 [36] G.R. Bhimanapati et al., Recent advances in two-dimensional materials beyond
- 1376 graphene, ACS nano 9 (2015) 11509.
- 1377 [37] T. Enoki, Y. Kobayashi, K.-I. Fukui, Electronic structures of graphene edges and
- nanographene, International Reviews in Physical Chemistry 26 (2007) 609.
- 1379 [38] Z. Zhen, H. Zhu, Graphene, Elsevier, 2018, p. 1-12.
- 1380 [39] R. Geetha Bai, K. Muthoosamy, S. Manickam, A. Hilal-Alnaqbi, Graphene-based
- 3D scaffolds in tissue engineering: fabrication, applications, and future scope in liver
- 1382 tissue engineering, International Journal of Nanomedicine 14 (2019).
- 1383 https://doi.org/10.2147/IJN.S192779
- 1384 [40] A. Kaplan, Z. Yuan, J.D. Benck, A.G. Rajan, X.S. Chu, Q.H. Wang, M.S. Strano,
- 1385 Current and future directions in electron transfer chemistry of graphene, Chemical
- 1386 Society Reviews 46 (2017) 4530.
- 1387 [41] N. Zhang, M.-Q. Yang, S. Liu, Y. Sun, Y.-J. Xu, Waltzing with the versatile
- platform of graphene to synthesize composite photocatalysts, Chemical reviews 115
- 1389 (2015) 10307.
- 1390 [42] H. Grajek, J. Jonik, Z. Witkiewicz, T. Wawer, M. Purchała, Applications of
- 1391 graphene and its derivatives in chemical analysis, Critical Reviews in Analytical
- 1392 Chemistry 50 (2020) 445.
- 1393 [43] C. Li, C. Zheng, F. Cao, Y. Zhang, X. Xia, The development trend of graphene
- derivatives, Journal of Electronic Materials 51 (2022) 4107.
- 1395 [44] J. Narayan, K. Bezborah, Recent advances in the functionalization, substitutional
- doping and applications of graphene/graphene composite nanomaterials, RSC
- 1397 advances 14 (2024) 13413.

- 1398 [45] R. Ghosh, M. Aslam, H. Kalita, Graphene derivatives for chemiresistive online Chemires and Chemires of Chemires and Chemires
- sensors: A review, Materials Today Communications 30 (2022) 103182.
- 1400 [46] R. Singh et al., Synthesis of Three-Dimensional Reduced-Graphene Oxide from
- 1401 Graphene Oxide, Journal of Nanomaterials 2022 (2022) 8731429.
- 1402 [47] A. Ahmed, A. Singh, S.-J. Young, V. Gupta, M. Singh, S. Arya, Synthesis
- techniques and advances in sensing applications of reduced graphene oxide (rGO)
- 1404 Composites: A review, Composites Part A: Applied Science and Manufacturing 165
- 1405 (2023) 107373.
- 1406 [48] A. Mondal, A. Prabhakaran, S. Gupta, V.R. Subramanian, Boosting photocatalytic
- 1407 activity using reduced graphene oxide (RGO)/semiconductor nanocomposites: issues
- 1408 and future scope, ACS omega 6 (2021) 8734.
- 1409 [49] P. Jadhav, G.M. Joshi, Recent trends in Nitrogen doped polymer composites: a
- 1410 review, Journal of Polymer Research 28 (2021) 73. https://doi.org/10.1007/s10965-
- 1411 021-02436-x
- 1412 [50] N. Sohal, B. Maity, S. Basu, Recent advances in heteroatom-doped graphene
- 1413 quantum dots for sensing applications, RSC advances 11 (2021) 25586.
- 1414 [51] M.B. Arvas, H. Gürsu, M. Gencten, Y. Sahin, Preparation of different heteroatom
- 1415 doped graphene oxide based electrodes by electrochemical method and their
- supercapacitor applications, Journal of Energy Storage 35 (2021) 102328.
- 1417 [52] S.J. Lee *et al.*, Heteroatom-doped graphene-based materials for sustainable energy
- 1418 applications: A review, Renewable and Sustainable Energy Reviews 143 (2021) 110849.
- 1419 [53] F. Zhang, E. Alhajji, Y. Lei, N. Kurra, H.N. Alshareef, Highly doped 3D graphene
- Na-ion battery anode by laser scribing polyimide films in nitrogen ambient, Advanced
- 1421 Energy Materials 8 (2018) 1800353.
- 1422 [54] E. Umar, M. Ikram, J. Haider, W. Nabgan, M. Imran, G. Nazir, 3D graphene-based
- 1423 material: Overview, perspective, advancement, energy storage, biomedical
- 1424 engineering and environmental applications a bibliometric analysis, Journal of
- 1425 Environmental Chemical Engineering 11 (2023) 110339.
- 1426 https://doi.org/https://doi.org/10.1016/j.jece.2023.110339

- 1427 [55] F.M. Vivaldi et al., Three-dimensional (3D) laser-induced graphene: struction Annual (3D) laser-induced graphene
- 1428 properties, and application to chemical sensing, ACS Applied Materials & Interfaces
- 1429 13 (2021) 30245.
- 1430 [56] W. Xiao, B. Li, J. Yan, L. Wang, X. Huang, J. Gao, Three dimensional graphene
- 1431 composites: preparation, morphology and their multi-functional applications,
- 1432 Composites Part A: Applied Science and Manufacturing 165 (2023) 107335.
- 1433 [57] A.M. Díez-Pascual, MDPI, 2021, p. 7726.
- 1434 [58] A. Hussain, Y. Weng, Y. Huang, Graphene and graphene-based nanomaterials:
- 1435 current applications and future perspectives, Drug Delivery Using Nanomaterials
- 1436 (2022) 209.
- 1437 [59] A. Gutiérrez-Cruz, A.R. Ruiz-Hernández, J.F. Vega-Clemente, D.G. Luna-Gazcón,
- J. Campos-Delgado, A review of top-down and bottom-up synthesis methods for the
- 1439 production of graphene, graphene oxide and reduced graphene oxide, Journal of
- 1440 Materials Science 57 (2022) 14543. https://doi.org/10.1007/s10853-022-07514-z
- 1441 [60] E. Boateng, A.R. Thiruppathi, C.-K. Hung, D. Chow, D. Sridhar, A. Chen,
- 1442 Functionalization of graphene-based nanomaterials for energy and hydrogen storage,
- 1443 Electrochimica Acta 452 (2023) 142340.
- 1444 [61] D.S. Rakshe, P. William, M. Jawale, A. Pawar, S.K. Korde, N. Deshpande,
- 1445 Synthesis and characterization of graphene based nanomaterials for energy
- 1446 applications, (2023).
- 1447 [62] J.M. Tour, Top-down versus bottom-up fabrication of graphene-based electronics,
- 1448 Chemistry of Materials 26 (2014) 163.
- 1449 [63] A.L. Olatomiwa, T. Adam, S.C. Gopinath, S.Y. Kolawole, O.H. Olayinka, U.
- 1450 Hashim, Graphene synthesis, fabrication, characterization based on bottom-up and
- top-down approaches: An overview, Journal of Semiconductors 43 (2022) 061101.
- 1452 [64] R. Boddula, N. Borane, N. Odedara, J. Singh, Graphene-Based Nanomaterials,
- 1453 CRC Press, 2024, p. 33-46.
- 1454 [65] H. Jiang, Chemical preparation of graphene-based nanomaterials and their
- applications in chemical and biological sensors, Small 7 (2011) 2413.
- 1456 [66] N. Borane, S. Aralekallu, R. Boddula, J. Singh, M.D. Kurkuri, Carbon-Based
- Nanomaterials in Biosystems, Elsevier, 2024, p. 91-120.

- 1458 [67] B.C. Brodie, XIII. On the atomic weight of graphite, Philosophical transaction and Colored Philosophical transaction of the Adolphical Science (Adolphical Science and Colored Philosophical Science and Colored Philosophical Science and Colored Philosophical Science (Adolphical Science and Colored Philosophical Science and Colored Philosophical Science (Adolphical Science and Colored Philosophical Science and Colored Philosophical Science (Adolphical Science and Colored Philosophical Science and Colored Philosophical Science (Adolphical Science and Colored Philosophical Science and Colored Philosophical Science (Adolphical Science and Colored Philosophical Science and Colored Philosophical Science (Adolphical Science and Colored Philosophical Science and Colored Philosophical Science (Adolphical Science and Colored Philosophical Science and Colored Philosophical Science (Adolphical Science and Colored Philosophical Science and Colored Philosophical Science (Adolphical Science and Colored Philosophical Science and Colored Philosophical Science (Adolphical Science and Colored Philosophical Science and Colored Philosophical Science (Adolphical Science and Colored Philosophical Science and Colored Philosophical Science (Adolphical Science and Colored Philosophical Science and Colored Philosophical Science (Adolphical Science and Colored Philosophical Science and Colored Philosophical Science (Adolphical Science and Colored Philosophical Science and Colored Philosophical Science (Adolphical Science and Colored Philosophical Science and Colored Philosophical Science (Adolphical Science and Colored Philosophical Science and Colored Philosophical Science (Adolphical Science and Colored Philosophical Science and Colored Philosophical Science (Adolphical Science and Colored Philosophical Science and Colored Philosophical Science (Adolphical Science and Colored Philosophical Science and Colored Philosophical Science (Adolphical Science and Colored Philosophical Science and Colored Philosophical Science (Adolphical
- the Royal Society of London (1859) 249.
- 1460 [68] D.C. Marcano et al., Improved synthesis of graphene oxide, ACS nano 4 (2010)
- 1461 4806.
- 1462 [69] H.L. Poh, F. Šaněk, A. Ambrosi, G. Zhao, Z. Sofer, M. Pumera, Graphenes
- 1463 prepared by Staudenmaier, Hofmann and Hummers methods with consequent
- thermal exfoliation exhibit very different electrochemical properties, Nanoscale 4
- 1465 (2012) 3515.
- 1466 [70] L. Shahriary, A.A. Athawale, Graphene oxide synthesized by using modified
- hummers approach, Int. j. renew. energy environ. eng 2 (2014) 58.
- 1468 [71] T. Dzhabiev, N. Denisov, D. Moiseev, A. Shilov, Formation of ozone during the
- 1469 reduction of potassium permanganate in sulfuric acid solutions, Russian Journal of
- 1470 Physical Chemistry A 79 (2005) 1755.
- 1471 [72] W. Gao et al., Ozonated graphene oxide film as a proton-exchange membrane,
- 1472 Angewandte Chemie International Edition 53 (2014) 3588.
- 1473 [73] M. Muradov, E. Huseynov, M. Conradi, M. Malok, T. Sever, M.B. Baghirov,
- 1474 Effects of gamma radiation on the properties of GO/PVA/AgNW nanocomposites,
- 1475 RSC Advances 15 (2025) 13574. https://doi.org/10.1039/D5RA01344E
- 1476 [74] S.K. Sharma, S. Sharma, Synthesis of Graphene Oxide and Impact of Its
- 1477 Functionalization in the Wastewater Treatment, Chemical Engineering & Technology
- 1478 48 (2025) e70009. https://doi.org/https://doi.org/10.1002/ceat.70009
- 1479 [75] C. Han, M.-Q. Yang, N. Zhang, Y.-J. Xu, Enhancing the visible light photocatalytic
- 1480 performance of ternary CdS-(graphene-Pd) nanocomposites via a facile interfacial
- mediator and co-catalyst strategy, Journal of Materials Chemistry A 2 (2014) 19156.
- 1482 [76] Y. Li, Z. Zhang, L. Pei, X. Li, T. Fan, J. Ji, J. Shen, M. Ye, Multifunctional
- 1483 photocatalytic performances of recyclable Pd-NiFe2O4/reduced graphene oxide
- nanocomposites via different co-catalyst strategy, Applied Catalysis B: Environmental
- 1485 190 (2016) 1.
- 1486 [77] D. Maarisetty, S.S. Baral, Synergistic effect of dual electron-cocatalyst modified
- 1487 photocatalyst and methodical strategy for better charge separation, Applied Surface
- 1488 Science 489 (2019) 930.

- 1489 [78] R. Akhter, S. Hussain, S.S. Maktedar, Advanced graphene-based (photo & lelection of the photo of the continuous properties of the continuous properties
- catalysts for sustainable & clean energy technologies, New Journal of Chemistry 48
- 1491 (2024) 437.
- 1492 [79] L. Ye, J. Fu, Z. Xu, R. Yuan, Z. Li, Facile one-pot solvothermal method to
- 1493 synthesize sheet-on-sheet reduced graphene oxide (RGO)/ZnIn2S4 nanocomposites
- with superior photocatalytic performance, ACS applied materials & interfaces 6 (2014)
- 1495 3483.
- 1496 [80] N. Meng, Y. Zhou, W. Nie, P. Chen, Synthesis of CdS-decorated RGO
- 1497 nanocomposites by reflux condensation method and its improved photocatalytic
- 1498 activity, Journal of Nanoparticle Research 18 (2016) 1.
- 1499 https://doi.org/10.1007/s11051-016-3522-y
- 1500 [81] J. Prakash, Mechanistic insights into graphene oxide driven photocatalysis as Co-
- catalyst and sole catalyst in degradation of organic dye pollutants, Photochem 2 (2022)
- 1502 651.
- 1503 [82] F. Khan, M.S. Khan, S. Kamal, M. Arshad, S.I. Ahmad, S.A. Nami, Recent
- advances in graphene oxide and reduced graphene oxide based nanocomposites for
- the photodegradation of dyes, Journal of Materials Chemistry C 8 (2020) 15940.
- 1506 [83] A. Mondal, A. Vomiero, 2D transition metal dichalcogenides-based
- electrocatalysts for hydrogen evolution reaction, Advanced Functional Materials 32
- 1508 (2022) 2208994.
- 1509 [84] N.H. Shudin, M. Aziz, M.H.D. Othman, M. Tanemura, M.Z.M. Yusop, The role of
- 1510 solid, liquid and gaseous hydrocarbon precursors on chemical vapor deposition
- 1511 grown carbon nanomaterials' growth temperature, Synthetic Metals 274 (2021) 116735.
- 1512 [85] P. Chavalekvirat, W. Hirunpinyopas, K. Deshsorn, K. Jitapunkul, P.
- 1513 Iamprasertkun, Liquid phase exfoliation of 2D materials and its electrochemical
- applications in the data-driven future, Precision Chemistry 2 (2024) 300.
- 1515 [86] T. HUANG, F. Bing, L. Peipei, Z. ZHANG, N. Qi, M. Zonghu, L. Kai, L. Qiang,
- 1516 Hydrothermal N-doping assisted synthesis of poplar sawdust-derived porous
- carbons for carbon capture, Journal of Fuel Chemistry and Technology 53 (2025) 1191.
- 1518 [87] N. Zhang, Y. Zhang, Y.-J. Xu, Recent progress on graphene-based photocatalysts:
- current status and future perspectives, Nanoscale 4 (2012) 5792.

- 1520 [88] X. An, C.Y. Jimmy, Graphene-based photocatalytic composites, Rsc Advances Madon Solution (188) And C.Y. Jimmy, Graphene-based photocatalytic composites, Rsc Advances Madon Solution (188) And C.Y. Jimmy, Graphene-based photocatalytic composites, Rsc Advances Madon Solution (188) And C.Y. Jimmy, Graphene-based photocatalytic composites, Rsc Advances Madon Solution (188) And C.Y. Jimmy, Graphene-based photocatalytic composites, Rsc Advances Madon Solution (188) And C.Y. Jimmy, Graphene-based photocatalytic composites, Rsc Advances Madon Solution (188) And C.Y. Jimmy, Graphene-based photocatalytic composites, Rsc Advances Madon Solution (188) And C.Y. Jimmy, Graphene-based photocatalytic composites, Rsc Advances Madon Solution (188) And C.Y. Jimmy, Graphene-based photocatalytic composites, Rsc Advances Madon Solution (188) And C.Y. Jimmy, Graphene-based photocatalytic composites (188) And C.Y. Jimmy, Graphene (188) And C.Y. Ji
- 1521 (2011) 1426.
- 1522 [89] F. Saeedi, R. Ansari, M. Haghgoo, Recent Advances of Graphene-Based Wearable
- 1523 Sensors: Synthesis, Fabrication, Performance, and Application in Smart Device,
- 1524 Advanced Materials Interfaces (2025) 2500093.
- 1525 [90] B.C. Yallur et al., Recent Advances in Graphene-Based Metal Oxide Composites
- 1526 for Supercapacitors: A Comprehensive Review, Advanced Sustainable Systems
- 1527 2500121.
- 1528 [91] H.S. Biswas, A.K. Kundu, S.S. Biswas, Recent Advancement of Graphene-TiO2
- 1529 Composite Nanomaterials and Their Applications in Energy Storage and Conversion:
- Novel Functions and Future Prospects Explored, Innovations in Next-Generation
- 1531 Energy Storage Solutions (2025) 425.
- 1532 [92] Y. Zhang, H. Wang, J. Zhang, Application of Graphene-Based Solar Driven
- 1533 Interfacial Evaporation-Coupled Photocatalysis in Water Treatment, Catalysts 15
- 1534 (2025) 336.
- 1535 [93] T. Shahzad, S. Nawaz, H. Jamal, T. Shahzad, F. Akhtar, U. Kamran, A Review on
- 1536 Cutting-Edge Three-Dimensional Graphene-Based Composite Materials: Redefining
- 1537 Wastewater Remediation for a Cleaner and Sustainable World, Journal of Composites
- 1538 Science 9 (2025) 18.
- 1539 [94] A. Badoni et al., Recent progress in understanding the role of graphene oxide,
- 1540 TiO2 and graphene oxide-TiO2 nanocomposites as multidisciplinary photocatalysts
- in energy and environmental applications, Catalysis Science & Technology (2025).
- 1542 [95] Y. Wu, C. Wang, L. Wang, C. Hou, Recent Advances in Iron Oxide-Based
- 1543 Heterojunction Photo-Fenton Catalysts for the Elimination of Organic Pollutants,
- 1544 Catalysts 15 (2025) 391.
- 1545 [96] A.K. Potbhare et al., Bioinspired graphene-based metal oxide nanocomposites for
- 1546 photocatalytic and electrochemical performances: an updated review, Nanoscale
- 1547 Advances 6 (2024) 2539.
- 1548 [97] T. Xu, J. Wang, X. Yu, Y. Niu, H. Li, Y. Wu, M. Li, J. Rong, A new generation of
- 1549 functional desalted carbon and nitrogen membrane with photocatalytic and
- adsorption properties, Computational Materials Science 258 (2025) 114014.

- 1551 [98] A. Khalajiolyaie, C. Jian, Advances in Graphene-Based Materials for Metal Managed Materials for Metal Me
- 1552 Sensing and Wastewater Treatment: A Review, Environments 12 (2025) 43.
- 1553 [99] W. Gao, H. Chi, Y. Xiong, J. Ye, Z. Zou, Y. Zhou, Comprehensive insight into
- 1554 construction of active sites toward steering photocatalytic CO2 conversion, Advanced
- 1555 Functional Materials 34 (2024) 2312056.
- 1556 [100] S. Wang, M. Xu, T. Peng, C. Zhang, T. Li, I. Hussain, J. Wang, B. Tan, Porous
- 1557 hypercrosslinked polymer-TiO2-graphene composite photocatalysts for visible-light-
- driven CO2 conversion, Nature communications 10 (2019) 676.
- 1559 [101] F.-X. Liang, Y. Gao, C. Xie, X.-W. Tong, Z.-J. Li, L.-B. Luo, Recent advances in the
- 1560 fabrication of graphene-ZnO heterojunctions for optoelectronic device applications,
- 1561 Journal of Materials Chemistry C 6 (2018) 3815.
- 1562 [102] S. Chandrasekaran, J.S. Chung, E.J. Kim, S.H. Hur, Exploring complex structural
- evolution of graphene oxide/ZnO triangles and its impact on photoelectrochemical
- water splitting, Chemical Engineering Journal 290 (2016) 465.
- 1565 [103] X. Li, J. Yu, M. Jaroniec, X. Chen, Cocatalysts for selective photoreduction of CO2
- into solar fuels, Chemical reviews 119 (2019) 3962.
- 1567 [104] P.M. Gawal, J. Ishrat, K. Bhattacharyya, A.K. Golder, Experimental and
- 1568 Theoretical Studies on Photocatalytic CO2 Reduction to HCOOH by Biomass-Derived
- 1569 Carbon Dots Embedded Phytochemical-Based CdS Quantum Dots, Langmuir (2025).
- 1570 [105] H.V. Babu, M.M. Bai, M. Rajeswara Rao, Functional π-conjugated two-
- 1571 dimensional covalent organic frameworks, ACS applied materials & interfaces 11
- 1572 (2019) 11029.
- 1573 [106] L. Jing, P. Li, Z. Li, D. Ma, J. Hu, Influence of π-π interactions on organic
- photocatalytic materials and their performance, Chemical Society Reviews (2025).
- 1575 [107] Y. Li, L. Wang, X. Gao, Y. Xue, B. Li, X. Zhu, Construction of a graphitic carbon
- 1576 nitride-based photocatalyst with a strong built-in electric field via π-π stacking
- interactions boosting photocatalytic CO 2 reduction, Journal of Materials Chemistry
- 1578 A 12 (2024) 7807.
- 1579 [108] K. Jayaramulu et al., Graphene-based metal-organic framework hybrids for
- applications in catalysis, environmental, and energy technologies, Chemical reviews
- 1581 122 (2022) 17241.

- 1582 [109] J. Yang, Z. Chen, L. Zhang, Q. Zhang, Covalent organic frameworks Viet Acticle Online
- photocatalytic reduction of carbon dioxide: A review, ACS nano 18 (2024) 21804.
- 1584 [110] I. Ahmad *et al.*, Recent progress in ZnO-based heterostructured photocatalysts:
- 1585 A review, Materials Science in Semiconductor Processing 180 (2024) 108578.
- 1586 https://doi.org/https://doi.org/10.1016/j.mssp.2024.108578
- 1587 [111] I. Ahmad, S. Shukrullah, M.Y. Naz, H.N. Bhatti, Dual S-scheme ZnO-g-C3N4-
- 1588 CuO heterosystem: a potential photocatalyst for H2 evolution and wastewater
- 1589 treatment, Reaction Chemistry & Engineering 8 (2023) 1159.
- 1590 https://doi.org/10.1039/D2RE00576J
- 1591 [112] I. Ahmad, S. Shukrullah, M.Y. Naz, H.N. Bhatti, A Cu medium designed Z-
- scheme ZnO-Cu-CdS heterojunction photocatalyst for stable and excellent H2
- evolution, methylene blue degradation, and CO2 reduction, Dalton Transactions 52
- 1594 (2023) 6343. https://doi.org/10.1039/D3DT00684K
- 1595 [113] I. Ahmad, S.A. AlFaify, K.M. Alanezi, M.Q. Alfaifi, M.M. Abduljawad, Y. Liu,
- 1596 Improved hydrogen production performance of an S-scheme Nb2O5/La2O3
- 1597 photocatalyst, Dalton Transactions 54 (2025) 1402.
- 1598 https://doi.org/10.1039/D4DT02913E
- 1599 [114] I. Ahmad et al., Boosted hydrogen evolution activity from Sr doped ZnO/CNTs
- 1600 nanocomposite as visible light driven photocatalyst, International Journal of
- 1601 Hydrogen Energy 46 (2021) 26711.
- 1602 https://doi.org/https://doi.org/10.1016/j.ijhydene.2021.05.164
- 1603 [115] I. Ahmad, M.Q. Alfaifi, S. Ben Ahmed, M.M. Abduljawad, Y.A. Alassmy, S.A.
- 1604 Alshuhri, T.L. Tamang, Strategies for optimizing sunlight conversion in
- semiconductor photocatalysts: A review of experimental and theoretical insights,
- 1606 International Journal of Hydrogen Energy 96 (2024) 1006.
- 1607 https://doi.org/https://doi.org/10.1016/j.ijhydene.2024.11.388
- 1608 [116] M.T. Vu, D. Thatikayala, B. Min, Porous reduced-graphene oxide supported
- 1609 hollow titania (rGO/TiO2) as an effective catalyst for upgrading
- electromethanogenesis, International Journal of Hydrogen Energy 47 (2022) 1121.
- 1611 [117] J. Wu, M. Gong, ZnO/graphene heterostructure nanohybrids for optoelectronics
- and sensors, Journal of Applied Physics 130 (2021).

- 1613 [118] Z. Tan, R. Wang, S. Yang, Z. Shi, D. Wang, Fabrication of Cu-Cu2QN dependence on the control of Cu-Cu2QN dependence on the cu-c
- 1614 carbon with high photo-Fenton catalytic activity using a Cu-nicotinic acid framework:
- 1615 Insight into structural transformation, Journal of Molecular Structure 1337 (2025)
- 1616 142248.
- 1617 [119] R. CHATURVEDI, R. PANDEY, S. SINGHANIA, A. GARG, Synergic Energy
- 1618 Storage Performance of MoS2/g-C3N4 composite on Screen-printed Carbon
- 1619 Electrode, Electrochimica Acta (2025) 147090.
- 1620 [120] G. Bharath et al., Synthesis of TiO2/RGO with plasmonic Ag nanoparticles for
- 1621 highly efficient photoelectrocatalytic reduction of CO2 to methanol toward the
- removal of an organic pollutant from the atmosphere, Environmental Pollution 281
- 1623 (2021) 116990.
- 1624 [121] J. Wekalao, High-sensitivity graphene-MoS₂ hybrid metasurface biosensor with
- machine learning optimization for hemoglobin detection, Plasmonics (2025) 1.
- 1626 [122] D. Kanakaraju, D.N. Joseph, P.P. Natashya, A. Pace, Pioneering TiO2/G-C3N4
- 1627 Heterostructures for Enhanced Organic Pollutant Removal, ChemistrySelect 10 (2025)
- 1628 e202405101.
- 1629 [123] S.K. Behura, C. Wang, Y. Wen, V. Berry, Graphene-semiconductor
- heterojunction sheds light on emerging photovoltaics, Nature Photonics 13 (2019) 312.
- 1631 [124] A. Di Bartolomeo, Graphene Schottky diodes: An experimental review of the
- rectifying graphene/semiconductor heterojunction, Physics Reports 606 (2016) 1.
- 1633 [125] Z. Zhu, I. Murtaza, H. Meng, W. Huang, Thin film transistors based on two
- dimensional graphene and graphene/semiconductor heterojunctions, RSC advances
- 1635 7 (2017) 17387.
- 1636 [126] S. Behura, C. Wang, Y. Wen, V. Berry, Graphene–Semiconductor Heterojunction
- 1637 Sheds Light on Emerging Photovoltaics, Nature Photonics 13 (2019).
- 1638 https://doi.org/10.1038/s41566-019-0391-9
- 1639 [127] Y.-J. Kim, J.-H. Lee, G.-C. Yi, Vertically aligned ZnO nanostructures grown on
- 1640 graphene layers, Applied Physics Letters 95 (2009) 213101.
- 1641 https://doi.org/10.1063/1.3266836
- 1642 [128] D. Maeso, A. Castellanos-Gomez, N. Agraït, G. Rubio-Bollinger, Fast Yet
- 1643 Quantum-Efficient Few-Layer Vertical MoS2 Photodetectors, Advanced Electronic

- 1644 Materials 5 (2019) 1900/FM Article Online
- 1645 https://doi.org/https://doi.org/10.1002/aelm.201900141
- 1646 [129] X. Ge, W. Qin, H. Zhang, G. Wang, Y. Zhang, C. Yu, A three-dimensional porous
- 1647 Co@C/carbon foam hybrid monolith for exceptional oil-water separation, Nanoscale
- 1648 11 (2019) 12161. https://doi.org/10.1039/C9NR02819F
- 1649 [130] X. Xu, X. Zhang, C. Hu, Y. Zheng, B. Lei, Y. Liu, J. Zhuang, Construction of
- 1650 NaYF4:Yb,Er(Tm)@CDs composites for enhancing red and NIR upconversion
- 1651 emission, Journal of Materials Chemistry C 7 (2019) 6231.
- 1652 https://doi.org/10.1039/C9TC01346F
- 1653 [131] A. Singh, S. Chahal, H. Dahiya, A. Goswami, S. Nain, Synthesis of Ag
- nanoparticle supported graphene/multi-walled carbon nanotube based nanohybrids
- for photodegradation of toxic dyes, Materials Express 11 (2021) 936.
- 1656 [132] A. Singh, S. Chahal, H. Dahiya, A. Goswami, S. Nain, Materials Express,
- 1657 Synthesis 4 (2021) 4.
- 1658 [133] Q. Ding, B. Song, P. Xu, S. Jin, Efficient electrocatalytic and photoelectrochemical
- hydrogen generation using MoS2 and related compounds, Chem 1 (2016) 699.
- 1660 [134] D. Vikraman, K. Akbar, S. Hussain, G. Yoo, J.-Y. Jang, S.-H. Chun, J. Jung, H.J.
- Park, Direct synthesis of thickness-tunable MoS2 quantum dot thin layers: Optical,
- structural and electrical properties and their application to hydrogen evolution, Nano
- 1663 Energy 35 (2017) 101.
- 1664 [135] S. Chen, Y. Pan, Enhancing catalytic properties of noble metal@ MoS2/WS2
- 1665 heterojunction for the hydrogen evolution reaction, Applied Surface Science 591
- 1666 (2022) 153168.
- 1667 [136] D. Zheng, G. Zhang, Y. Hou, X. Wang, Layering MoS2 on soft hollow g-C3N4
- 1668 nanostructures for photocatalytic hydrogen evolution, Applied Catalysis A: General
- 1669 521 (2016) 2.
- 1670 [137] Z. Wang, J. Huang, J. Mao, Q. Guo, Z. Chen, Y. Lai, Metal-organic frameworks
- and their derivatives with graphene composites: preparation and applications in
- electrocatalysis and photocatalysis, Journal of Materials Chemistry A 8 (2020) 2934.
- 1673 [138] E.F. Joel, G. Lujanienė, Progress in graphene oxide hybrids for environmental
- applications, Environments 9 (2022) 153.

- 1675 [139] Y.-J. Park, H. Lee, H.L. Choi, M.C. Tapia, C.Y. Chuah, T.-H. Bae, Mixing Managara
- dimensional nanocomposites based on 2D materials for hydrogen storage and CO2
- capture, npj 2D Materials and Applications 7 (2023) 61.
- 1678 [140] T. Zhou et al., Polyethyleneimine-induced in-situ chemical epitaxial growth
- 1679 ultrathin 2D/2D graphene carbon nitride intralayer heterojunction with elevating
- photocatalytic activity: Performances and mechanism insight, International Journal of
- 1681 Hydrogen Energy 51 (2024) 884.
- 1682 [141] T.A. Shifa, F. Wang, Y. Liu, J. He, Heterostructures Based on 2D Materials: A
- Versatile Platform for Efficient Catalysis, Advanced Materials 31 (2018) 1804828.
- 1684 https://doi.org/10.1002/adma.201804828
- 1685 [142] H. Boumeriame et al., Graphitic carbon nitride/few-layer graphene
- 1686 heterostructures for enhanced visible-LED photocatalytic hydrogen generation,
- 1687 International Journal of Hydrogen Energy 47 (2022) 25555.
- 1688 [143] H. Li, B. Zhu, B. Cheng, G. Luo, J. Xu, S. Cao, Single-atom Cu anchored on N-
- doped graphene/carbon nitride heterojunction for enhanced photocatalytic H2O2
- production, Journal of Materials Science & Technology 161 (2023) 192.
- 1691 [144] M. Chen, M. Li, S.L.J. Lee, X. Zhao, S. Lin, Constructing novel graphitic carbon
- 1692 nitride-based nanocomposites-from the perspective of material dimensions and
- interfacial characteristics, Chemosphere 302 (2022) 134889.
- 1694 [145] D. Adekoya, S. Zhang, M. Hankel, 1D/2D C3N4/graphene composite as a
- preferred anode material for lithium ion batteries: importance of heterostructure
- design via DFT computation, ACS applied materials & interfaces 12 (2020) 25875.
- 1697 [146] K. Sridharan, S. Shenoy, S.G. Kumar, C. Terashima, A. Fujishima, S.
- 1698 Pitchaimuthu, Advanced two-dimensional heterojunction photocatalysts of
- 1699 stoichiometric and non-stoichiometric bismuth oxyhalides with graphitic carbon
- 1700 nitride for sustainable energy and environmental applications, Catalysts 11 (2021) 426.
- 1701 [147] X. Li et al., 2D-1D-2D multi-interfacial-electron transfer scheme enhanced g-
- 1702 C3N4/MWNTs/rGO hybrid composite for accelerating CO2 photoreduction, Journal
- 1703 of Alloys and Compounds 940 (2023) 168796.

- Open Access Article. Published on 13 November 2025. Downloaded on 18/11/2025 9:21:00 PM.

 This article is licensed under a Creative Commons Attribution-NonCommercial 3.0 Unported Licence
- 1704 [148] J. Jia, Q. Zhang, K. Li, Y. Zhang, E. Liu, X. Li, Recent advances on g-C3N4. base MA00750J
- 1705 Z-scheme photocatalysts: Structural design and photocatalytic applications,
- 1706 International Journal of Hydrogen Energy 48 (2023) 196.
- 1707 [149] X. Zeng, Z. Wang, G. Wang, T.R. Gengenbach, D.T. McCarthy, A. Deletic, J. Yu,
- 1708 X. Zhang, Highly dispersed TiO2 nanocrystals and WO3 nanorods on reduced
- 1709 graphene oxide: Z-scheme photocatalysis system for accelerated photocatalytic water
- disinfection, Applied Catalysis B: Environmental 218 (2017) 163.
- 1711 [150] J. Low, C. Jiang, B. Cheng, S. Wageh, A.A. Al-Ghamdi, J. Yu, A review of direct
- 1712 Z-scheme photocatalysts, Small methods 1 (2017) 1700080.
- 1713 [151] X. Miao, X. Shen, J. Wu, Z. Ji, J. Wang, L. Kong, M. Liu, C. Song, Fabrication of
- an all solid Z-scheme photocatalyst g-C3N4/GO/AgBr with enhanced visible light
- photocatalytic activity, Applied Catalysis A: General 539 (2017) 104.
- 1716 [152] Z. Qian, B. Pathak, J. Nisar, R. Ahuja, Oxygen-and nitrogen-chemisorbed carbon
- 1717 nanostructures for Z-scheme photocatalysis applications, Journal of nanoparticle
- 1718 research 14 (2012) 895.
- 1719 [153] D. Zhou, D. Li, Z. Chen, Recent advances in ternary Z-scheme photocatalysis on
- 1720 graphitic carbon nitride based photocatalysts, Frontiers in Chemistry 12 (2024)
- 1721 1359895. https://doi.org/10.3389/fchem.2024.1359895
- 1722 [154] M. Li et al., Novel Z-scheme visible-light photocatalyst based on
- 1723 CoFe2O4/BiOBr/Graphene composites for organic dye degradation and Cr (VI)
- 1724 reduction, Applied Surface Science 478 (2019) 744.
- 1725 [155] W. Li, X. Wang, M. Li, S.-a. He, Q. Ma, X. Wang, Construction of Z-scheme and
- pn heterostructure: Three-dimensional porous g-C3N4/graphene oxide-Ag/AgBr
- 1727 composite for high-efficient hydrogen evolution, Applied Catalysis B: Environmental
- 1728 268 (2020) 118384.
- 1729 [156] Z. Chen, S. Sun, J. Prakash, Design and engineering of graphene nanostructures
- as independent solar-driven photocatalysts for emerging applications in the field of
- energy and environment, Molecular Systems Design & Engineering 7 (2022) 213.
- 1732 [157] S. Huang, M. Hu, L. He, S. Ren, X. Wu, S. Cui, Construction of manganese
- 1733 ferrite/zinc ferrite anchored graphene-based hierarchical aerogel photocatalysts

- 1734 following Z-scheme electron transfer for visible-light-driven carbon dio Not represent the following transfer for visible-light-driven carbon dio Not represent the following transfer for visible-light-driven carbon dio Not represent the following transfer for visible-light-driven carbon dio Not represent the following transfer for visible-light-driven carbon dio Not represent the following transfer for visible-light-driven carbon dio Not represent the following transfer for visible-light-driven carbon dio Not represent the following transfer for visible-light-driven carbon dio Not represent the following transfer for visible-light-driven carbon dio Not represent the following transfer for visible-light-driven carbon dio Not represent the following transfer for visible-light-driven carbon dio Not represent the following transfer for visible-light-driven carbon dio Not represent the following transfer for visible-light-driven carbon dio Not represent the following transfer for visible-light-driven carbon dio Not represent the following transfer for visible-light-driven carbon dio Not represent the following transfer for visible-light-driven carbon dio Not represent the following transfer for visible-light-driven carbon dio Not represent the following transfer for visible-light-driven carbon dio Not represent the following transfer for visible-light-driven carbon dio Not represent the following transfer for visible-light-driven carbon dio Not represent the following transfer for visible-light-driven carbon driven dio Not represent the following transfer for visible-light-driven carbon driven drive
- 1735 reduction, Journal of Colloid and Interface Science (2025) 137678.
- 1736 [158] U. C Gowda, H. Priyadarshini, K. Prashantha, M. Shkir, S. Appu, G. Nagaraju,
- 1737 S.G. Kumar, Enhanced Photocatalytic Performances of Ag-Bivo4/Tio2@ Graphene-
- 1738 Based Z-Scheme Heterojunction.
- 1739 [159] M. Chu, J. Bian, Z. Zhang, Z. Zhao, L. Jing, Graphene-Regulated Interfacial Z-
- 1740 Scheme Charge Transfer for CO2 Photoreduction to CO with Nearly 100% Selectivity,
- 1741 The Journal of Physical Chemistry C (2025).
- 1742 [160] M.T. Baig, Z. Zahid, M. Taugeer, C.-H. Park, J.P. Park, C.-H. Choi, T. Yoon, A.
- 1743 Mohammad, State-of-the-art developments in metal/metal oxide and graphene-based
- nano-hybrid systems for photocatalytic degradation of tetracycline antibiotics, Journal
- of Industrial and Engineering Chemistry (2025).
- 1746 [161] A. Meera, M. Mahalakshmi, B. Neppolian, The strategy on selecting the
- 1747 oxidation photocatalyst NiWO4 as a co-catalyst to enhance the performance of
- 1748 TiO2/rGO for H2 production under solar light, International Journal of Hydrogen
- 1749 Energy 144 (2025) 186.
- 1750 [162] P.-Q. Wang, Y. Bai, P.-Y. Luo, J.-Y. Liu, Graphene–WO3 nanobelt composite:
- 1751 Elevated conduction band toward photocatalytic reduction of CO2 into hydrocarbon
- 1752 fuels, Catalysis Communications 38 (2013) 82.
- 1753 https://doi.org/https://doi.org/10.1016/j.catcom.2013.04.020
- 1754 [163] Y. Xia, B. Cheng, J. Fan, J. Yu, G. Liu, Near-infrared absorbing 2D/3D
- 2755 ZnIn2S4/N-doped graphene photocatalyst for highly efficient CO2 capture and
- 1756 photocatalytic reduction, Science China Materials 63 (2020) 552.
- 1757 https://doi.org/10.1007/s40843-019-1234-x
- 1758 [164] W.-J. Ong, L.-L. Tan, S.-P. Chai, S.-T. Yong, Graphene oxide as a structure-
- 1759 directing agent for the two-dimensional interface engineering of sandwich-like
- graphene-g-C3N4 hybrid nanostructures with enhanced visible-light photoreduction
- of CO2 to methane, Chemical Communications 51 (2015) 858.
- 1762 https://doi.org/10.1039/C4CC08996K
- 1763 [165] H.-C. Hsu et al., Graphene oxide as a promising photocatalyst for CO2 to
- methanol conversion, Nanoscale 5 (2013) 262. https://doi.org/10.1039/C2NR31718D

- 1765 [166] I. Shown et al., Highly Efficient Visible Light Photocatalytic Reduction of CO2000 A007503
- 1766 Hydrocarbon Fuels by Cu-Nanoparticle Decorated Graphene Oxide, Nano Letters 14
- 1767 (2014) 6097. https://doi.org/10.1021/nl503609v
- 1768 [167] J. Cheng, M. Zhang, G. Wu, X. Wang, J. Zhou, K. Cen, Photoelectrocatalytic
- 1769 Reduction of CO2 into Chemicals Using Pt-Modified Reduced Graphene Oxide
- 1770 Combined with Pt-Modified TiO2 Nanotubes, Environmental Science & Technology
- 1771 48 (2014) 7076. https://doi.org/10.1021/es500364g
- 1772 [168] L.M. Pastrana-Martínez, A.M.T. Silva, N.N.C. Fonseca, J.R. Vaz, J.L. Figueiredo,
- 1773 J.L. Faria, Photocatalytic Reduction of CO2 with Water into Methanol and Ethanol
- 1774 Using Graphene Derivative-TiO2 Composites: Effect of pH and Copper(I) Oxide,
- 1775 Topics in Catalysis 59 (2016) 1279. https://doi.org/10.1007/s11244-016-0655-2
- 1776 [169] L.-L. Tan, W.-J. Ong, S.-P. Chai, A.R. Mohamed, Noble metal modified reduced
- 1777 graphene oxide/TiO2 ternary nanostructures for efficient visible-light-driven
- 1778 photoreduction of carbon dioxide into methane, Applied Catalysis B: Environmental
- 1779 166-167 (2015) 251. https://doi.org/https://doi.org/10.1016/j.apcatb.2014.11.035
- 1780 [170] Z. Xiong, Y. Luo, Y. Zhao, J. Zhang, C. Zheng, J.C.S. Wu, Synthesis,
- 1781 characterization and enhanced photocatalytic CO2 reduction activity of graphene
- 1782 supported TiO2 nanocrystals with coexposed {001} and {101} facets, Physical
- 1783 Chemistry Chemical Physics 18 (2016) 13186. https://doi.org/10.1039/C5CP07854G
- 1784 [171] R. Gusain, P. Kumar, O.P. Sharma, S.L. Jain, O.P. Khatri, Reduced graphene
- 1785 oxide-CuO nanocomposites for photocatalytic conversion of CO2 into methanol
- under visible light irradiation, Applied Catalysis B: Environmental 181 (2016) 352.
- 1787 https://doi.org/https://doi.org/10.1016/j.apcatb.2015.08.012
- 1788 [172] L.-L. Tan, W.-J. Ong, S.-P. Chai, A.R. Mohamed, Photocatalytic reduction of CO2
- with H2O over graphene oxide-supported oxygen-rich TiO2 hybrid photocatalyst
- under visible light irradiation: Process and kinetic studies, Chemical Engineering
- 1791 Journal 308 (2017) 248. https://doi.org/https://doi.org/10.1016/j.cej.2016.09.050
- 1792 [173] Q. Zhang, L. Huang, S. Kang, C. Yin, Z. Ma, L. Cui, Y. Wang, CuO/Cu2O
- 1793 nanowire arrays grafted by reduced graphene oxide: synthesis, characterization, and
- application in photocatalytic reduction of CO2, RSC Advances 7 (2017) 43642.
- 1795 https://doi.org/10.1039/C7RA07310K

- 1796 [174] S. Sorcar, J. Thompson, Y. Hwang, Y.H. Park, T. Majima, C.A. Grimes Virtual Online
- Durrant, S.-I. In, High-rate solar-light photoconversion of CO2 to fuel: controllable
- transformation from C1 to C2 products, Energy & Environmental Science 11 (2018)
- 1799 3183. https://doi.org/10.1039/C8EE00983J
- 1800 [175] S. Kumar, R.K. Yadav, K. Ram, A. Aguiar, J. Koh, A.J.F.N. Sobral, Graphene
- oxide modified cobalt metallated porphyrin photocatalyst for conversion of formic
- 1802 acid from carbon dioxide, Journal of CO2 Utilization 27 (2018) 107.
- 1803 https://doi.org/https://doi.org/10.1016/j.jcou.2018.07.008
- 1804 [176] P. Devi, J.P. Singh, Visible light induced selective photocatalytic reduction of
- 1805 CO2 to CH4 on In2O3-rGO nanocomposites, Journal of CO2 Utilization 43 (2021)
- 1806 101376. https://doi.org/https://doi.org/10.1016/j.jcou.2020.101376
- 1807 [177] X. Wang, Q. Li, C. Zhou, Z. Cao, R. Zhang, ZnO rod/reduced graphene oxide
- sensitized by α-Fe2O3 nanoparticles for effective visible-light photoreduction of CO2,
- 1809 Journal of Colloid and Interface Science 554 (2019) 335.
- 1810 https://doi.org/https://doi.org/10.1016/j.jcis.2019.07.014
- 1811 [178] H.-T. Lien *et al.*, Solar to hydrocarbon production using metal-free water-soluble
- bulk heterojunction of conducting polymer nanoparticle and graphene oxide, The
- Journal of Chemical Physics 154 (2021) 164707. https://doi.org/10.1063/5.0042716
- 1814 [179] T. Wu, C. Zhu, D. Han, Z. Kang, L. Niu, Highly selective conversion of CO2 to
- 1815 C2H6 on graphene modified chlorophyll Cu through multi-electron process for
- 1816 artificial photosynthesis, Nanoscale 11 (2019) 22980.
- 1817 https://doi.org/10.1039/C9NR07824J
- 1818 [180] K.M. Kamal et al., Synergistic enhancement of photocatalytic CO2 reduction by
- plasmonic Au nanoparticles on TiO2 decorated N-graphene heterostructure catalyst
- 1820 for high selectivity methane production, Applied Catalysis B: Environment and
- 1821 Energy 307 (2022) 121181.
- 1822 https://doi.org/https://doi.org/10.1016/j.apcatb.2022.121181
- 1823 [181] H.R. Park, A.U. Pawar, U. Pal, T. Zhang, Y.S. Kang, Enhanced solar
- photoreduction of CO2 to liquid fuel over rGO grafted NiO-CeO2 heterostructure
- 1825 nanocomposite, Nano Energy 79 (2021) 105483.
- 1826 https://doi.org/https://doi.org/10.1016/j.nanoen.2020.105483

- Open Access Article. Published on 13 November 2025. Downloaded on 18/11/2025 9:21:00 PM.

 BY-NC

 This article is licensed under a Creative Commons Attribution-NonCommercial 3.0 Unported Licence.
- 1827 [182] W. Tu et al., Robust Hollow Spheres Consisting of Alternating Title Adolorson
- 1828 Nanosheets and Graphene Nanosheets with High Photocatalytic Activity for CO2
- 1829 Conversion into Renewable Fuels, Advanced Functional Materials 22 (2012) 1215.
- 1830 https://doi.org/https://doi.org/10.1002/adfm.201102566
 - 1831 [183] N. Nandal, P.K. Prajapati, B.M. Abraham, S.L. Jain, CO2 to ethanol: A selective
 - photoelectrochemical conversion using a ternary composite consisting of graphene
 - 1833 oxide/copper oxide and a copper-based metal-organic framework, Electrochimica
 - 1834 Acta 404 (2022) 139612.
 - 1835 https://doi.org/https://doi.org/10.1016/j.electacta.2021.139612
 - 1836 [184] J. Yu, J. Jin, B. Cheng, M. Jaroniec, A noble metal-free reduced graphene oxide-
 - 1837 CdS nanorod composite for the enhanced visible-light photocatalytic reduction of
 - 1838 CO2 to solar fuel, Journal of Materials Chemistry A 2 (2014) 3407.
 - 1839 https://doi.org/10.1039/C3TA14493C
 - 1840 [185] Y.T. Liang, B.K. Vijayan, O. Lyandres, K.A. Gray, M.C. Hersam, Effect of
 - 1841 Dimensionality on the Photocatalytic Behavior of Carbon-Titania Nanosheet
 - 1842 Composites: Charge Transfer at Nanomaterial Interfaces, The Journal of Physical
 - 1843 Chemistry Letters 3 (2012) 1760. https://doi.org/10.1021/jz300491s
 - 1844 [186] W. Tu, Y. Zhou, Q. Liu, S. Yan, S. Bao, X. Wang, M. Xiao, Z. Zou, An In Situ
 - 1845 Simultaneous Reduction-Hydrolysis Technique for Fabrication of TiO2-Graphene 2D
 - 1846 Sandwich-Like Hybrid Nanosheets: Graphene-Promoted Selectivity of Photocatalytic-
 - 1847 Driven Hydrogenation and Coupling of CO2 into Methane and Ethane, Advanced
 - 1848 Functional Materials 23 (2013) 1743.
 - 1849 https://doi.org/https://doi.org/10.1002/adfm.201202349
 - 1850 [187] S. Liu, B. Weng, Z.-R. Tang, Y.-J. Xu, Constructing one-dimensional silver
 - 1851 nanowire-doped reduced graphene oxide integrated with CdS nanowire network
 - 1852 hybrid structures toward artificial photosynthesis, Nanoscale 7 (2015) 861.
 - 1853 https://doi.org/10.1039/C4NR04229H
 - 1854 [188] J. Hou, H. Cheng, O. Takeda, H. Zhu, Three-Dimensional Bimetal-Graphene-
 - 1855 Semiconductor Coaxial Nanowire Arrays to Harness Charge Flow for the
 - 1856 Photochemical Reduction of Carbon Dioxide, Angewandte Chemie International
 - 1857 Edition 54 (2015) 8480. https://doi.org/https://doi.org/10.1002/anie.201502319

- 1858 [189] X. An, K. Li, J. Tang, Cu2O/Reduced Graphene Oxide Composites of Composites
- 1859 Photocatalytic Conversion of CO2, ChemSusChem 7 (2014) 1086.
- 1860 https://doi.org/https://doi.org/10.1002/cssc.201301194
- 1861 [190] X. Li, Q. Wang, Y. Zhao, W. Wu, J. Chen, H. Meng, Green synthesis and photo-
- catalytic performances for ZnO-reduced graphene oxide nanocomposites, Journal of
- 1863 Colloid and Interface Science 411 (2013) 69.
- 1864 https://doi.org/https://doi.org/10.1016/j.jcis.2013.08.050
- 1865 [191] P. Li, Y. Zhou, H. Li, Q. Xu, X. Meng, X. Wang, M. Xiao, Z. Zou, All-solid-state
- 1866 Z-scheme system arrays of Fe2V4O13/RGO/CdS for visible light-driving
- 1867 photocatalytic CO2 reduction into renewable hydrocarbon fuel, Chemical
- 1868 Communications 51 (2015) 800. https://doi.org/10.1039/C4CC08744E
- 1869 [192] J. Park, T. Jin, C. Liu, G. Li, M. Yan, Three-Dimensional Graphene-TiO2
- 1870 Nanocomposite Photocatalyst Synthesized by Covalent Attachment, ACS Omega 1
- 1871 (2016) 351. https://doi.org/10.1021/acsomega.6b00113
- 1872 [193] M. Song et al., Facile synthesis of MOF–808/RGO-based 3D macroscopic aerogel
- for enhanced photoreduction CO₂, Journal of Colloid and Interface Science 668 (2024)
- 471. https://doi.org/https://doi.org/10.1016/j.jcis.2024.04.195
- 1875 [194] J. Zhang, S. Shao, D. Zhou, Q. Xu, T. Wang, ZnO nanowire arrays decorated 3D
- 1876 N-doped reduced graphene oxide nanotube framework for enhanced photocatalytic
- 1877 CO2 reduction performance, Journal of CO2 Utilization 50 (2021) 101584.
- 1878 https://doi.org/https://doi.org/10.1016/j.jcou.2021.101584
- 1879 [195] Y.T. Liang, B.K. Vijayan, K.A. Gray, M.C. Hersam, Minimizing Graphene Defects
- 1880 Enhances Titania Nanocomposite-Based Photocatalytic Reduction of CO2 for
- 1881 Improved Solar Fuel Production, Nano Letters 11 (2011) 2865.
- 1882 https://doi.org/10.1021/nl2012906
- 1883 [196] B. Kaur et al., Catalytic performance of Graphdiyne for CO2 reduction and
- charge dynamics progress, Journal of Environmental Chemical Engineering (2025)
- 1885 116904.
- 1886 [197] F.-Y. Liu, H.-L. Chen, K.-Y. Hsiao, Y.-M. Dai, C.-C. Chen, I.-C. Chen, Unveiling
- photochemical CO2 reduction processes on PbBiO2I/GO surfaces: Insights from in-

- situ Raman spectroscopy, Applied Catalysis B: Environment and Energy 364 (2002) Applied Catalysis B: Environment Applied Catalysis B: Environment Applied Catalysis B: Environment Applied Catalysis Applied Catalysis
- 1889 124844.
- 1890 [198] Z. Zhang, L. Li, S. Gao, P. Yang, Graphene interface modification to improve
- efficiency and stability at MAPbI3/ZnO interface for perovskite solar cells: A first-
- 1892 principles study, Solar Energy 287 (2025) 113236.
- 1893 [199] U.U. Rehman, R.S. Almufarij, A. Abd-Elwahed, K.U. Sahar, E. Hussain, A.
- 1894 Ashfaq, K. Mahmood, C.-M. Wang, Improving efficiency of germanium-based
- 1895 perovskite solar cells with graphene interface layer: a strategy to minimize charge
- recombination, Journal of Physics and Chemistry of Solids 198 (2025) 112487.
- 1897 [200] S. Fu, H. Zhang, K.-J. Tielrooij, M. Bonn, H.I. Wang, Tracking and controlling
- 1898 ultrafast charge and energy flow in graphene-semiconductor heterostructures, The
- 1899 Innovation 6 (2025).
- 1900 [201] X. Zhou et al., Weakness-complementing Z-scheme black phosphorus/TiO2
- 1901 heterojunction with efficient charge separation and photocatalytic overall water
- splitting activity, Journal of Colloid and Interface Science 689 (2025) 137240.
- 1903 [202] A. Kamboukos, N. Todorova, I. Yarovsky, Exploring 2D Graphene-Based
- 1904 Nanomaterials for Biomedical Applications: A Theoretical Modeling Perspective,
- 1905 Small Science (2025) 2400505.
- 1906 [203] S. Samajdar, M. Biswas, D. Sarkar, J. Pramanik, J. Mukhopadhyay, S. Ghosh,
- 1907 Double heterojunction photocatalysts: strategic fabrication and mechanistic insights
- towards sustainable fuel production, Chemical Communications 61 (2025) 6069.
- 1909 [204] X. Zhu, Y. Hu, G. Wu, W. Chen, N. Bao, Two-dimensional nanosheets-based soft
- 1910 electro-chemo-mechanical actuators: recent advances in design, construction, and
- 1911 applications, ACS nano 15 (2021) 9273.
- 1912 [205] X. Lan, N. Luo, Z. Li, J. Peng, H.-M. Cheng, Status and prospect of two-
- dimensional materials in electrolytes for all-solid-state lithium batteries, ACS nano 18
- 1914 (2024) 9285.
- 1915 [206] Z. Zhou, W. Qi, Z. Li, L. Yang, Z. Lin, R. Guan, N-P Type Charge Compensatory
- 1916 Synergistic Effect for Schottky and Efficient Photoelectrocatalysis Applications:
- 1917 Doping Mechanism in (Nb/Re)@ WS2/Graphene Heterojunctions, Chemistry-A
- 1918 European Journal 31 (2025) e202403963.

- 1919 [207] F. Gomes et al., Advancing Dye-Sensitized Solar Cells: Synergistic Effection Advancing Dye-Sensitized Solar Cells:
- 1920 Polyaniline, Graphene Oxide, and Carbon Nanotubes for Enhanced Efficiency and
- 1921 Sustainability Developments, Recent patents on nanotechnology (2025).
- 1922 [208] D. Das, M. Das, S. Sil, P. Sahu, P.P. Ray, Effect of Higher Carrier Mobility of the
- 1923 Reduced Graphene Oxide-Zinc Telluride Nanocomposite on Efficient Charge
- 1924 Transfer Facility and the Photodecomposition of Rhodamine B, ACS Omega 7 (2022)
- 1925 26483. https://doi.org/10.1021/acsomega.2c02472
- 1926 [209] G.S. Natarajamani, V.P. Kannan, S. Madanagurusamy, Synergistic ramifications
- of a sustainable ultra-sensitive NH3 sensor: Thermally reduced graphene oxide/ZnO
- 1928 hybrid composite for sub-PPM detection, Journal of Environmental Chemical
- 1929 Engineering 13 (2025) 116079.
- 1930 [210] T. Sewela, R. Ocaya, T. Malevu, Recent insights into the transformative role of
- 1931 Graphene-based/TiO2 electron transport layers for perovskite solar cells, Energy
- 1932 Science & Engineering 13 (2025) 4.
- 1933 [211] F. Ullah, B.H. Guan, M. Zafar, N. e Hira, H. Khan, M.S.M. Saheed, Synergistic
- 1934 enhancement in PEC hydrogen production using novel GQDs and CuO modified
- 1935 TiO2 based heterostructure photocatalyst, Materials Chemistry and Physics 340 (2025)
- 1936 130781.
- 1937 [212] D. Maarisetty, R. Mary, D.-R. Hang, P. Mohapatra, S.S. Baral, The role of material
- 1938 defects in the photocatalytic CO2 reduction: Interfacial properties, thermodynamics,
- 1939 kinetics and mechanism, Journal of CO2 Utilization 64 (2022) 102175.
- 1940 [213] C.A. Celaya, C. Delesma, P. Valadés-Pelayo, O.A. Jaramillo-Quintero, C.O.
- 1941 Castillo-Araiza, L. Ramos, P. Sebastian, J. Muñiz, Exploring the potential of graphene
- oxide as a functional material to produce hydrocarbons via photocatalysis: Theory
- 1943 meets experiment, Fuel 271 (2020) 117616.
- 1944 [214] M.Y. Akram, T. Ashraf, M.S. Jagirani, A. Nazir, M. Saqib, M. Imran, Recent
- advances in graphene-based single-atom photocatalysts for CO2 reduction and H2
- 1946 production, Catalysts 14 (2024) 343.
- 1947 [215] J.O. Olowoyo, M. Kumar, B. Singh, V.O. Oninla, J.O. Babalola, H. Valdés, A.V.
- 1948 Vorontsov, U. Kumar, Self-assembled reduced graphene oxide-TiO2 nanocomposites:

- Synthesis, DFTB+ calculations, and enhanced photocatalytic reduction of 1003 Advictor of 10
- 1950 methanol, Carbon 147 (2019) 385.
- 1951 [216] Y. Cui, X. Huang, T. Wang, L. Jia, Q. Nie, Z. Tan, H. Yu, Graphene quantum
- 1952 dots/carbon nitride heterojunction with enhanced visible-light driven photocatalysis
- of nitric oxide: An experimental and DFT study, Carbon 191 (2022) 502.
- 1954 [217] A. Olatomiwa, T. Adam, C. Edet, A. Adewale, A. Chik, M. Mohammed, S.C.
- 1955 Gopinath, U. Hashim, Recent advances in density functional theory approach for
- optoelectronics properties of graphene, Heliyon 9 (2023).
- 1957 [218] M. Khenfouch, M. Baïtoul, M. Maaza, White photoluminescence from a grown
- 1958 ZnO nanorods/graphene hybrid nanostructure, optical Materials 34 (2012) 1320.
- 1959 [219] B. Weng, Y.-J. Xu, What if the electrical conductivity of graphene is significantly
- 1960 deteriorated for the graphene-semiconductor composite-based photocatalysis?, ACS
- 1961 Applied Materials & Interfaces 7 (2015) 27948.
- 1962 [220] Y. Xiang, L. Xin, J. Hu, C. Li, J. Qi, Y. Hou, X. Wei, Advances in the applications
- of graphene-based nanocomposites in clean energy materials, Crystals 11 (2021) 47.
- 1964 [221] G. Marineau-Plante et al., Effect of mesogenic side groups on the redox,
- 1965 photophysical, and solar cell properties of diketopyrrolopyrrole-trans-bis
- 1966 (diphosphine) diethynylplatinum (II) polymers, ACS Applied Polymer Materials 3
- 1967 (2021) 1087.
- 1968 [222] H. Kasap, 2019.
- 1969 [223] A.G. Al-Gamal, A.M. Elseman, K.I. Kabel, Advances in Nitrogen-Functionalized
- 1970 Graphene for Enhanced Photovoltaic Applications, Solar RRL 9 (2025) 2500002.
- 1971 [224] E. Flórez, C. Jimenez-Orozco, N. Acelas, Unravelling the influence of surface
- 1972 functional groups and surface charge on heavy metal adsorption onto carbonaceous
- materials: an in-depth DFT study, Materials Today Communications 39 (2024) 108647.
- 1974 [225] M. Yang, B. Qin, C. Si, X. Sun, B. Li, Electrochemical reactions catalyzed by
- 1975 carbon dots from computational investigations: functional groups, dopants, and
- 1976 defects, Journal of Materials Chemistry A 12 (2024) 2520.
- 1977 [226] Y. Li, W. Niu, T. Chen, Y. Sun, M. Yu, Integrating vacancy engineering and
- 1978 energy-level adapted coupling of electrocatalyst for enhancement of carbon dioxide
- 1979 conversion, Applied Catalysis B: Environmental 321 (2023) 122037.

- 1980 [227] S. Xu, E.A. Carter, CO2 photoelectrochemical reduction catalyzed by a GaP₁₀(001) Million catalyzed by a Million catalyzed
- 1981 photoelectrode, ACS Catalysis 11 (2021) 1233.
- 1982 [228] X. Xu, C. Liu, Z. Sun, T. Cao, Z. Zhang, E. Wang, Z. Liu, K. Liu, Interfacial
- engineering in graphene bandgap, Chemical Society Reviews 47 (2018) 3059.
- 1984 [229] S. Nakaharai, T. Iijima, S. Ogawa, S. Suzuki, S.-L. Li, K. Tsukagoshi, S. Sato, N.
- 1985 Yokoyama, Conduction tuning of graphene based on defect-induced localization,
- 1986 ACS nano 7 (2013) 5694.
- 1987 [230] M. Kumar Kumawat, S. Kumar, T. Mohanty, Tailoring functional properties of
- 1988 graphene oxide by defect-assisted surface and interface modifications, Journal of
- 1989 Materials Research 37 (2022) 3394.
- 1990 [231] I. Shtepliuk, Defect-induced modulation of a 2D ZnO/graphene heterostructure:
- 1991 exploring structural and electronic transformations, Applied Sciences 13 (2023) 7243.
- 1992 [232] K.P. Dhakal et al., Local strain induced band gap modulation and
- 1993 photoluminescence enhancement of multilayer transition metal dichalcogenides,
- 1994 Chemistry of Materials 29 (2017) 5124.
- 1995 [233] D. Maarisetty, S.S. Baral, Defect engineering in photocatalysis: formation,
- chemistry, optoelectronics, and interface studies, Journal of Materials Chemistry A 8
- 1997 (2020) 18560.
- 1998 [234] M. Shen, L. Zhang, J. Shi, Defect engineering of photocatalysts towards elevated
- 1999 CO2 reduction performance, ChemSusChem 14 (2021) 2635.
- 2000 [235] B. Wang, G. Du, S. Tan, S. Guo, Z. Zhu, G.-F. Huang, W.-Q. Huang, R. Jiang,
- 2001 Constructing a Double Type-Ii G-C3n4/Cds/Mos2 (Gcsm) Heterojunction with Dual-
- 2002 Enhanced Redox Capability for Efficient Photocatalytic Pollutant Degradation,
- 2003 Shengxia and Guo, Shengwei and Zhu, ZhongHua and Huang, Gui-Fang and Huang,
- 2004 Wei-Qing and Jiang, Ru, Constructing a Double Type-Ii G-C3n4/Cds/Mos2 (Gcsm)
- 2005 Heterojunction with Dual-Enhanced Redox Capability for Efficient Photocatalytic
- 2006 Pollutant Degradation.
- 2007 [236] S. Zhang, X. Zhang, W. Shi, H. Weiyan, X. Wang, The Study on the Construction
- of S-Scheme G-C3n4/Mof Heterojunctions Through Interface and Built-In Electric
- 2009 Field Modulation and Their Photocatalytic Degradation Performance of Tetracycline,
- 2010 Xiaojing, The Study on the Construction of S-Scheme G-C3n4/Mof Heterojunctions

- Through Interface and Built-In Electric Field Modulation and Their Photocataly 13 (A00750)
- 2012 Degradation Performance of Tetracycline.
- 2013 [237] Y. Wang, Y. Liu, H. Zhang, X. Duan, J. Ma, H. Sun, W. Tian, S. Wang,
- 2014 Carbonaceous materials in structural dimensions for advanced oxidation processes,
- 2015 Chemical Society Reviews (2025).
- 2016 [238] Q. Tian, Q. Li, T. Zhang, W. Huang, C. Zhao, B. Hu, X. Xu, Molecular Orbital
- 2017 Level Micro-Electric Field in Green Fenton-Like Chemistry for Water Treatment: From
- 2018 Mechanism Understanding to Scale-Up Applications, Advanced Materials (2025)
- 2019 e09280.
- 2020 [239] N.N. Rabin, H. Ohmagari, M.S. Islam, M.R. Karim, S. Hayami, A procession on
- 2021 photocatalyst for solar fuel production and waste treatment, Journal of Inclusion
- 2022 Phenomena and Macrocyclic Chemistry 94 (2019) 263.
- 2023 [240] M.D. Ali, A. Starczewska, T.K. Das, M. Jesionek, Exploration of Sp-Sp2 Carbon
- 2024 Networks: Advances in Graphyne Research and Its Role in Next-Generation
- Technologies, International Journal of Molecular Sciences 26 (2025) 5140.
- 2026 [241] F. Liu, G. Wei, B. Hu, A review on n-type chemical doping of graphene films:
- preparation, characterization and applications, Nanoscale (2025).
- 2028 [242] L.K. Putri, W.-J. Ong, W.S. Chang, S.-P. Chai, Heteroatom doped graphene in
- 2029 photocatalysis: A review, Applied Surface Science 358 (2015) 2.
- 2030 https://doi.org/https://doi.org/10.1016/j.apsusc.2015.08.177
- 2031 [243] J. Jianga, Y. Zhanga, W. Suna, J. Penga, W. Shib, Y. Quc, E. Liud, A review of
- 2032 updated red phosphorus-based photocatalysts, (2025).
- 2033 [244] W. Zhu, B. Zhang, Y. Yang, M. Zhao, Y. Fang, Y. Cui, J. Tian, Enhanced
- 2034 Electrocatalytic Performance of P-Doped MoS2/rGO Composites for Hydrogen
- Evolution Reactions, Molecules 30 (2025) 1205.
- 2036 [245] S. Zhi, Q. Dai, H. Wang, D. Wu, L. Zhao, C. Hu, L. Dai, Heteroatom-Doped
- 2037 Carbon Materials for Multifunctional Noncatalytic Applications, ACS nano (2025).
- 2038 [246] H. Noorizadeh, R.H. Al Omari, A. Kumar, A.F. Al-Hussainy, S. Mohammed, A.
- 2039 Sinha, S. Ray, Indium Phosphide Quantum Dots as Green Nanosystems for
- 2040 Environmental Detoxification: Surface Engineering, Photocatalytic Mechanisms, and
- 2041 Comparative Material Insights, Environmental Science: Advances (2025).

- 2042 [247] Z.A. Sandhu, U. Farwa, M. Danish, M.A. Raza, A. Talib, H. Amjad, R. Riaza, Mew Carticle Online
- 2043 Al-Sehemi, Sustainability and photocatalytic performance of MOFs: Synthesis
- strategies and structural insights, Journal of Cleaner Production (2024) 143263.
- 2045 [248] D.S. Constantino, M.M. Dias, A.M. Silva, J.L. Faria, C.G. Silva, Intensification
- 2046 strategies for improving the performance of photocatalytic processes: A review,
- 2047 Journal of Cleaner Production 340 (2022) 130800.
- 2048 [249] S. Sadana, N. Rajamohan, R. Manivasagan, N. Raut, S. Paramasivam, G. Gatto,
- 2049 A. Kumar, Graphene-based materials for photocatalytic and environmental sensing
- applications, RESULTS IN ENGINEERING 27 (2025).
- 2051 [250] I. Razzaq et al., Graphene-Based Polymer Composites for High-Performance
- 2052 Chemical Sensing and Detection: A Critical Review, Advanced Materials
- 2053 Technologies e00578.
- 2054 [251] R. Atchudan, T.N.J.I. Edison, S. Perumal, D. Karthikeyan, Y.R. Lee, Facile
- 2055 synthesis of zinc oxide nanoparticles decorated graphene oxide composite via simple
- 2056 solvothermal route and their photocatalytic activity on methylene blue degradation,
- Journal of Photochemistry and Photobiology B: Biology 162 (2016) 500.
- 2058 [252] M. Ahmad, E. Ahmed, Z. Hong, N. Khalid, W. Ahmed, A. Elhissi, Graphene-
- 2059 Ag/ZnO nanocomposites as high performance photocatalysts under visible light
- irradiation, Journal of alloys and compounds 577 (2013) 717.
- 2061 [253] X. Liu, A. Hu, Z. Liu, K. Ding, W. Xia, H. Shangguan, C. Zhang, T. Fu, Review
- 2062 on fundamental and recent advances of strain engineering for enhancing
- photocatalytic CO2 reduction, Advanced Energy Materials 15 (2025) 2405320.
- 2064 [254] L.T. Mambiri, University of Louisiana at Lafayette, 2025.
- 2065 [255] L. Jiang, X. Zhi, X. Bai, Y. Jiao, Atomic-level insights into cation-mediated
- 2066 mechanism in electrochemical nitrogen reduction, Journal of the American Chemical
- 2067 Society 147 (2025) 16935.
- 2068 [256] G.G. Nezhad, H. Esfandian, M.S. Lashkenari, Synthesis and Electrocatalytic
- 2069 Performance of Cu-Pb/RGO Composite for Efficient CO₂ Reduction to Methanol,
- 2070 Results in Engineering (2025) 105436.

- 2071 [257] S.J. Armaković, S. Armaković, A. Bilić, M.M. Savanović, ZnQ-Bases Androice Online
- 2072 Photocatalysts: Synergistic Effects of Material Modifications and Machine Learning
- 2073 Optimization, Catalysts 15 (2025) 793.
- 2074 [258] Q. Adfar, S. Hussain, S.S. Maktedar, Insights into energy and environmental
- 2075 sustainability through photoactive graphene-based advanced materials: perspectives
- and promises, New Journal of Chemistry (2025).
- 2077 [259] S. Sambyal, P. Raizada, A. Chawla, A.A.P. Khan, S. Thakur, V.-H. Nguyen, P.
- 2078 Singh, Tuning ZnCdS heterostructures for enhanced photocatalysis: hybrid
- 2079 architectures for sustainable energy and environmental applications, Journal of
- 2080 Materials Chemistry A (2025).
- 2081 [260] G.I. Edo et al., Green Biosynthesis of Nanoparticles Using Plant Extracts:
- 2082 Mechanisms, Advances, Challenges, and Applications, BioNanoScience 15 (2025) 267.
- 2083 [261] V. Jayant, R. Kumar, P. Tyagi, M. Yusuf, Green Chemistry, Elsevier, 2025, p. 67-
- 2084 96.
- 2085 [262] G.B. Mahendran, S.J. Ramalingam, J.B.B. Rayappan, S. Kesavan, T. Periathambi,
- 2086 N. Nesakumar, Green preparation of reduced graphene oxide by Bougainvillea glabra
- 2087 flower extract and sensing application, Journal of Materials Science: Materials in
- 2088 Electronics 31 (2020) 14345. https://doi.org/10.1007/s10854-020-03994-4
- 2089 [263] J. Singh, D.D. Nguyen, P. Leclere, P. Nguyen-Tri, Recent Advancements in
- 2090 Graphene-Based Nanocomposites for Enhanced Photocatalysis in Environmental
- 2091 Remediation: A Comprehensive Review, Reviews of Environmental Contamination
- 2092 and Toxicology 263 (2025) 13.
- 2093 [264] P. Rana, P. Singh, V. Puri, Q. Van Le, T. Ahamad, T.T. Le, V.-H. Nguyen, P.
- 2094 Raizada, Flat meets functional: face-to-face 2D/2D S-scheme photocatalysts for
- efficient CO 2-to-fuel conversion, Sustainable Energy & Fuels (2025).
- 2096 [265] S.H. Osman, S.K. Kamarudin, M.H. Jamil, E. Alfianto, N. Shaari, Z. Zakaria, 3D
- 2097 Graphene-Coupled Aerogel Nanoarchitectures: Emerging Paradigm Toward
- 2098 Sustainable Applications in Fuel Cell, Korean Journal of Chemical Engineering (2025)
- 2099 1.
- 2100 [266] H. Ali et al., Defect-driven innovations in photocatalysts: Pathways to enhanced
- 2101 photocatalytic applications, InfoMat e70040.

- 2102 [267] S.H. Emon, M.I. Hossain, M. Khanam, D.K. Yi, Expanding Horizons: Taking Addicte Online
- 2103 Advantage of Graphene's Surface Area for Advanced Applications, (2025).
- 2104 [268] L. Ma et al., Metal organic frameworks for photocatalytic CO 2 reduction to CO
- with high selectivity: Mechanism and strategy, Nano Research (2025).
- 2106 [269] J. Yu, G. Wang, B. Cheng, M. Zhou, Effects of hydrothermal temperature and
- 2107 time on the photocatalytic activity and microstructures of bimodal mesoporous TiO2
- 2108 powders, Applied Catalysis B: Environmental 69 (2007) 171.
- 2109 https://doi.org/https://doi.org/10.1016/j.apcatb.2006.06.022
- 2110 [270] M. Tang, Y. Xia, D. Yang, J. Liu, X. Zhu, R. Tang, Effects of hydrothermal time
- 2111 on structure and photocatalytic property of titanium dioxide for degradation of
- 2112 rhodamine b and tetracycline hydrochloride, Materials 14 (2021) 5674.
- 2113 [271] T.T.P.N.X. Trinh et al., Hydrothermal synthesis of titanium dioxide/graphene
- 2114 aerogel for photodegradation of methylene blue in aqueous solution, Journal of
- 2115 Science: Advanced Materials and Devices 7 (2022) 100433.
- 2116 https://doi.org/https://doi.org/10.1016/j.jsamd.2022.100433
- 2117 [272] A.a. Zhou, J. Bai, W. Hong, H. Bai, Electrochemically reduced graphene oxide:
- 2118 Preparation, composites, and applications, Carbon 191 (2022) 301.
- 2119 https://doi.org/https://doi.org/10.1016/j.carbon.2022.01.056
- 2120 [273] A.G. Marrani, A. Motta, F. Amato, R. Schrebler, R. Zanoni, E.A. Dalchiele, Effect
- of electrolytic medium on the electrochemical reduction of graphene oxide on Si (111)
- 2122 as probed by XPS, Nanomaterials 12 (2021) 43.
- 2123 [274] R.Y.N. Gengler, D.S. Badali, D. Zhang, K. Dimos, K. Spyrou, D. Gournis, R.J.D.
- 2124 Miller, Revealing the ultrafast process behind the photoreduction of graphene oxide,
- 2125 Nature Communications 4 (2013) 2560. https://doi.org/10.1038/ncomms3560
- 2126 [275] H.W. Cho, J.J. Wu, Photoreduction of graphene oxide enhanced by sacrificial
- 2127 agents, J Colloid Interface Sci 438 (2015) 291.
- 2128 https://doi.org/10.1016/j.jcis.2014.10.006
- 2129 [276] H. Singh et al., Revisiting the Green Synthesis of Nanoparticles: Uncovering
- 2130 Influences of Plant Extracts as Reducing Agents for Enhanced Synthesis Efficiency and
- 2131 Its Biomedical Applications, Int J Nanomedicine 18 (2023) 4727.
- 2132 https://doi.org/10.2147/ijn.S419369

- 2133 [277] Y. Wang, J. Yu, W. Xiao, Q. Li, Microwave-assisted hydrothermal synthesis of April 2013
- 2134 graphene based Au-TiO 2 photocatalysts for efficient visible-light hydrogen
- 2135 production, Journal of Materials Chemistry A 2 (2014) 3847.
- 2136 [278] P. Zhang, X. Teng, X. Feng, S. Ding, G. Zhang, Preparation of Bi2WO6
- 2137 photocatalyst by high-energy ball milled Bi2O3-WO3 mixture, Ceramics International
- 2138 42 (2016) 16749. https://doi.org/https://doi.org/10.1016/j.ceramint.2016.07.148
- 2139 [279] L. Zhang, L. Jin, B. Liu, J. He, Templated growth of crystalline mesoporous
- 2140 materials: from soft/hard templates to colloidal templates, Frontiers in chemistry 7
- 2141 (2019) 22.
- 2142 [280] R.J. Li, W.J. Niu, W.W. Zhao, B.X. Yu, C.Y. Cai, L.Y. Xu, F.M. Wang,
- 2143 Achievements and Challenges in Surfactants-Assisted Synthesis of MOFs-Derived
- 2144 Transition Metal-Nitrogen-Carbon as a Highly Efficient Electrocatalyst for ORR,
- 2145 OER, and HER, Small 21 (2025) 2408227.
- 2146 [281] Z. Tong, Y. Hai, B. Wang, F. Lv, Z. Zhong, R. Xiong, Activated g-C3N4
- 2147 Photocatalyst with Defect Engineering for Efficient Reduction of CO2 in Water, The
- 2148 Journal of Physical Chemistry C 127 (2023) 11067.
- 2149 https://doi.org/10.1021/acs.jpcc.3c02076
- 2150 [282] M. Mehrpooya, F. Bayatlar, Photocatalytic Reactors for CO2 Reduction: Review
- on Simulation Studies, Archives of Computational Methods in Engineering (2025) 1.
- 2152 [283] Z. Sun, X. He, L. Duan, Multifunctional Soft and Solid Materials for Integrated
- 2153 CO2 Capture and Utilization: Prospects and Opportunities, Advanced Functional
- 2154 Materials (2025) e24549.
- 2155 [284] S. Chakraborty, S.C. Peter, Solar-Fuel Production by Photodriven CO2
- 2156 Reduction: Facts, Challenges, and Recommendations, ACS Energy Letters 10 (2025)
- 2157 2359.
- 2158 [285] M. Zhan, M. Xu, W. Lin, H. He, C. He, Graphene Oxide Research: Current
- Developments and Future Directions, Nanomaterials 15 (2025) 507.
- 2160 [286] M. Ramezani, O. Rahmani, A review of recent progress in the graphene
- 2161 syntheses and its applications, Mechanics of Advanced Materials and Structures
- 2162 (2024) 1.

2176

- 2163 [287] C. Amutha, A. Gopan, I. Pushbalatatha, M. Ragavi, J.A. Rene MADOJ Rene MADOJ Rene MADOJ SOJ
- Nanotechnology in Societal Development, Springer, 2024, p. 481-503.
- 2165 [288] H.-Y. Zhuo, X. Zhang, J.-X. Liang, Q. Yu, H. Xiao, J. Li, Theoretical
- 2166 understandings of graphene-based metal single-atom catalysts: stability and catalytic
- 2167 performance, Chemical reviews 120 (2020) 12315.
- 2168 [289] H. Chen, Y. Zheng, J. Li, L. Li, X. Wang, AI for nanomaterials development in
- clean energy and carbon capture, utilization and storage (CCUS), ACS nano 17 (2023)
- 2170 9763.
- 2171 [290] R. Awasthy, S. Flint, R. Sankarnarayana, R.L. Jones, A framework to improve
- 2172 university-industry collaboration, Journal of Industry-University Collaboration 2
- 2173 (2020) 49.
- 2174 [291] N. Kalaiselvan, T. Mathimani, Solar-driven green hydrogen generation for
- revolutionizing the future of zero-carbon energy, Fuel 375 (2024) 132538.

Materials Advances Accepted Manuscript

This article is licensed under a Creative Commons Attribution-NonCommercial 3.0 Unported Licence.

No primary research results, software or code have been included and no new data Article Online Shakoo750J were generated or analysed as part of this review.